

Text and references accompanying Nevada Bureau of Mines and Geology Map 184

Geologic Map of the Welcome Quadrangle and an Adjacent Part of the Wells Quadrangle, Elko County, Nevada

by

Allen J. McGrew¹ and Arthur W. Snoke²

¹University of Dayton, Ohio

²University of Wyoming, Laramie

2015

ABSTRACT

Located in central Elko County, the Welcome and adjacent part of the Wells quadrangles expose a remarkable array of critical relationships for understanding the geologic history of the State of Nevada and the interior of the southwestern U.S. Cordillera. Covering the northern end of the East Humboldt Range and adjacent Clover Valley and Clover Hill, this map includes the northern terminus of the Ruby Mountains-East Humboldt Range metamorphic core complex. The oldest rocks in the State of Nevada (the gneiss complex of Angel Lake), and Nevada's only exposures of Archean rock, form the core of a multi-kilometer scale, southward-closing recumbent fold-nappe, the Winchell Lake nappe (WLN). Although intensely metamorphosed and profoundly ductilely attenuated, the WLN folds a series of pre-metamorphic thrust allochthons that collectively form an essentially complete sequence of Paleoproterozoic to Mississippian metasedimentary rocks. The WLN transported what may be Nevada's most deeply exhumed rocks, with peak pressures ranging to 10 kb, peak temperatures in excess of 750 °C, and widespread partial melting and stromatic migmatization, all related to Late Cretaceous to Paleocene tectonism. Overprinting the metamorphic core is a WNW-directed kilometer-scale shear zone that, together with the detachment fault that forms its roof, accommodated tens of kilometers of extensional displacement in mid- to late Cenozoic time, diachronously exhuming the terrain from mid-crustal depths by late Miocene time. In addition, the high-grade rocks are extensively intruded by one of the Nevada's most diverse suites of magmatic rocks, ranging in age from Archean to Miocene and in composition from mafic

to felsic. On the west flank of Clover Hill, a west-dipping detachment-fault system separates the high-grade metamorphic core from an overlying plexus of brittlely deformed, partly correlative but lower grade to non-metamorphosed Paleozoic rocks. In turn, a sequence of partly syntectonic volcanic and sedimentary rocks ranging in age from Eocene to Miocene structurally overlie the fault-bounded Paleozoic units. The Cenozoic sequence includes late Eocene and Oligocene ignimbrites and volcanoclastic rocks, Miocene sedimentary rocks and megabreccias, a Miocene rhyolite complex, and younger sedimentary rocks and vitric tuffs. The presence of the most distal northeasterly exposure of a key Oligocene volcanic marker, the 29 Ma tuff of Campbell Creek, suggests that a broad, low-relief (unfaulted) terrain was dissected by paleovalleys that extended at least 200 km to the west. Bracketed between the tuff of Campbell Creek and a 15.5 Ma tuffaceous sandstone at the base of the Miocene Humboldt Formation is a proximal sedimentary sequence known as the sedimentary sequence of Clover Creek that includes conglomerate, sedimentary breccia, sandstone, and megabreccia as well as intercalations of fossiliferous lacustrine strata. The megabreccias consist of unmetamorphosed mid-Paleozoic rocks (chiefly Upper Devonian Guilmette Formation) interpreted as rock-avalanche deposits shed from evolving normal-fault scarps inferred to have bounded the basin to the east. Disconformably overlying the sedimentary sequence of Clover Creek is a thick sequence of Miocene Humboldt Formation that is tilted steeply down against the detachment fault system, documenting large-scale displacement on the detachment system extending to at least as young ca. 9 Ma. Finally, bounding the range today on both east and west are large, normal-fault systems that were active in Quaternary time, including the Clover Hill fault, which may

represent a southerly extension of the blind fault that caused the 2008 M_w 6.0 Wells earthquake.

INTRODUCTION AND PREVIOUS WORK

The Welcome 7.5' quadrangle and part of the adjacent Wells 7.5' quadrangle, Elko County, Nevada, include the northern East Humboldt Range, Clover

Valley (a basin filled with Cenozoic sedimentary, volcanic and volcanoclastic rocks), and on the east, a north-trending line of hills including Clover Hill and the northern end of Signal Hill (figure 1) (Sharp, 1939a, 1940; Snelson, 1957). The East Humboldt Range (EHR) together with the Ruby Mountains to the south and the Wood Hills to the east, have gained widespread attention as a classic example of a Cordilleran metamorphic core

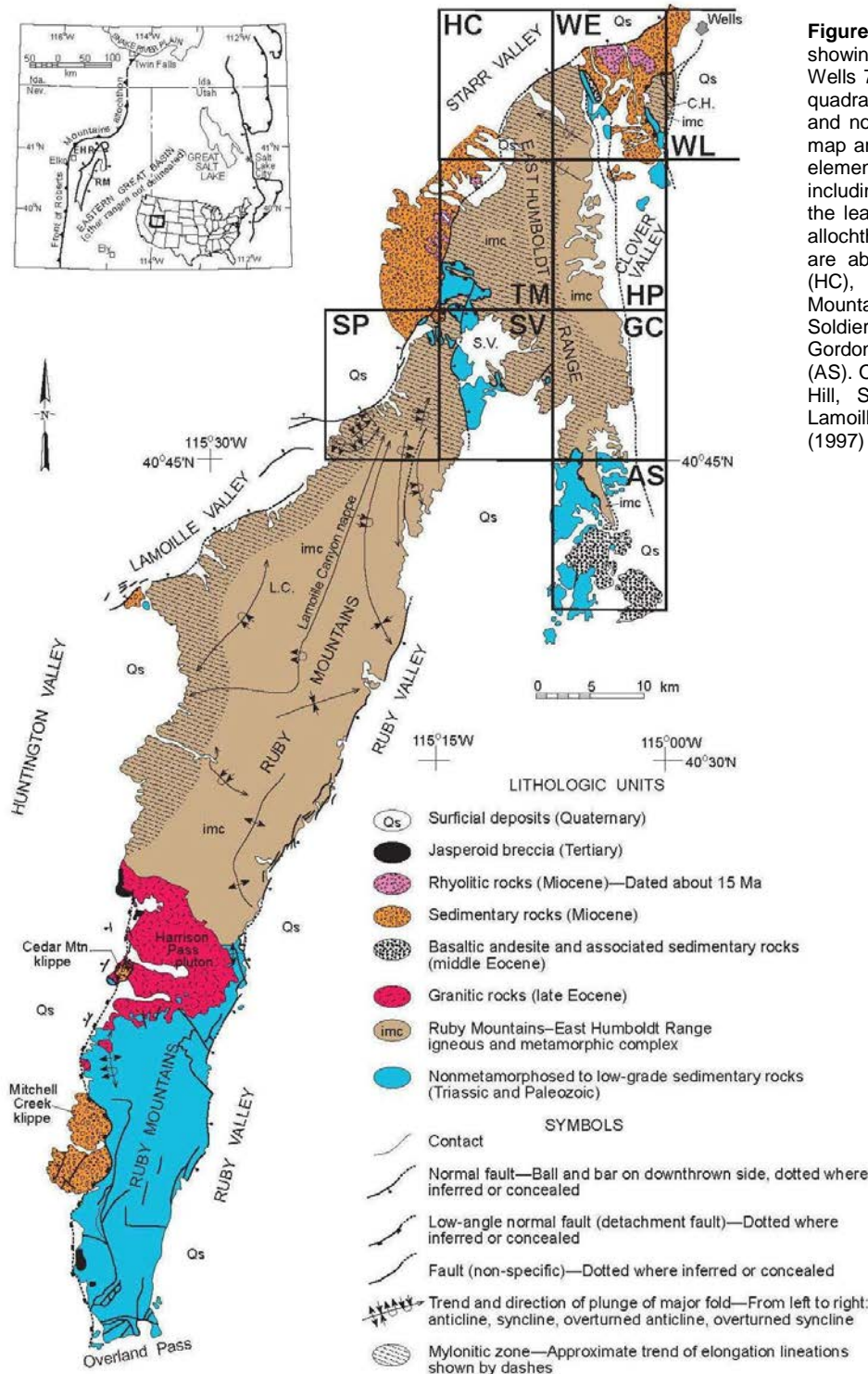


Figure 1. Generalized geologic map showing the location of the Welcome and Wells 7.5' quadrangles relative to other 7.5' quadrangles in the East Humboldt Range and northern Ruby Mountains. Inset shows map area in relation to other major tectonic elements of the western U.S. Cordillera, including the Sevier fold-and-thrust belt and the leading edge of the Roberts Mountains allochthon. The names of 7.5' quadrangles are abbreviated as follows: Herder Creek (HC), Welcome (WE), Wells (WL), Tent Mountain (TM), Humboldt Peak (HP), Soldier Peak (SP), Secret Valley (SV), Gordon Creek (GC), and Arizona Springs (AS). Other abbreviations are: C.H. – Clover Hill, S.V. – Secret Valley, and L.C. – Lamoille Canyon. Modified from Snoke et al. (1997) and Colgan et al. (2010).

complex (Howard, 1980; Snoke, 1980; Snoke and Miller, 1988; Snoke et al., 1990; McGrew, 1992; Snoke et al., 1997; McGrew et al., 2000; Sullivan and Snoke, 2007).

The EHR forms a high, narrow, north-trending horst block bounded both east and west by Quaternary normal faults (Sharp, 1939a; Wesnousky and Willoughby, 2003; Ramelli and dePolo, 2011). Gently westward-dipping metamorphic foliations throughout the lower plate suggest that the range is tilted to the west.

With a ridgeline cresting above 3000 m elevation for most of its length, the EHR was high enough to experience extensive Pleistocene glaciation, which produced some of its most noteworthy geographic features, including Chimney Rock and a series of deeply incised cirque basins that commonly host cirque lakes, such as Smith Lake and Angel Lake (figure 2a). Accordingly, the EHR, and in particular the Angel Lake cirque in the Welcome quadrangle, have also received considerable attention for the records they preserve of Quaternary climatic change (Sharp, 1938, Wayne, 1984, Munroe and Laabs, 2011).

As outlined in the *Structural Architecture* section, the Welcome quadrangle and an adjacent part of the Wells quadrangle expose a dissected natural cross section representing structural levels ranging from deep-crustal gneissic rocks (including the only exposures of Archean basement in Nevada) to Quaternary basin fill cut by active normal faults. As such, this map area exposes critical relationships for reconstructing the history and architecture of the crust of the northeastern Great Basin.

The earliest systematic reports of the geology of the EHR date from the 40th Parallel Survey led by Clarence King (1878). It was later the focus of early studies on Basin and Range structure and geomorphology (Sharp, 1939a, 1940). Prior to our study, the general geology of the EHR was mapped by Snelson (1957) and parts of the Humboldt Peak and Welcome quadrangles were mapped by Lush (1982) at 1:24,000 scale. Several field-trip guides have summarized various aspects of the geology of the Welcome and westernmost part of the Wells quadrangles (e.g., Snoke et al., 1997, Henry et al., 2011, Munroe and Laabs, 2011).

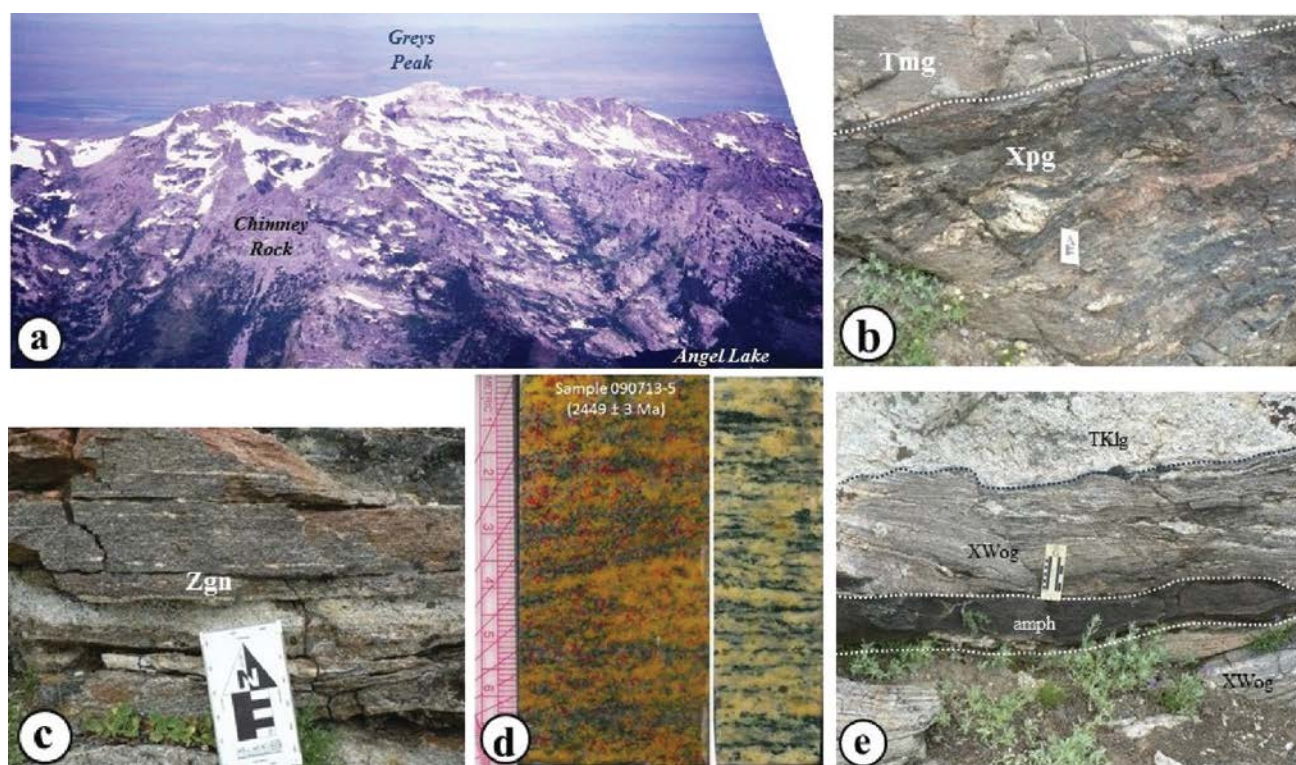


Figure 2. Photographs of field relationships. (a) East face of the northern EHR in the Welcome quadrangle. Major landmarks are labeled – Chimney Rock, Greys Peak, and Angel Lake. (b) Migmatitic biotite-sillimanite schist characteristic of the paragneiss of Greys Peak. Note folding of leucosomes and local offsets by normal-sense shear bands. 29 Ma biotite monzogranitic orthogneiss at top of photo is slightly discordant. (c) Outcrop photo of feldspathic biotite metaquartzite (probable McCoy Creek Group in the paragneiss of Greys Peak) forming an annealed mylonite near sample locality 4134-23 in the contact zone with the metamorphosed Cambrian to Mississippian(?) undivided unit. (d) Hand sample photo of sample 090713-5, which yielded an early Paleoproterozoic SHRIMP-RG U-Pb zircon age of 2449 ± 3 Ma (Premo and McGrew). The surface, stained for K-feldspar, was cut perpendicular to lineation, whereas the unstained surface was cut perpendicular to foliation and parallel to lineation. Ruler on left is in centimeters. (e) Typical outcrop of gray migmatitic biotite monzogranitic orthogneiss of Chimney rock illustrating characteristic striped appearance (central and lower part of photo) with a layer of amphibolite (middle of photo) and a thick layer of younger pegmatite (top of photo).

STRUCTURAL ARCHITECTURE

Several major features dominate the tectonic architecture of the EHR. As noted above, the EHR forms a west-tilted horst block bounded on both the east and the west by major normal fault systems (Sharp, 1939a, 1940). The steep eastern flank of the range exposes a natural cross section through migmatitic upper amphibolite-facies rocks representing middle and deep-crustal levels, whereas the western flank of the range forms a dip slope on the gently west-dipping Ruby Mountains-East Humboldt Range (RM-EHR) mylonitic shear zone (figure 1) (Hurlow, 1987). From north-to-south, the range is broadly arched with the deepest structural levels in the center of the range in the vicinity of Lizzies Basin in the Humboldt Peak quadrangle. The Welcome quadrangle covers the northern end of the range, which is dominated by a large, southward-closing recumbent isoclinal fold, the Winchell Lake fold-nappe (WLN) described in greater detail below (cross section A–A'). Maximum pressures during Late Cretaceous metamorphism ranged up to ~10 kb indicating that these rocks were exhumed from the deepest crustal levels observed anywhere in Nevada (McGrew et al., 2000; Hallett, 2012; Hallett and Spear, 2014). WNW-directed mylonitic fabrics overprint these rocks with increasing intensity at higher structural levels, but there is no sharply defined base to the mylonitic shear zone. However, the mylonitic character of the gneisses diminishes greatly with depth and there is a reversal in bulk shear-sense from WNW-directed, normal-sense shear at higher structural levels to mostly ESE-directed normal-sense shear at deeper structural levels (McGrew, 1992).

The core of the WLN is exposed in the cirque wall above Angel Lake where it consists of the Paleoproterozoic to Neoproterozoic(?) paragneiss of Angel Lake. This unit is in turn enfolded by the Paleoproterozoic to Neoproterozoic orthogneiss of Chimney Rock, which is extensively exposed in a belt extending from Smith Lake to the south side of Chimney Rock (figure 2a) (Lush et al., 1988; Premo et al., 2008; McGrew and Snoke, 2010; Premo et al., 2010; McGrew and Premo, 2011; Premo et al., 2014). Folded around the Neoproterozoic to Paleoproterozoic paragneiss and orthogneiss is the paragneiss of Greys Peak, a sequence inferred to be derived from Neoproterozoic and Paleoproterozoic strata. It wraps around the closure of the WLN near the northwestern corner of the Humboldt Peak quadrangle. Collectively, the Neoproterozoic to Paleoproterozoic rocks will be referred to as the *gneiss complex of Angel Lake*. The stratigraphic assignments suggest that the rocks face stratigraphically outward from the core of the WLN.

Folded around the gneiss complex of Angel Lake is a sequence of quartzite, pelitic schist, and marble interpreted to represent a profoundly attenuated, multiply metamorphosed and polyphase-deformed section of

Neoproterozoic and Paleozoic (miogeoclinal) sequence of the eastern Great Basin. Curiously, the inferred stratigraphic facing direction of this sequence is inward toward the outward-facing Precambrian rocks in the core of the fold-nappe. The gneiss complex of Angel Lake faces outward as would be expected for an anticlinal fold; however, the metamorphosed miogeoclinal sequence faces inward toward the core of the fold, as would be expected for a syncline. This perplexing structural relationship is discussed in greater detail in the *Structural Analysis* section, but in any interpretation it requires a major pre-metamorphic, pre-folding, low-angle tectonic contact between the miogeoclinal sequence and the gneiss complex of Angel Lake. At least one older generation of isoclinal folds are also refolded by the WLN, further testifying to a complex history of large-scale tectonism before Late Cretaceous emplacement of the WLN (McGrew, 1992).

The base of the WLN is marked by an inferred pre-metamorphic tectonic slide that emplaces it over a still deeper sequence of inferred miogeoclinal metasedimentary rocks and an underlying sequence of quartzite, pelitic schist, and subordinate marble here referred to as the *Lizzies Basin block*. Only the northernmost exposures of the Lizzies Basin block are observed in the Welcome quadrangle, at elevations below 8800 ft (2680 m) in section 16 near the southern edge of the quadrangle. The paragneiss sequence forming the deepest structural levels of the Lizzies Basin block correlates at least in part with Neoproterozoic to Lower Cambrian McCoy Creek Group and Prospect Mountain Quartzite. At the deepest structural levels on the east flank of the range, wholesale migmatization (67–90% leucogranite) commonly obliterates the last vestiges of original stratigraphic relationships. Intruding the Lizzies Basin block and the tectonic slides that bound it is a thick hornblende-biotite quartz diorite sheet that intrudes into the lower limb of the WLN at the base of Chimney Rock, thus cutting the basal tectonic slide of the WLN which therefore must predate the 40 Ma age of the quartz diorite (Wright and Snoke, 1993).

Along the east flank of the EHR and faulted down against the high-grade terrain described above is a NNW-trending belt of normal fault-bounded Mississippian to Permian sedimentary rocks. A broad mantle of Quaternary glacial deposits along the east flank of the range commonly mantles and hides the fault contact between these sedimentary rocks and the high-grade core. Finally, paralleling the EHR to the east is a smaller west-tilted horst block forming a line of hills, the largest of which is Clover Hill in the easternmost Welcome quadrangle extending into the western part of the adjacent Wells quadrangle. The rocks in Clover Hill correlate with high structural levels in the EHR, and the down-dropped half-graben between the two affords a unique opportunity to assess the structural relationship between the brittlely extended Paleozoic to Neogene cover sequence and the underlying mylonitic zone and

metamorphic core. Like upper levels of the adjacent EHR, kinematic indicators in the Clover Hill mylonites record WNW-directed normal-sense shear (Snoko, 1992). A gently, west-dipping detachment-fault system separates the underlying mylonitic to cataclastically deformed metamorphic rocks from an overlying series of fault-bounded slices of progressively younger and lower grade metasedimentary rocks along the northern, western, and southwestern flanks of the gently domed Clover Hill (Snoko, 1992). We correlate this detachment system with the Ruby Mountains-East Humboldt Range (RM-EHR) detachment-fault system, which extends approximately 150 km along the west flank of the RM-EHR metamorphic core complex.

At the northern end of the EHR, the normal fault that delineates the western side of the range arcs northeastward, dropping the Marys River basin (known as Starr Valley in this area) down to the northwest. This fault system is marked by well-developed Quaternary fault scarps extending ~75 km along strike (Wesnousky and Willoughby, 2003). Although Wesnousky and Willoughby refer to this fault as the RM-EHR normal fault, we seek to avoid confusion with the older RM-EHR detachment fault by following the prior usage of Mueller and Snoko (1992a) who considered this fault to be part of the Marys River fault system. In the Welcome quadrangle, the Marys River fault system truncates the range-bounding fault system on the east side of the EHR. Wesnousky and Willoughby (2003) estimated Quaternary slip rates on the Marys River fault system at 0.06–0.13 mm/yr, with a recurrence interval between 5000 and 40,000 years. The last major earthquake was bracketed between 4800 and 7600 BP (Wesnousky and Willoughby, 2003).

No detailed neotectonic study has yet been conducted of the eastern range-front fault system, but we interpret that the range-front fault cuts an Angel Lake stage glacial moraine forming a prominent ravine along North Fork Angel Creek above 7350 ft (2240 m) elevation at 41° 01' 45.7" N, 115° 03' 52.5" W. Wayne (1984) correlates the Angel Lake stage with the last glacial maximum at approximately 22,000 BP (correlating to the Pinedale glaciation of the Rocky Mountains or the Late Wisconsin Stage of the continental interior). Dohrenwend et al. (1991) infer that the Clover Hill fault juxtaposes Quaternary older alluvium against bedrock based on photogeologic reconnaissance. Henry and Colgan (2011) argue that the Clover Valley fault projects northward into the blind Town Creek Flat basin fault that produced the M_w 6.0 Wells earthquake on February 21, 2008. Taken together, these relationships suggest that an appreciable seismic risk surrounds the EHR, albeit with a long recurrence interval, on the order of thousands or tens of thousands of years.

DISCUSSION OF MAP UNITS

Introduction

As outlined above, rock units within the Welcome quadrangle range from Archean to Holocene in age, with the crest of the range in the western half of the quadrangle consisting mostly of high-grade metamorphic and associated igneous rocks, whereas the eastern flank of the range and adjoining basin consist of down-faulted Paleozoic sedimentary rocks and Cenozoic sedimentary and volcanic rocks, in part covered by unconsolidated late Cenozoic glacial, colluvial, alluvial fan, and active fluvial deposits. Clover Hill on the eastern side of the Welcome quadrangle and extending into the adjacent Wells quadrangle is a small horst-block of high-grade metamorphic footwall rocks inferred to correlate up-dip with the uppermost structural levels of the metamorphic core exposed in the main range of the EHR to the west.

Due to high-grade metamorphism, migmatization, extreme plastic attenuation of units, and multiple phases of deformation, understanding the original character and correlation of protoliths in the metamorphic core of the EHR poses a challenge. Nevertheless, some rock units can be traced southward into a non-migmatitic and lower grade terrain in the southeastern EHR (Gordon Creek and Arizona Spring quadrangles) (Taylor, 1984; Snoko et al., 1997; Sicard, 2012; Sicard and Snoko, unpublished data) where the stratigraphic sequence resembles the metamorphosed Paleozoic miogeoclinal sequence of the Wood Hills to the east (Thorman, 1970). Using a similar approach, Howard (1971) also concluded that the rocks of the northern Ruby Mountains correlate with stratigraphic formations of the Neoproterozoic to Upper Devonian miogeoclinal sequence.

The gross stratigraphic architecture of the miogeocline can be recognized even in the highest grade rocks of the EHR. In broad outline this sequence consists of a basal unit of quartzite and schist inferred to correlate with the Neoproterozoic McCoy Creek Group and overlying Lower Cambrian Prospect Mountain Quartzite, an overlying sequence of calcite marble (Cambrian to Ordovician), a distinctive thin, white metaquartzite (Ordovician Eureka Quartzite), an overlying sequence of dolomitic marble (Devonian to Ordovician), a younger graphitic calcite marble unit (Upper Devonian Guilmette Formation), a unit of graphitic schist that may correlate with the Mississippian to Devonian Pilot Shale, and additional calcite marble (presumably Mississippian Joana limestone and possibly Tripon Pass formation). Although the Pilot Shale has not been reported from either the Wood Hills or northern Ruby Mountains, multiply deformed Pilot Shale (crenulated phyllite and intercalated meta-limestone) has also been mapped in the footwall of the detachment-fault system in the southern EHR in the Arizona Spring quadrangle immediately

Table 1. Mineral Abbreviations

Mineral	Abbreviation	Mineral	Abbreviation	Mineral	Abbreviation
Allanite	aln	Diopside	di	Opaque phases	opq
Amphibole	amph	Epidote	ep	Phlogopite	phl
Andalusite	and	Forsterite	fo	Plagioclase	pl
Anorthite	an	Garnet	gt	Potassium Feldspar	Ksp
Apatite	ap	Graphite	gr	Quartz	qz
Biotite	bt	Grossular	grs	Rutile	ru
Calcite	cc	Hematite	hem	Scapolite	scap
Clinopyroxene	cpx	Hornblende	hb	Sillimanite	sill
Clinozoisite	czo	Ilmenite	ilm	Staurolite	st
Cordierite	crd	Kyanite	ky	Titanite	ttn
Corundum	crn	Magnetite	mt	Tremolite	tr
Chlorite	chl	Monazite	mz	Zircon	zr
		Muscovite	mu		

above metamorphosed Guilmette Formation (Taylor, 1984).

In contrast with either the Ruby Mountains or Wood Hills, the northern EHR also exposes demonstrably older rocks in the Precambrian gneiss complex of Angel Lake occupying the core of the WLN (figure 2). As elaborated below, recent and continuing new work applying U-Pb SHRIMP-RG zircon geochronology to this sequence has significantly enhanced our understanding of the age relationships and potential regional correlations and tectonic significance of these units (Metcalfe and Drew, 2011; Premo et al., 2008, 2010; McGrew and Snoko, 2010; McGrew and Premo, 2011; Premo et al, 2014).

Metamorphosed Mississippian to Neoproterozoic(?) rock units

Paragneiss of Angel Lake (Paleoproterozoic to Neoproterozoic?)

Field Description and Petrography: Occupying the core of the WLN in the central part of the Angel Lake cirque, the paragneiss of Angel Lake (**XWpg**) includes migmatitic biotite and biotite-sillimanite schist (rarely containing garnet) (figure 2b); micaceous quartzofeldspathic paragneiss; rare quartzite; and localized sheets, pods, and other small bodies of amphibolite and garnet amphibolite interpreted as metamorphosed mafic intrusions. Garnet where present is commonly partly to wholly replaced by symplectites of pl + bt (in schist) or pl + hb (in amphibolite), indicating a decompressional $P-T$ path. (Mineral abbreviations used throughout this report are summarized in table 1). This map unit is distinguished by the paucity of quartzite, the absence of marble, and the amphibolite bodies. The biotite-sillimanite schist is intensely migmatized, commonly containing >33% leucosome (figure 2b). Metapsammitic paragneiss commonly contains 60–80% quartz, 10–20% biotite, 5–15% feldspar, and <4% each of sillimanite and/or muscovite. Likely these rocks represent an immature original sedimentary sequence, such as graywacke. Quartz is coarse grained (600–2000 μm), although it

commonly shows coarse subgrain polygonization and dynamic recrystallization near the edges of grains. Where surrounded by quartz, feldspar grains typically show little to no evidence of crystal-plastic strain, the strain being partitioned primarily into the surrounding quartz matrix, but more feldspathic components of the rock show undulose extinction and coarse subgrain polygonization of feldspars as well as quartz.

Geochronology and Correlation: Recently obtained SHRIMP-RG U-Pb results from the paragneiss of Angel Lake record Archean to early Paleoproterozoic ages on detrital zircon, but the details of the age relationships vary (McGrew and Premo, 2011; Premo et al., 2014). In general, the zircon age systematics show a nearly unimodal provenance age of ~2550 Ma, but with minimum provenance ages as young as ~2450 Ma in some samples, and with maximum ages represented by two analyses at 3340 Ma and 3740 Ma, respectively (Premo et al., 2014). In general, these age relationships strikingly resemble those for the orthogneiss of Chimney Rock described below, suggesting that the orthogneiss may have been a dominant proximal source for the paragneiss. However, the rare occurrence of much older grains suggests a distal link to ancient crust, most reasonably the Archean Wyoming province. Finally, metamorphic rims record two distinct episodes of secondary zircon growth, one at ~1770 Ma and the final phase at 70 to 85 Ma. Thus, the age of the original sediment can be bracketed between the youngest detrital zircon population (~2450 Ma) and the oldest secondary zircon overgrowths, ~ 1770 Ma. A few samples lack the 2450 Ma zircon population so a youngest Neoproterozoic depositional age for part of the sequence remains possible.

Rocks of Neoproterozoic to early Paleoproterozoic age are not exposed elsewhere in Nevada, so the outcrops in the Welcome quadrangle represent the farthest southwest exposures of Archean to early Paleoproterozoic basement in North America. The nearest exposures of Precambrian basement rocks occur in the Albion-Raft River-Grouse Creek metamorphic core complex of northwestern Utah and southeastern Idaho and in Utah's

Farmington Canyon Complex exposed at Antelope Island and along the Wasatch mountain front near Salt Lake City and Ogden. In the Albion and Raft River Mountains a potentially correlative metasedimentary sequence consisting of muscovite-biotite-quartz schist, plagioclase-quartz-biotite schist, and uncommon quartzite is known as the Older Schist (Compton, 1972, 1975; Compton et al., 1977). Both Armstrong (1968) and Compton et al. (1977) interpret these metasedimentary rocks as country rock to Neoproterozoic granitic to granodioritic orthogneiss of the Green Creek Complex (Compton et al., 1977; Strickland et al., 2011).

The Farmington Canyon Complex exposes a suite of metasedimentary rocks broadly resembling the paragneiss of Angel Lake and consisting of biotite-feldspar-quartz gneiss, biotite and biotite-sillimanite schist, uncommon quartzite, local small bodies of amphibolite, and rare calc-silicate rock, with all of the above rock types grading northward into migmatites and ultimately into quartz monzonitic orthogneiss (Eardley and Hatch, 1940; Bryant, 1988; Yonkee et al., 2000). Paleoproterozoic upper amphibolite- to granulite-facies metamorphism strongly disturbed U-Pb zircon age systematics in the Farmington Canyon Complex at ~1670 Ma, approximately 100 m.y. later than the secondary zircon growth that has thus far been documented in the gneiss complex of Angel Lake (Mueller et al., 2011; Premo et al., 2014).

Paragneiss of Greys Peak (Neoproterozoic to Paleoproterozoic)

Field description and petrography: The paragneiss of Greys Peak (**ZXpg**) typically consists mostly of micaceous feldspathic metaquartzite (figure 2c) and metapsammitic paragneiss, biotite-sillimanite schist (locally with garnet), and widespread but volumetrically small meter-scale layers and boudins of melanocratic orthoamphibolite and garnet amphibolite. The paragneiss is migmatitic throughout, but on the upper limb of the WLN it commonly contains <33% leucogranite, whereas on the lower limb of the fold-nappe the percentage of leucogranite commonly exceeds 50%. More pelitic or feldspathic components of the unit tend to host a higher percentage of leucogranite than do more quartz-rich horizons on both limbs of the fold. Like other units in the northern EHR, the paragneiss of Greys Peak is undoubtedly profoundly ductilely attenuated relative to original stratigraphic thickness, but structural thicknesses in the range of 30–60 m are characteristic from the Angel Lake cirque southward. However, on the upper limb of the fold-nappe above Smith Lake the structural thickness abruptly increases to ~300 m and in the same area pale green metaquartzite colored by chromian mica (fuchsite) joins the lithologic assemblage along with more extensive outcrops of cleaner metaquartzite, including some pure white, vitreous metaquartzite. Although a contact was not mappable, we suspect that the impure

Neoproterozoic unit (possibly basal McCoy Creek formation) may unconformably overlie an older, possibly Paleoproterozoic sequence in this area, analogous to the Huntsville sequence (McCoy Creek equivalent) which unconformably overlies the Paleoproterozoic–Neoproterozoic Facer Formation in the hanging wall of the Willard thrust in the Wasatch mountains between Brigham City and Ogden, Utah (Crittenden and Sorenson, 1980; P.K. Link, personal comm., 2013). Supporting this inference, the fuchsite quartzite yields an Archean detrital zircon suite lacking any Grenville-aged detritus (Premo et al., 2014).

Structural Relationships: The folded contact separating the paragneiss of Greys Peak from the undivided calcite and dolomitic marble unit (**MCmu**) is inferred to be tectonic because the stratigraphic sequence is out of order. Supporting this inference, some rocks near the contact show a distinctive, finely foliated, ribbon-like character suggestive of an annealed mylonite (figure 2c). The opposite contact of this unit with the orthogneiss of Chimney Rock could be another premetamorphic tectonic contact or it could be unconformable.

Geochronology and Correlation: The allochthonous character of the Angel Lake gneiss complex combined with the lithologic contrasts identified above originally led Lush et al. (1988) and McGrew (1992) to infer an older, Paleoproterozoic age for the paragneiss of Greys Peak. However, new U-Pb SHRIMP-RG dating of the mostly well-rounded detrital zircon grains from this sequence yields nearly concordant ages ranging from 880 Ma to 1880 Ma (W. R. Premo, personal comm., 2013), thus definitively establishing a Neoproterozoic or younger age. The presence of well-developed Grenville-aged peaks in these samples argues against a Cambrian or younger age as the supply of Grenville-aged zircons to the western Cordilleran continental margin appears to have been choked off by the Sauk I transgression (Link et al., 2011). Furthermore, the strong lithologic contrast between this impure meta-clastic sequence and the carbonate-dominated Paleozoic sedimentary rocks of the eastern Great Basin leads us to infer a Neoproterozoic age and favors correlation with the McCoy Creek Group of the eastern Great Basin. However, based on the lithologic contrasts noted above, we suggest that this sequence may include deeper levels in the McCoy Creek Group than exposed elsewhere in northeastern Nevada, and may also include unconformably underlying Paleoproterozoic–Neoproterozoic rocks correlative with the Facer Formation as argued above.

The McCoy Creek Group has been described from a variety of lower metamorphic grade occurrences throughout the northeastern Great Basin, including the Bull Run Mountains and Copper Mountains to the north and northwest (Ehman and Clark, 1990; McGrew,

unpublished data); Albion and Pilot Mountains to the northeast and east (Woodward, 1967; Miller, 1983; 1984); and Cherry Creek, Egan, Schell Creek, Snake and Deep Creek Ranges to the south and southeast (Misch and Hazzard, 1962; Woodward, 1965; Rodgers, 1984; Schneck, 1986). Although there is considerable facies variability between these occurrences, in general the McCoy Creek Group consists of a thick sequence of alternating feldspathic metaquartzite, metasiltstone, metapelitic rocks, metaconglomerate (possibly representing diamictite) and subsidiary marble and calc-silicate rock, with the entire package containing variable volumes of metamorphosed mafic igneous rock. A widespread sequence of calc-silicate rock and/or impure marble commonly occurs in the upper part of the McCoy Creek Group, but this distinctive marker is absent in the paragneiss of Greys Peak, lending credence to the inference that the paragneiss of Greys Peak may represent deeper stratigraphic levels. In addition, the rare but distinctive pale green fuchsitic metaquartzite resembles rock types reported from the Albion-Raft River-Grouse Creek metamorphic core complex in northwestern Utah and southeastern Idaho, which may also be partly Neoproterozoic and partly Paleoproterozoic in age based on detrital zircon geochronology (Armstrong, 1968; Compton, 1972; Link and Johnston, 2008; Strickland et al., 2011). The Albion-Raft River-Grouse Creek sequence includes metaquartzite (including pale green fuchsitic metaquartzite), schist, metapsammite, and meta-tuff with inferred metabasite intrusions, and like the paragneiss of Greys Peak it lacks significant marble or calc-silicate rock.

Metaconglomerate and metaquartzite unit (Neoproterozoic)

A mappable lens of mylonitic quartz-pebble metaconglomerate and impure metaquartzite (**Zc**) occurs surrounded by the **Mcmu** unit on the upper part of the east face of Clover Hill. The off-white to light gray clasts in the metaconglomerate appear to be derived from original quartz or quartzite pebbles rather than chert. This unit is correlated with Units G or F of the McCoy Creek Group (Miller, 1983).

Metamorphosed Prospect Mountain and McCoy Creek Group (Cambrian to Neoproterozoic, undivided)

Field Description and Petrography: The metamorphosed Prospect Mountain Quartzite consists predominantly of metaquartzite and micaceous feldspathic metaquartzite, commonly with micaceous partings and with subordinate biotite-muscovite and biotite-sillimanite-garnet schist and rare calc-silicate paragneiss and amphibolite. This unit (**Zpm**) mostly is correlated to the Prospect Mountain Quartzite but may

locally include elements of the Neoproterozoic McCoy Creek Group. This composite unit is commonly migmatitic, with more pelitic and/or feldspathic horizons harboring a higher percentage of leucosome than do purer metaquartzite layers. This suggests that a considerable fraction of the leucogranitic rock is locally derived or only slightly remobilized. Leucosomes are typically stromatic, being segregated into pods and sheets parallel to bulk foliation with concentrated biotite and sillimanite commonly forming selvages at the boundaries. The proportion of leucogranitic rock also increases as a function of structural depth, with the lower limb of the Winchell Lake fold-nappe hosting far more leucogranitic rock than the upper limb. Characteristic mineral assemblages in pelitic schist horizons include biotite, sillimanite, relict kyanite, garnet, plagioclase, sparse muscovite or locally K-feldspar, and quartz. Kyanite is found only on the upper limb of the WLN, and is everywhere thickly mantled by sillimanite in the EHR, although it is nearly pristine on Clover Hill (Snoke, 1992). Accessory phases commonly include rutile (typically as inclusions in garnet), ilmenite, and titanite.

Correlation: Originally named by Hague (1883) for exposures on Prospect Peak southwest of Eureka, Nevada, the Prospect Mountain Quartzite crops out throughout the eastern Great Basin, and is considered to be mostly Early Cambrian in age, although it likely extends into the late Neoproterozoic. In areas of lower metamorphic grade such as the Schell Creek Range, it commonly consists of slabby to massive, commonly cross-bedded medium- to coarse-grained sandstone with 80–90% quartz and 10–20% feldspar, rare conglomeratic horizons, and with shaly or argillaceous horizons ranging from partings on bedding surfaces to layers no more than a few meters thick composing <5% of the sequence (e.g., Misch and Hazzard, 1962). In the Ruby Mountains it consists of foliated brown to gray-weathering coarse-grained feldspathic metaquartzite with muscovite, biotite, sparse hematite or locally magnetite, and sillimanite (Sharp, 1942; Howard, 1971; Hudec, 1990). The full stratigraphic thickness of the Prospect Mountain Quartzite is rarely preserved, but it is commonly at least 450 m (1500 ft) thick. In the central Ruby Mountains Hudec (1990) reports a relatively little deformed partial section with a structural thickness of 1220 m (4000 ft thick). As noted above, the McCoy Creek Group crops out widely throughout northeastern Nevada forming a thick sequence of alternating feldspathic metaquartzite, metasiltstone, metapelitic rocks, metaconglomerate (possibly representing diamictite) and subsidiary marble and calc-silicate rock, with deeper stratigraphic levels intruded by variable amounts of metamorphosed mafic igneous rock. In its type area in the Schell Creek Range, the McCoy Creek Group is nearly 2700 m thick (Misch and Hazzard, 1962).

Calcite and dolomite marble with calc-silicate paragneiss, calc-schist, and white metaquartzite (Mississippian to Cambrian, undivided)

Overlying the Prospect Mountain Quartzite is a sequence dominated by calcite and dolomite marble but also including abundant calc-silicate paragneiss, calc-schist, and white metaquartzite (**M€mu**). Together with the underlying Prospect Mountain Quartzite these units are interpreted to correlate with the Mississippian to Cambrian carbonate-rich shelf sequence of the eastern Great Basin (Howard, 1971). However, in contrast to the Ruby Mountains and Wood Hills, this sequence in the northern EHR includes units that we correlate with metamorphosed Pilot Shale and overlying metacarbonate rocks. Hence we extend its range into the Mississippian. Where mappable at 1:24,000 scale, this unit has been subdivided as itemized below, but due to profound structural disruption, extreme ductile attenuation, and megaboudinage of units, it has commonly been impossible to break out the individual components of the sequence, in which instances it was mapped as Mississippian to Cambrian marble, undivided.

Marble of Verdi Peak (Ordovician to Cambrian, undivided)

Field description and petrography: Situated between the metamorphosed Prospect Mountain Quartzite and the distinctive, pure white, metamorphosed Eureka Quartzite is a sequence consisting of coarse-grained, white to pale gray, locally graphitic, muscovite- and/or phlogopite-bearing calcite and calc-silicate marble; yellow-brown weathering metadolomite; calc-silicate paragneiss; localized calcareous schist; and white metaquartzite (**O€m**). In the Welcome quadrangle, characteristic mineral assemblages in the marble of Verdi Peak include $cc \pm dol \pm plag \pm di \pm tr \pm ep \pm gt \pm phl \pm ttn \pm scap$ (Peters and Wickham, 1994). Like all units in the EHR the marble of Verdi Peak commonly hosts sheets or boudins of coarse-grained muscovite \pm biotite leucogranitic or pegmatitic orthogneiss. However, the proportions of leucogranitic rock are dramatically less than in adjacent metamorphosed Prospect Mountain Quartzite (commonly <10% leucogranite in the marble versus >30% in meta-clastic rocks).

Correlation: The presence of metamorphosed miogeoclinal rocks in the RM-EHR-Wood Hills metamorphic core complex was first recognized in the somewhat lower grade and nonmigmatitic domain of the Wood Hills where metamorphosed fossils are locally preserved (Thorman, 1970). Howard (1971) subsequently extended the correlation to the higher grade, more structurally attenuated and disrupted rocks of the Ruby Mountains, where he described a sequence of calcite and dolomite marble with subsidiary

calcareous rock and schist that he correlated with Cambrian limestone and shale and the overlying Ordovician Pogonip Group. For this suite of rocks he adopted the name “marble of Verdi Peak” (Howard, 2000; Howard and MacCready, 2004), and we extend that usage here.

In eastern Elko County, McCollum and Miller (1990) systematized a nomenclature for the Upper Cambrian stratigraphy that, from base to top, includes the following: Toano Limestone (silty limestone and calcareous siltstone); Clifside Limestone (limestone and silty limestone); Morgan Pass Formation (shale and silty limestone); Decoy Limestone (massive, clean limestone); Shafter Formation (thin bedded silty limestone); Oasis Formation (limestone, dolomite, and calcareous siltstone); Dunderberg Shale (dark gray to black shale and argillaceous limestone grading upward into tan or olive shale with crinoidal limestone) (Walcott, 1908; Nolan et al., 1956); and Notch Peak Formation (limestone and dolostone with bedding-parallel stringers and lenses of chert) (Walcott, 1908). The overlying Pogonip Group (Nolan et al., 1956) is subdivided where possible into the following: Garden City Formation (argillaceous, nodular limestone) (Richardson, 1913); Kanosh Shale (dolomite and shaly or cherty limestone, locally with quartz arenite) (Hintze, 1951); Lehman Formation (limestone) (Hintze, 1951); Swan Peak Quartzite (Richardson, 1913); and Crystal Peak Dolomite (Webb, 1956). Camilleri (2010) subsequently extended this nomenclature to the greenschist-facies metamorphic rocks of the Pequop Mountains. In aggregate, the reference section through the Upper Cambrian stratigraphy in the Toano Range together with the Ordovician Pogonip Group has a thickness of nearly 4 km, whereas the correlative, greenschist-facies sequence in the Pequop Mountains has a moderately attenuated structural thickness of approximately 2440 m (8000 ft) (Camilleri, 2010). In contrast, in the Welcome quadrangle the marble of Verdi Peak is metamorphosed to upper amphibolite facies and profoundly ductilely attenuated to structural thicknesses of 20–60 m, just 1%–2.5% of the original stratigraphic thickness of the unmetamorphosed reference section. Large-scale boudinage and fold transposition render it impossible to subdivide the stratigraphy to the formation level.

Metamorphosed Eureka Quartzite (Ordovician)

In the Welcome quadrangle, the inferred Eureka Quartzite consists of 0–10 ft (0–3 m) of massive, coarsely recrystallized, exceptionally pure metaquartzite (**Oe**). Commonly vitreous gray on fresh fractures, it weathers to white. Locally it contains diopside and may have gray streaks due to the presence of sparse, disseminated graphite. Like other metamorphic rocks in the EHR, the metamorphosed Eureka Quartzite is profoundly plastically attenuated relative to original stratigraphic thickness.

In its unmetamorphosed state the Eureka Quartzite (Hague, 1883; Kirk, 1933) is a distinctive, widespread and commonly exceptionally pure quartz arenite that lies disconformably on Middle Ordovician Pogonip Group and is overlain by Upper Ordovician to Lower Devonian dolomitic units. Whereas the basal contact forms a widespread unconformity of regional significance, the upper contact is locally conformable and elsewhere disconformable (Nolan et al., 1956; Merriam, 1963). Accordingly, the thickness is highly variable, but most thickness estimates range between 200 and 1000 feet (60–300 m). In the southern Ruby Mountains the Eureka Quartzite is missing due to local stratigraphic disconformity, but farther north Howard (1971, 2000) reports a tectonically thinned section with 0–10 ft (0–3 m) of metamorphosed Eureka Quartzite similar to the northern EHR. The Wood Hills also hosts metamorphosed Eureka Quartzite ranging from 0 to 400 ft (130 m) thick due to intense plastic attenuation on fold limbs and thickening in the hinge zones of folds (Thorman, 1970; Camilleri, 2010). A similar section of thinned, metamorphosed Eureka Quartzite occurs in the Arizona Spring quadrangle of the southeastern EHR.

Dolomitic marble (Devonian to Ordovician, undivided)

The dolomitic marble unit (**DOd**) consists of white to dark gray, medium- to coarse-grained dolomitic marble with subordinate metapsammite and calc-silicate rock. Locally it also includes calcite marble that may correlate in part with the overlying Guilmette Formation. Due to metamorphic recrystallization and deformation, the dolomite cannot be subdivided to formation level, but in the unmetamorphosed reference section it is inferred to correlate with Ordovician to Silurian Fish Haven and Laketown Dolomites (Richardson, 1913); Silurian Roberts Mountain Formation and Devonian to Silurian Lone Mountain Dolomite (Merriam, 1940); and Devonian Sevy and Simonson Dolostone (Nolan, 1935). On the southwestern flank of Clover Hill, a fault-bounded slice of metadolomite and metasandstone occurs above mylonitic marble of the marble of Verdi Peak (**OCm**) and below unmetamorphosed Upper Devonian Guilmette Formation (**Dg**). The metadolomite is gray with a granoblastic texture and is typically brecciated. White metasandstone is interlayered with the metadolomite. These low-grade (greenschist-facies?) rocks are correlated with the Middle Devonian Simonson Dolostone. In the Pequop Mountains these units exhibit an aggregate thickness of approximately 3300 ft (1000 m) (Camilleri, 2010), but like other units in the northern EHR, profound plastic attenuation commonly reduces this unit to a structural thickness less than 120 ft (36 m), and in some localities it is missing altogether due to megaboudinage.

Metamorphosed Guilmette Formation (Upper Devonian)

In the high-grade core of the northern EHR, the metamorphosed Guilmette Formation consists of color-banded, commonly graphitic, fine- to medium-grained calcite ± dolomite marble overlying the inferred Devonian to Ordovician dolomitic marble sequence. However, where this lithologic type is highly metamorphosed it has been included with the undivided Mississippian to Cambrian unit (**MCmu**). Due to high-grade metamorphism and extensive structural complication, it is difficult to rule out the possibility that it could in part include marble derived either from the underlying Devonian to Ordovician sequence or even overlying metamorphosed Joana or Tripon Pass formations.

Graphitic schist and calcareous paragneiss (Mississippian to Upper Devonian?)

Field Description and petrography: This unit is well exposed only on the upper limb of the WLN, where it includes graphitic quartzo-feldspathic metapsammite, semi-pelitic schist, graphite-bearing pelitic schist, and graphite-bearing calc-silicate paragneiss, all containing abundant hematite and hence weathering rusty red-brown. Characteristic peak metamorphic assemblages in pelitic schist from this unit include $bt + sill + gt + ilm + plag + qz + ap + mnz + zrc + gr [+ melt]$ (McGrew et al., 2000; Hallett, 2012; Hallett and Spear, 2014). Also preserved is a relict, lower temperature, higher pressure subassemblage including $ky + st + ru + mnz$, with the kyanite occurring as large matrix porphyroblasts thickly mantled by sillimanite, and the staurolite and rutile preserved as rare inclusions in garnet.

Although this unit is typically migmatitic wherever it occurs, on the upper limb of the WLN it commonly hosts <25% leucosome and small leucogranitic bodies whereas the visually estimated proportion of leucogranite increases to >67% over a distance of <2 km as the unit is traced into the hinge zone of the fold (in the adjacent Humboldt Peak quadrangle). On the lower limb of the fold-nappe this unit does not exceed 5 m in thickness and is commonly observed only as rafts of rusty-weathering, graphitic biotite-rich melanosome suspended in small bodies of leucogranite several meters in size (McGrew et al., 2000).

Correlation: The graphitic schist unit most likely correlates with the Pilot Shale (Spencer, 1917). In the vicinity of the EHR, unmetamorphosed Pilot Shale has been mapped in the Ruby Mountains (Willden and Kistler, 1979), Spruce Mountain (Hope, 1972), the Pequop Mountains (Thorman, 1970; Camilleri, 2010), and on the east side of Signal Hill in the northeastern part of the Humboldt Peak quadrangle (Snelson, 1957; Lush, 1982). In these areas, it consists of thin- to medium-

bedded, light to dark gray or black carbonaceous shale and tan to olive-weathering shale and argillaceous limestone. In the southern Ruby Mountains near Overland Pass, the Pilot Shale ranges from 120–180 m (400–600 ft) in thickness, whereas in the Pequop Mountains, Thorman (1970) reports a thickness of approximately 155 m (500 ft). In the Welcome quadrangle, the graphitic schist sequence is typically ductilely attenuated to a structural thickness of 12–25 m (40–80 ft) on the upper limb of the WLN. In addition, metamorphosed Pilot Shale occurs in the southern EHR in the footwall of the detachment system, where it has been deformed and metamorphosed under greenschist-facies conditions (Taylor, 1984). If the correlation of the graphitic schist sequence with the Pilot Shale is correct, then the stratigraphically overlying marble would likely correspond to the Joana Limestone and perhaps the Tripon Pass Limestone (Spencer, 1917; Oversby, 1973). However, here the overlying marble unit has not been broken out from the undivided Mississippian to Cambrian marble unit (**M€mu**).

Unmetamorphosed Paleozoic Sedimentary Rocks

Introduction

The unmetamorphosed Paleozoic sedimentary rocks of the Welcome quadrangle are chiefly exposed in a north-northwest–striking belt of moderately to steeply east-dipping strata, subdivided by steeply dipping faults constituting part of the range-front normal-fault system. This fault-bounded stratigraphy includes: Mississippian Diamond Peak Formation, Pennsylvanian Ely Limestone, Lower Permian Pequop Formation, and Permian Murdock Mountain Formation. The Murdock Mountain Formation is in normal fault contact with middle Eocene rocks of the **Tvs** unit. This fault could be a faulted unconformity, and the offset does not have to be large. The Diamond Peak Formation is structurally above a series of thin, fault-bounded slices of metamorphosed Guilmette Formation, Devonian to Ordovician dolomitic marble, and Ordovician to Cambrian marble (marble of Verdi Peak).

Dolostone (Devonian to Silurian, undivided)

At the southern end of Clover Hill, an unmetamorphosed, composite dolostone unit (**DSd**) occurs as a fault slice between structurally higher, unmetamorphosed Upper Devonian Guilmette Formation (see below) and structurally lower Ordovician to Cambrian marble of Verdi Peak. The lithologic character of the undivided dolostone unit suggests that some elements of the Silurian Laketown Dolomite may be included in the unit. However, the bulk of the unit consists of Lower Devonian Sevy Dolomite and Middle

Devonian Simonson Dolostone (Lush, 1982). The same unit underlies most of Signal Hill, located immediately to the south, in the Humboldt Peak quadrangle (McGrew, in review). The lithotypes chiefly include: laminated black, fine- to medium-grained dolostone, thick-bedded medium- to dark-gray dolostone, and quartz sandstone (Lush, 1982). The unit is commonly brecciated and cemented by carbonate and/or siliceous matrix between the fragments.

Guilmette Formation (Upper Devonian)

Unmetamorphosed Guilmette Formation (**Dg**) occurs as a fault-bounded slice on the southwestern flank of Clover Hill (Lush, 1982). This rock unit consists of massively bedded to platy, dark gray limestone, which is highly veined by calcite. The unit is commonly brecciated, and, at some localities, bedding is difficult to recognize (Lush, 1982). The non-metamorphosed Guilmette Formation is commonly fossiliferous containing stromatoporoids, bryozoa, corals, crinoid debris, gastropods, and brachiopods (Snelson, 1957; Lush, 1982).

The megabreccia deposits in the Tertiary sedimentary sequence of Clover Creek are chiefly composed of brecciated Guilmette Formation, although a few megabreccias are brecciated gray sugary meta-dolostone with quartz meta-sandstone layers, correlated with the Middle Devonian Simonson Dolostone (see the section titled *Tertiary stratified rocks* for additional details on the megabreccia deposits).

Diamond Peak Formation (Mississippian)

The Mississippian Diamond Peak Formation (**Mdp**) consists of chert-pebble conglomerate, brown quartzite or sandstone, siltstone, shale, and gray limestone (Nolan et al., 1956). The chert clasts are multi-colored, chiefly black, gray, tan, or green. Thorman (1970) estimated the thickness of the Diamond Peak Formation to be 1350 ft (412 m) in the Wood Hills and 1190 ft (363 m) in the Pequop Mountains. With regard to the regional stratigraphy of northeast Nevada, the Mississippian Chainman Formation lies stratigraphically below the Diamond Peak Formation and is, in part, the lateral equivalent to it. However, the Chainman Formation is not exposed in the Welcome quadrangle.

Ely Limestone (Pennsylvanian)

The Ely Limestone, originally named and defined by Lawson (1906), was applied to massively bedded cherty limestones exposed in the Robinson mining district, White Pine County, Nevada. Steele (1960) restricted the Ely Limestone to Pennsylvanian age strata and named the overlying Permian limestone the Riepe Spring Limestone. He described the Pennsylvanian Ely Limestone as a sequence of alternating beds of resistant

thick-bedded limestone and slabby slope-forming limestones, yielding a bluff-and-bench topography. In the Welcome quadrangle, the Ely Limestone (**Pe**) is a ridge-forming, thick-bedded light olive gray to dark gray fine- to medium-grained limestone (Snelson, 1957). Olive gray to grayish black nodular and lenticular chert is common in the unit. Snelson (1957) reported two fossil collections from the Ely Limestone exposed in the map area. His locality A56 (see map for approximate location) yielded: *Cleiothyridina orbicularis*, *Dictyoclostus* sp., *Hustedia mormoni*, *Linoproductus* sp., *Marginifera M. haydenesis*, *Marginifera wabashensis*, *Neospirifer* n. sp., *Neospirifer triplicatus*, and *Triplophyllites* sp. From his locality N16 (see map for approximate location), he reported: *Cleiothyridina orbicularis*, *Composita* sp., *Derbya* sp., *Dictyoclostus?* sp., *Marginifera* cf. *M. muricatina*, *Neospirifer* sp.; a pectinoid; *Triplophyllites?* sp.; and trepostome bryozoans.

Pequop Formation of Steele (1960) (Lower Permian)

The name Pequop Formation was originally coined by Steele (1959) for a thick sequence of thin-bedded, fusulinid-bearing limestone exposed in the central Pequop Mountains, Nevada. This rock unit was formally named in Steele (1960). At the type locality according to Steele (1960, p. 106), the unit "...is composed of purplish-gray, irregularly bedded, platy, silty limestones with interbedded fusuline coquinas." This stratigraphic unit is Early Permian in age ranging from latest Wolfcampian to early Leonardian (Marcantel, 1975; Stevens, 1979) and is roughly equivalent to the Arcturus Formation (Lawson, 1906) of east-central Nevada.

Exposures of the Pequop Formation (**Pp**) in the Welcome quadrangle are part of the northwest-striking belt of unmetamorphosed Paleozoic rocks that form a fore-range immediately east of the main range of the EHR. The Pequop Formation is fault-bounded by Pennsylvanian Ely Limestone to the west and Lower to Upper Permian rocks of the Park City Group to the east. The dominant rock types in the Pequop Formation in the Welcome quadrangle are thin-bedded silty limestone to thick-bedded limestone and yellow-weathering, fine-grained calcareous sandstone. Fusulinid-rich coquina is scarce.

Snoke (1980, Appendix 1) reported fauna from this unit in the Secret Valley and Tent Mountain quadrangles, which yielded early Leonardian ages based on fusulinid fauna; e.g., *Pseudofusulina* sp. and *Parafusulina* sp.

Murdock Mountain Formation (Permian)

The Murdock Mountain Formation (Wardlaw et al., 1979) is a unit within the Park City Group, that is interpreted as a transitional facies between the Plympton Formation and the Rex Chert Member of the Phosphoria Formation. The Murdock Mountain Formation includes: dolomite with chert, bedded chert, fine-grained sandstone, and conglomerate (Wardlaw et al., 1979, their figure 5). The rocks mapped as Murdock Mountain Formation in the Welcome quadrangle consist chiefly of these rock types as well as gray limestone, suggesting that the mapped unit may include elements of the overlying Gerster Formation. In the Arizona Spring quadrangle (southeastern EHR), Taylor (1984) delineated the tripartite sequence of Kaibab Limestone, Plympton Formation, and Gerster Limestone as the Park City Group in that map area.

Tertiary stratified rocks

Introduction

Snelson (1957) mapped and studied the Tertiary rocks in the northeastern EHR and subdivided the Tertiary section into three mappable units: Clover Valley, Starr Valley, and Willow Creek units. The Clover Valley unit roughly equates to our Tertiary volcanic and sedimentary rocks (**Tvs**), whereas the Starr Valley unit includes the sedimentary sequence of Clover Creek (**Tcc**) and Humboldt Formation, Unit 1 (**Th₁**). The Willow Creek unit is equivalent to our Willow Creek rhyolite suite (**Tr₁**, **Tr₂**, **Trvb**, and **Tr₃**). Snelson (1957) also delineated a volcanic unit at the southern end of the EHR, which he referred to as the Warm Springs unit. This unit and the **Tvs** unit have been radiometrically dated by ⁴⁰Ar/³⁹Ar methods as middle to late Eocene and are considered part of the Northeast Nevada Volcanic Field (Brooks et al., 1995a, b).

Volcanic and sedimentary rocks (upper Oligocene and middle to upper Eocene)

The oldest exposed stratified Cenozoic rocks in the northeastern EHR form a heterogeneous sequence of volcanic, volcanoclastic, and epiclastic rocks (**Tvs**) in a north-northwest-striking band bounded by a composite contact that varies along strike from an unconformity to a high-angle normal fault of modest displacement. The **Tvs** unit is unconformably overlain by rocks of the sedimentary sequence of Clover Creek to the northeast. The **Tvs** unit consists of andesitic lava flows grading into flow breccia, rhyolitic lapilli tuff, volcanogenic diamictite, polymictic conglomerate and breccia (figure 3a), and intercalated scarce lenses of sandstone.

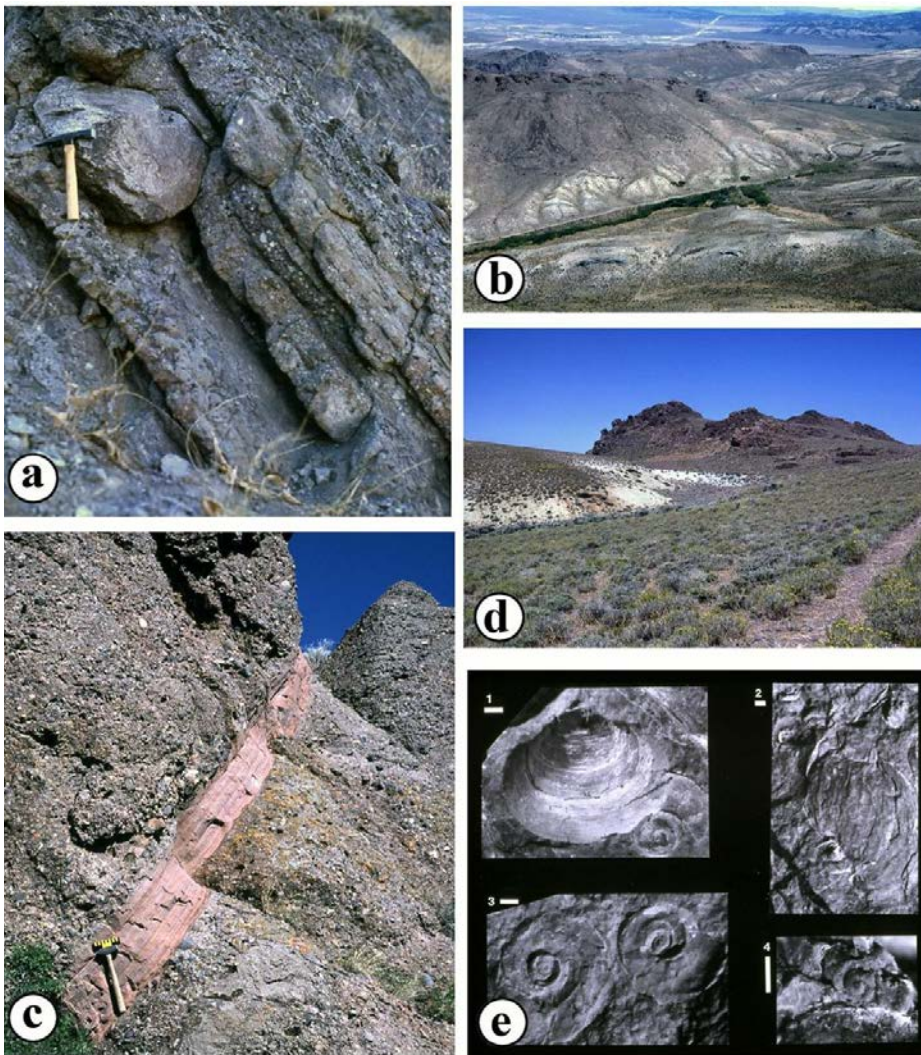


Figure 3. Photographs of Tertiary field relationships, rock types, and fossils. (a) Boulder of flow-banded rhyolite (under hammer) in volcaniclastic conglomerate (in Tvs unit), Clover Creek canyon. (b) In foreground, bold outcrops of megabreccia lenses (Tmb, rock-avalanche deposits), consisting of brecciated, unmetamorphosed Upper Devonian Guilmette Formation, within the sedimentary sequence of Clover Creek (Tcc). Stratigraphically above the Tcc unit are tuffaceous siltstone and sandstone with lenticular conglomeratic beds of the Th₁ unit (pale-colored slopes above creek); and in turn, quartz + feldspar-phyric rhyolite porphyry (Tr₂) lies above the sedimentary rocks, Clover Creek canyon. The town of Wells, Nevada, is in the background. (c) Dipping red sandstone bed within massive conglomerate beds of an alluvial-fan deposit, sedimentary sequence of Clover Creek (Tcc), Clover Creek canyon. (d) Slope-forming, volcaniclastic siltstone, sandstone, and conglomerate with intercalated fossiliferous, lacustrine micritic limestone (Th₁) overlain by massive, resistant rhyolite porphyry (Tr₂) of the middle Miocene Willow Creek rhyolite suite, Willow Creek. (e) Examples of the molluscan fauna from lacustrine beds in the Humboldt Formation (Th₁). 1, Sphaerium species indeterminate; 2, Lymnaeidae, genus and species indeterminate; 3, Biomphalaria species indeterminate; 4, Valvata species indeterminate. Scale bar is 1 mm. Courtesy of Steven C. Good (West Chester University, Pennsylvania).

The age of the **Tvs** unit ranges from middle Eocene to early Oligocene, based on $^{40}\text{Ar}/^{39}\text{Ar}$ radiometric dating of volcaniclastic rocks. Brooks et al. (1995a, b) reported an $^{40}\text{Ar}/^{39}\text{Ar}$ biotite date of 38.0 ± 0.5 Ma (sample 90B31B, Locality 3 on map) from an ash-flow tuff collected from this unit. These authors noted that the spectrum was disturbed, and they considered this date as a minimum age, although it clearly indicates evidence of Eocene volcanism in this unit. Brooks et al. (1995b) also reported two whole-rock chemical analyses of andesitic lava flows from the **Tvs** unit exposed in the northern EHR (their table 3, samples 90B31A and 90B31B). The major oxides in these samples indicate an intermediate composition ($\text{SiO}_2 = 62.0\text{--}65.4$ wt. %, $\text{CaO} = 3.49\text{--}4.48$ wt. %, $\text{Na}_2\text{O} + \text{K}_2\text{O} = 3.85\text{--}6.09$ wt. %). Sr and Ba contents are relatively high (481–2,965 and 1,083–2,239 ppm, respectively).

An important recent discovery regarding the age range of this unit is the presence of the early Oligocene tuff of Campbell Creek as a member within the **Tvs** unit (Henry et al., 2012). These authors reported an $^{40}\text{Ar}/^{39}\text{Ar}$ age on sanidine of $28.93 \pm .07$ Ma (their sample H10-79,

Locality 4 on map). A whole-rock chemical analysis of this sample is reported in their table 1. These data indicate a high- SiO_2 rhyolite (77.76 wt. %) with exceptionally high Sr (4029 ppm) and Ba (8108 ppm) contents. The tuff of Campbell Creek is a voluminous ash-flow tuff, erupted from a caldera in north-central Nevada (Desatoya Mountains), which spread widely through paleovalleys across northern Nevada and the Sierra Nevada. The occurrence of the tuff of Campbell Creek in the **Tvs** unit of the northern EHR is the easternmost known exposure of this tuff, and its poorly welded character indicates a distal location relative to the eruptive center (Henry et al., 2012, their figure 4D).

The sum of the available $^{40}\text{Ar}/^{39}\text{Ar}$ ages from the **Tvs** unit indicates a composite depositional history that lasted ~10 m.y. from the middle to late Eocene Northeast Nevada Volcanic Field (Brooks et al., 1995 a, b) to the early Oligocene tuff of Campbell Creek (Henry et al., 2012). A disconformity is suspected but not yet recognized between the Eocene rocks and the ash-flow tuff unit. Unfortunately, no paleontological data are presently available from this unit.

Sedimentary sequence of Clover Creek (lower Miocene?)

The Cenozoic rocks stratigraphically above the upper Eocene to lower Oligocene volcanic and sedimentary rocks (**Tvs**) are referred to in this report as the *sedimentary sequence of Clover Creek* (**Tcc**). This unit consists chiefly of thick-bedded conglomerate and sedimentary breccia with intercalated megabreccia (figure 3b), calcareous sandstone, and fine-grained lacustrine limestone. Near the base of **Tcc**, pebbles of volcanic rock derived from the **Tvs** unit are a conspicuous component of the detritus. However, at higher stratigraphic levels, this unit is characterized by conglomerate and sedimentary breccia with abundant detritus from the Mississippian Diamond Peak and Chainman Formations. Sorting is poor in these rock types, and the clasts are angular to subangular. In the Clover Creek area, a discontinuous zone of megabreccia bodies and associated lacustrine limestone lie stratigraphically above the conglomerate and sedimentary breccia. Megabreccia and associated lacustrine limestone are also widespread in the central part of Welcome quadrangle, north of the Angel Lake Road.

The megabreccia bodies occur as lens-like masses that vary from ~10 m to ~500 m in length (figure 3b). In general, they are pervasively brecciated and characterized by angular clasts in a fine-grained matrix. However, vestiges of relict bedding are locally preserved in the larger megabreccia masses. The amount of matrix varies from sparse to abundant. Where the matrix is sparse, the megabreccia commonly exhibits a jigsaw-puzzle structure. Where the matrix is abundant, the clasts are matrix-supported in a silty to muddy matrix. In these megabreccias, some of the clasts are subangular to subrounded, suggesting they have been rotated during deposition.

Unmetamorphosed limestone of the Upper Devonian Guilmette Formation is the typical rock type of the megabreccias, but metamorphosed dolomite and sandstone (Middle Devonian Simonson Dolostone) are the principal rock types in several megabreccia bodies. The source area of these megabreccias is uncertain. However, Guilmette Formation is exposed at the northwest end of the adjacent Wood Hills (Thorman, 1970; Camilleri, 2010), and unmetamorphosed Guilmette Formation and Devonian and Silurian metdolomite/dolomite occur in fault-bounded slices associated with the detachment-fault system exposed along the southwestern flank and southern end of Clover Hill.

Based on their monolithologic character, lenticular nature, pervasive brecciation, and association with lacustrine deposits, we interpret the megabreccias as rock-avalanche deposits derived from actively evolving normal fault scarps. As such, they probably record extensional unroofing of the Wood Hills terrane farther

east. Adding credence to this inference, the stratigraphic levels represented by the megabreccias (as deep as Middle Devonian Simonson Dolostone) are 1.5–4 km deeper than the Upper Mississippian to Triassic stratigraphic levels inferred to have been exposed at the Earth's surface before Cenozoic extension based on the position of the basal Cenozoic unconformity southeast of the RM-EHR (Armstrong, 1972; Gans and Miller, 1983; Long, 2012).

The upper part of the sedimentary sequence of Clover Creek is characterized by thick-bedded, clast-supported, blue-gray to red conglomerate with calcareous sandstone intercalations (figure 3c). The clasts are subrounded to rounded and locally exhibit imbrication. There is much lithic clast diversity within these conglomerates, but the clasts consist chiefly of Upper Paleozoic limestone and calcareous sandstone as well as conspicuous detritus from the Diamond Peak and Chainman Formations. Dolomite and Upper Devonian Guilmette Formation are subordinate clast types. Scarce sugary-textured quartzite (metamorphosed Eureka Quartzite), calcite marble, and porphyritic volcanic clasts can be found in many exposures. Some of the volcanic clasts contain biotite as well as small quartz phenocrysts. The volcanic clasts comprise <1% of the clast types in these conglomerates. The occurrence of low-grade metamorphic clasts in this unit adds support for the above inference that extensional unroofing had begun by this time and suggests that progressively deeper levels in the footwall were being breached as extension proceeded. Locally fossiliferous lacustrine limestone is also a constituent of this unit. This limestone is typically platy, faintly to strongly laminated, and yellow-tan to brownish on the fresh break.

The age of the sedimentary sequence of Clover Creek is uncertain. However, it must be younger than 29 Ma based on the presence of the tuff of Campbell Creek stratigraphically below it. The Miocene Humboldt Formation (Sharp, 1939b; Wallace et al., 2008) is deposited on the sequence of Clover Creek. This contact is sharp and defined by the abundance of volcanoclastic debris in the Humboldt Formation. Volcanoclastic debris in the sedimentary sequence of Clover Creek is typically sparse, suggesting that its deposition pre-dated the regionally extensive volcanism related to the track of the Yellowstone hotspot. Nonetheless, a white-weathering tuffaceous sandstone in close stratigraphic association with the megabreccia zone exposed in the Clover Creek area yielded a group of Cenozoic $^{40}\text{Ar}/^{39}\text{Ar}$ sanidine ages with a distinct peak at ~24.5 Ma and with the youngest sanidine grain dated at 23.87 ± 0.03 Ma (C.D. Henry, personal commun., 2014). These data indicate that the upper part of the sedimentary sequence of Clover Creek could not have been deposited before the latest Oligocene and probably not after the onset of Yellowstone track volcanism at ~16.5 Ma. Finally, in wells drilled in the Marys River basin, north of the East Humboldt Range, Frerichs and Pekarek (1994)

recognized a thick stratigraphic sequence that included organic-rich shales that contain an early Miocene ostracod fauna. They referred to this sequence as the “Lower Humboldt” formation. Therefore, based on integration of these data, we have assigned an age of early Miocene? to the sedimentary sequence of Clover Creek.

Humboldt Formation (middle to upper Miocene)

The name *Humboldt* has been used to refer to various Cenozoic sedimentary rocks in northeast Nevada since the members of the Fortieth Parallel Survey applied the term to the Neogene rocks extensively exposed in western Utah and eastern Nevada (King, 1878, p. 434–443). Subsequent studies have attempted to redefine and/or restrict the stratigraphic usage of Humboldt (e.g., Sharp, 1939b; Van Houten, 1956; Smith and Ketner, 1976). Radiometric dating ($^{40}\text{Ar}/^{39}\text{Ar}$) and paleontological faunal ages indicate that the Humboldt Formation spans middle to late Miocene time, approximately 16–10 Ma (Wallace et al., 2008). Within this time interval rhyolite volcanism was dominant from ~16–15 Ma.

In the Welcome quadrangle, we have subdivided the Humboldt Formation into two units: unit 1 (**Th₁**) and unit 2 (**Th₂**), stratigraphically separated by volcanic/volcaniclastic rocks of the middle Miocene Willow Creek rhyolite suite. The lower unit, Humboldt Formation unit 1 (**Th₁**), is deposited on the sedimentary sequence of Clover Creek. This stratigraphic boundary is interpreted as a disconformity because of the abrupt lithologic change from conglomerate and sandstone, with sparse volcanic detritus, to the volcaniclastic-rich Humboldt Formation. The Humboldt Formation unit 1 is distinguished by pale-green to pale yellow to whitish slings underlain by platy tuffaceous siltstone, siliceous siltstone, and very fine-grained sandstone (figure 3d). Vitric ash is a component of the unit. Locally resistant outcrops of volcaniclastic pebble conglomerate and very coarse-grained sandstone are characteristic of the unit. Also, brown to tan lacustrine limestones form distinctive layers. Some of these limestones are pelletal and contain scarce ostracods. Platy, calcareous mudstone locally contains pelecypod and snail shells (figure 3e) as well as plant remains. Good et al. (1995) reported that the molluscan fauna is composed of Sphaeriidae bivalves and three gastropod species (figure 3e). The molluscan biota has been disturbed from life position, but does not appear to have been transported. All the molluscan taxa identified in the **Th₁** unit prefer quiet, shallow water lacustrine habitats. Fossil localities are indicated on the map with the symbol “f”. Eleven anorthoclase grains from a tuffaceous sandstone collected by K.A. Howard and J.P. Colgan from locality 2 (shown on map) were dated at the New Mexico Geochronology Research Laboratory by C.D. Henry and yielded an $^{40}\text{Ar}/^{39}\text{Ar}$ age of 15.52 ± 0.12 Ma. These data definitively indicate that

the **Th₁** unit is middle Miocene in age and support its assignment to the Humboldt Formation.

Stratigraphically above the Willow Creek rhyolite suite (see description that follows), the Humboldt Formation unit 2 (**Th₂**) includes the following: tuffaceous sandstone and siltstone, polymictic conglomerate, lacustrine limestone, accretionary lapilli tuff, and vitric ash. In a railroad cut near Wells, Mueller (1992) and Mueller and Snoke (1993b, field trip STOP 6, their figure 15, p. 28–29) report a fission-track zircon age of 9.57 ± 1.3 Ma from a vitric ash bed (sample OP-1) within a moderately tilted and faulted sequence of the upper Humboldt Formation dipping ~35–45° SE. In addition, Mueller (1992) reported a fission-track zircon age of 8.3 ± 0.9 Ma (his sample WE-1, see plate for fission-track sample locality 1) from the upper part of this unit in the Welcome quadrangle. Metamorphosed Eureka Quartzite (commonly graphite-bearing) and calcite marble are distinctive clasts in the conglomeratic rocks, suggesting a source from unroofing of a metamorphic terrain such as the adjacent Wood Hills ~15 km east of the map area (Thorman 1970; Camilleri, 2010). These metamorphic rock clasts are not mylonitic in contrast to the metamorphic rocks that crop out on Clover Hill. Therefore, at the time of deposition of the Humboldt Formation unit 2, the early Oligocene mylonitic shear zone was not yet exposed, whereas the structurally higher Wood Hills terrain was apparently a local source area. Other distinctive clasts in the conglomeratic rocks of the Humboldt Formation unit 2 include pieces of the Willow Creek rhyolite complex even though rhyolite dikes intrude the lower part of this unit. Thus, silicic volcanism must have occurred synchronously with the early stages of the deposition of this stratigraphic unit in the middle to late Miocene.

Willow Creek rhyolite suite (middle Miocene)

The oldest unit in the Willow Creek rhyolite suite is a sequence of rhyolite flows (**Tr₁**). These rhyolites weather brownish red to brick red to orange red, contain small phenocrysts of quartz and feldspar (1–2 mm diameter), are commonly vesicular, and locally exhibit flow banding and folds. A vitrophyric variety contains green clinopyroxene. Intercalated sedimentary rocks are orange-red to yellow-weathering siliceous siltstone. Associated with these flows are lenticular masses of rhyolitic quartz+feldspar porphyry (**Tr₂**), which intruded along the contact between the older rhyolite (**Tr₁**) and subjacent unit 1 of the Humboldt Formation (**Th₁**) (figure. 3d). Near the mouth of Clover Creek canyon, the intrusive mass of quartz+feldspar porphyry transects the contact. The massive, intrusive rhyolites (**Tr₂**) are conspicuously porphyritic characterized by quartz phenocrysts commonly 3–4 mm in diameter, and locally up to 7–8 mm in diameter. A prominent slabby cleavage is common and autobrecciation is widespread. These rhyolitic rocks weather brown to red brown to deep red,

but are pearly gray to red brown on the fresh break. The intrusive rhyolite is commonly vitrophyric near the contacts with the wall rocks, and local contact metamorphism of the underlying Humboldt Formation is apparent at some localities. Coupled with the emplacement of this rhyolite was the intrusion of similarly porphyritic rhyolite dikes and small bodies into the roof-rocks of the intrusion, consisting of the older rhyolite flows (**Tr₁**).

Other components of the Willow Creek rhyolite suite include a maroon microporphyritic rhyolite (**Tr₃**), which stratigraphically overlies an orange-weathering, volcanoclastic breccia (**Trvb**). The latter units are restricted to a fault-bounded block exposed near the front of the range. The volcanoclastic breccia consists chiefly of angular clasts of porphyritic rhyolite in a fine-grained siliceous matrix. The volcanoclastic breccia also contains angular, pebble-sized clasts to subrounded cobbles of white metaquartzite (metamorphosed Ordovician Eureka Quartzite). Scarce meter-scale clasts of **Tr₃** occur within the **Trvb** unit, suggesting that these lithologic units are relatively synchronous in origin even though the mapped exposures of the **Tr₃** rhyolite lie above the volcanoclastic breccia (**Trvb**). The volcanoclastic breccia may be a talus deposit developed on the flank of an emergent rhyolite dome. The rounded metaquartzite clasts are probably detritus derived from contemporaneous alluvial fan deposits (e.g., the Humboldt Formation).

Snoke et al., (1997) reported late Miocene K-Ar (sanidine) ages from these rhyolites in the interval 14.8 to 13.4 Ma, determined by E.H. McKee (U.S. Geological Survey). However, a recent ⁴⁰Ar/³⁹Ar age of 15.25 ± 0.04 Ma determined on sanidine from the **Tr₂** unit (Brueseke and Hames, unpublished data, personal comm., 2013; Locality 1 on the geologic map) indicates that the previously reported K-Ar ages do not accurately record the true age range of volcanism in the Willow Creek rhyolite suite. The Willow Creek rhyolite suite correlates with the middle Miocene Jarbidge Rhyolite, extensively exposed in northern Elko County (Coats, 1964, 1987; Brueseke et al., 2014).

Small volume basaltic lava flows (**Tvb**) are associated with the Willow Creek rhyolite suite in two areas of the Welcome quadrangle (western half of section 14, T37N R61E). This basalt is vesicular and amygdaloidal. The lava contains blocky to tabular phenocrysts of plagioclase feldspar up 7–8 mm in length. This basalt lava is inferred to be middle Miocene, based on its association with the middle Miocene rhyolite suite and local intrusion of ~15.5 Ma basalt dikes along the length of the RM-EHR, from the Harrison Pass area to Angel Lake (Hudec, 1990; this report).

Landslide deposit (upper Miocene)

Brecciated and silicified quartz porphyry rhyolite (**Tr₂**) resting on Humboldt Formation unit 2 is

interpreted as a late Miocene landslide deposit. This unit is older than the Boulder conglomerate unit (**QTbc**).

Boulder conglomerate unit (upper Miocene or Pliocene?)

The flat-lying boulder conglomerate unit (**QTbc**) overlies the Humboldt Formation and Willow Creek rhyolite suite forming an angular unconformity. The age of the unit is uncertain, but regional stratigraphic relationships suggest a Quaternary–Pliocene(?) age (Wallace et al., 2008). The unit is poorly sorted, and the matrix consists of angular clasts that reach ~2 cm in diameter, grit, sand, and silt. Boulders or cobbles include: rock types of the Willow Creek rhyolite suite, a variety of upper to middle Paleozoic sedimentary-rock clasts, metamorphosed Eureka Quartzite (equigranular to mylonitic texture), gray calcite marble with muscovite or siliceous layers, lacustrine limestone, and dark gray amygdaloidal pyroxene basalt with tabular plagioclase microphenocrysts. The source of the vesicular basalt is an interesting conundrum. Several small outcrops of vesicular basalt are associated with the Willow Creek rhyolite suite (see map for localities). Also, Sharp (1939a) showed a much larger outcropping of basalt within Clover Valley, about 4 mi (~6.4 km) east-southeast of the mouth of Leach Creek on his Plate 1, a feature locally known as The Mound near the western margin of the Tobar quadrangle (section 8, T35N R62E) southeast of the Welcome quadrangle. Based on the inferred southern extension of the Clover Hill fault, this locality is part of the hanging-wall of this Holocene–Pleistocene normal fault. Thus The Mound is a potential source of the basaltic cobbles in the boulder conglomerate unit, but only if the Clover Valley fault and the uplift of Clover Hill post-dated the deposition of this unit, as explained below.

The boulder conglomerate unit may represent a high-energy fluvial deposit related to the ancestral course of the Humboldt River. Therefore, the boulder conglomerate unit may have important implications for the course of the ancestral Humboldt River and its relationship to Pleistocene Lake Clover (Reheis et al., 2002; Munroe and Laabs, 2013). Because it lies with angular unconformity on Humboldt Formation unit 2, we infer that the boulder conglomerate unit postdates rotation on the detachment fault as well as other normal faults related to middle Miocene crustal extension (Colgan et al., 2010; Henry et al., 2011). The boulder conglomerate unit crops out at ~6000–6200 ft. (~1830–1890 m) on the northwestern flank of Clover Hill, whereas the present source of the Humboldt River at Humboldt Wells, about 0.7 km north of Wells, Nevada, is just 5618 ft. (1714 m), thus raising the possibility that the uplift of Clover Hill may have blocked the course of the paleo-Humboldt River. This hypothesis can be tested by petrographic and geochemical analysis and radiometric dating of the hypothesized basaltic source

rock at The Mound as compared to basaltic clasts from the boulder conglomerate unit. This would also offer the possibility of better constraining the age of the boulder conglomerate unit and, if confirmed, would place an older age bracket on the initiation of the Clover Hill normal fault bounding the east side of Clover Hill.

Intrusive Rocks

Orthogneiss of Chimney Rock (Neoproterozoic to Paleoproterozoic)

Field description and petrography: The orthogneiss of Chimney Rock (**XWog**) characteristically consists of coarse-grained, gray biotite monzogranitic orthogneiss, locally with white K-feldspar augen up to 1 cm in diameter, and commonly showing a distinctive striped appearance due to segregation of biotite parallel to foliation (figures 2d and 2e). Migmatization is nearly ubiquitous, with stromatic leucosomes defining strong compositional banding that further enhances the “striped” aspect of this rock. Locally the boundaries of thinner leucosomes are diffuse and poorly defined, but many leucosomes form veins with well-defined contacts (especially those with thicknesses greater than ~1 cm). Pegmatitic and leucogranitic sills also commonly intrude the complex. Like all components of the gneiss complex of Angel Lake, small amphibolite and garnet amphibolite bodies form widespread, meter-scale pods and layers interpreted as metamorphosed mafic intrusions (figure 2e). Petrographically, the orthogneiss is rather uniform in character typically containing 35–40% K-feldspar, 20–30% quartz, 15–25% oligoclase, 3–5% biotite, and locally up to 3% each of garnet, allanite, muscovite, and opaque minerals. Where present, garnet forms small grains less than 500 μm in diameter, which are locally cut by microveins of biotite and/or chlorite at high angle to foliation. Feldspar grains locally may also be cut by microfractures at high angle to foliation and in many localities the feldspars show evidence of crystal-plastic strain, including undulose extinction, subgrain polygonization, dynamic recrystallization to finer grain size at grain boundaries or along transecting normal-sense shear bands, and local replacement by pockets of myrmekite. In the more intensely sheared rocks, quartz is extensively recrystallized and foliation is dissected on a microscopic scale by anastomosing extensional shear bands and foliation boudinage.

Geochemistry: Geochemically, the orthogneiss of Chimney Rock resembles a granite, and in particular it overlaps in most respects with the major-, minor-, and trace-element chemistry of the early Oligocene biotite monzogranitic orthogneiss unit described below. Silica contents range from 72% to 76% with A/CNK ratios of 1.08–1.13 indicating mildly peraluminous compositions (Batum, 2000). Rare-earth element patterns normalized to chondrites show strong enrichments of the light rare-

earth elements with moderate to deep negative europium anomalies and relatively flat profiles in the heavy rare-earth elements (McGrew, unpublished data).

Geochronology: An Archean age for the orthogneiss of Chimney Rock was first reported based on U-Pb dating of zircon by traditional ID-TIMS methods on sample RM-9, a characteristic coarse-grained, migmatitic biotite monzogranitic orthogneiss (U-Pb Locality A on map). This sample yielded a strongly discordant array (>50% discordance) based on five multi-milligram size fractions with an Archean upper intercept of 2520 ± 110 Ma interpreted as the crystallization age of the gneiss and a lower intercept of 196 ± 32 Ma (Lush et al., 1988). Premo et al. (2008, 2010) subsequently investigated zircons from the same sample using SHRIMP-RG U-Pb methods, yielding an upper intercept of 2516 ± 17 Ma but with at least 50% of the sample consisting of Late Cretaceous zircon overgrowths on older cores with Neoproterozoic or Paleoproterozoic apparent ages. In addition, they noted that a number of the oldest grains showed clear detrital morphologies. Accordingly, they reinterpreted the sample as a Late Cretaceous orthogneiss derived from anatexis of Proterozoic sediment containing mostly Neoproterozoic zircon (Premo et al., 2008). In a subsequent *Comment and Reply*, McGrew and Snoke (2010) reasserted the Archean age interpretation, arguing that Late Cretaceous migmatization had strongly disturbed the older U-Pb zircon systematics. While conceding that the Late Cretaceous rim ages likely represent the age of migmatization and that little faith could be placed in the strongly discordant Proterozoic apparent ages, Premo et al. (2010) nevertheless maintained that the parent rock was likely a metasedimentary rather than igneous rock based on the relative abundance of grains with detrital morphologies and the broad age range of the Archean grains (2510–2580 Ma), even for the least discordant grains with the lowest common lead (<1%).

In this report, we infer a magmatic origin for the orthogneiss as argued by McGrew and Snoke (2010) based on its relatively homogeneous petrographic character and its mineralogic and chemical composition, which is characteristic of a high-silica granite. In addition, we point out the similarity of this sample to the Green Creek gneiss of the Basin Creek area of the Grouse Creek Mountains, which also shows a strongly discordant apparent age array with an upper intercept of 2532 ± 33 Ma (Strickland et al., 2011).

Regardless of the interpretation of sample RM-9, above, McGrew subsequently collected a much less migmatized orthogneiss sample near Chimney Rock (sample 090713-5) that yielded a much better constrained discordia based on grains that were less than 10% discordant with an upper intercept of 2449 ± 3 Ma (U-Pb Locality C on map) (McGrew and Premo, 2011). Although crust of ca. 2450 Ma age is not common globally (e.g., Voice et al., 2011), orthogneiss of this age

is widespread around the margins of the Wyoming province. Similar ages have been reported from the southeastern Wyoming province (e.g., the Baggot Rocks granitic suite: Premo and Van Schmus, 1989), southwestern Montana (e.g., Kellogg et al., 2003) and the Farmington Canyon Complex of Utah, where Mueller et al. (2011) reported a statistically overlapping age of 2446 ± 11 Ma on quartzo-feldspathic gneiss, which was also interpreted as probable orthogneiss. Moreover, the timing of this phase of magmatism approximately corresponds with proposed rifting at ca. 2480 Ma along the eastern margin of the Wyoming province north of the Cheyenne belt (Dahl et al., 2006) that may have been associated with a proposed global rifting event at ca. 2.45 Ga associated with the break-up of the supercontinent Kenorland (e.g., Heaman, 1997).

Leucogranite (Paleogene to Cretaceous)

Field description and petrography: Leucogranitic rocks are ubiquitous in the metamorphic core of the northern EHR and are inferred to be predominantly Late Cretaceous to Oligocene in age. Most leucogranitic bodies range from fine, centimeter-scale stringers of leucosome apparently still in their source rock (e.g., Hallett, 2012) to lit-par-lit intrusions decimeters to meters-long to small intrusive bodies up to 12 m thick. Batum (2000) completed a detailed investigation of granite petrogenesis that identified three major phases of leucogranitic intrusion as summarized below. The oldest phase is strongly foliated, typically concordant, and locally boudinaged in more ductile host rock types such as marble or metaquartzite. Typically these bodies are leucogranite in composition but extend to leucocratic granodiorite, with major mineral assemblages including $pl + Ksp + qz + bt \pm mu \pm gt \pm sill$, and accessory phases including apatite, zircon, and opaque oxides. Where intrusive into carbonate country rock the accessory minerals allanite, titanite, tremolite, and zoisite are also observed (Batum, 2000). Secondary minerals include calcite, chlorite (replacing biotite), Fe-Ti oxides, rutile, and hematite. Plagioclase is oligoclase, whereas K-feldspar commonly forms large (up to 40 mm) rounded augen of perthitic microcline. Coarse, granoblastic textures are typical at deeper structural levels, whereas mylonitic or protomylonitic fabrics are increasingly evident at higher structural levels in the mylonitic zone. Both plagioclase and K-feldspar are intensely strained, exhibiting extensive microfracturing, warping or kinking of albite twins, and subgrain development in augen, merging at grain boundaries into a matrix of fine, dynamically recrystallized polygonal grains of feldspar and quartz. Bleb-like intergrowths of myrmekite in microcline are common, suggesting amphibolite-facies deformation (Simpson and Wintsch, 1989). Quartz is also polygonized and commonly forms ribbons that warp around feldspar augen. Sillimanite occurs both as inclusions in garnet and as fibrous intergrowths with

muscovite. Garnet, where present, forms anhedral to subhedral porphyroclasts up to 5 mm diameter that are commonly poikiloblastic with inclusions of biotite, quartz, sillimanite, and opaque oxides (Batum, 2000).

The well-foliated, mostly concordant leucogranitic bodies described above are commonly cut by less strongly foliated dikes and sheets of leucogranite, some of which are themselves cut by normal-sense shear bands. Some of the cross-cutting bodies form step-like geometries with flats parallel to foliation alternating with ramps across foliation, whereas others branch into foliation-parallel sills and discordant dikes. Compositionally, the later stage leucogranitic sheets resemble the earlier, concordant leucogranites, with mineral assemblages consisting of $pl + Ksp + qz \pm bt \pm mu \pm gt$ with accessory apatite, zircon, oxide phases and (restricted to intrusions into marble) allanite, titanite, diopside, cordierite, and zoisite (Batum, 2000). Leucogranites of this stage are typically coarser grained, with feldspar augen up to 50 mm in diameter. Plagioclase typically shows weak normal zoning in the oligoclase range, is commonly myrmekitic, and locally displays graphic intergrowths with quartz. Potassium feldspar typically occurs as perthitic microcline. Biotite and muscovite forms stringers parallel to foliation that warp around feldspar porphyroclasts, as do quartz ribbons.

The final stage of leucogranitic intrusion is marked by late-stage, very weakly foliated, highly discordant dikes ranging in composition from muscovite syenite to leucogranite to muscovite biotite quartz monzonite to leucogranodiorite (Batum, 2000). Some dikes exhibit fine-grained muscovite garnet aplite cores with margins of muscovite pegmatite. In addition, border phases of leucogranitic rock commonly fringe biotite monzogranitic sheets (see below). Based on field relationships, the final stage of leucogranitic intrusion is inferred to range into the late Oligocene or perhaps even early Miocene. Mineralogically, the most typical assemblage is $pl + Ksp + qz + bt \pm mu \pm gt \pm sill$, and accessory phases including apatite, zircon, allanite, titanite, tremolite, diopside, and oxides (again, with the calcic accessory phases being restricted to intrusions into carbonate host rock) (Batum, 2000). Although generally less deformed than other leucogranitic rocks, these dikes are locally transected by thin mylonitic zones.

Geochemistry: The oldest leucogranitic rocks show a slightly narrower compositional range than the later phases, with CaO ranging from ~1.0% to 2.9% and SiO₂ ranging from ~71% to 75.6% in the first generation leucogranites as contrasted with CaO values in the range ~0.7 to 3.4% and SiO₂ ranging from ~63.1% to 75.4% in the later generation leucogranites (Batum, 2000). Using CaO as the differentiation index, both suites exhibit increasing trends in SiO₂ and K₂O with CaO and decreasing trends in Fe₂O₃ (as total iron), MgO, TiO₂ and P₂O₅.

Hornblende-biotite quartz diorite orthogneiss (middle Eocene)

Field description and petrography: The hornblende biotite quartz diorite forms an extensive, thick sill extending the length of the Humboldt Peak quadrangle to the south, but in the Welcome quadrangle this unit is represented only by a few isolated outcrops between 8400 and 8600 ft. (2560–2620 m) elevation in the southwestern part of the quadrangle. It is well foliated, mostly medium-grained, equigranular, and compositionally relatively homogeneous. Andesine showing strong normal zoning composes most of the rock (typically >60%) with 10–20% quartz, sparse or absent K-feldspar, and biotite and hornblende in variable proportions together composing 15–30% of the rock. Titanite is commonly the most conspicuous accessory phase and is joined by apatite, zircon, allanite, epidote, rarely garnet, and opaque minerals.

Geochemistry: Geochemically, the hornblende biotite quartz diorite forms a calc-alkaline intrusive suite ranging from 54–66% SiO₂ with A/CNK ratios ranging from 0.93 to 1.12 (slightly metaluminous to mildly peraluminous) (McGrew, unpublished data). With SiO₂ as the differentiation index, this suite shows increasing trends in the alkalis and decreasing trends in all other major elements, particularly Al₂O₃, CaO, and MgO. Rb/Sr ratios range from 0.10 to 0.27 and Wright and Snoke (1993) report initial ⁸⁷Sr/⁸⁶Sr = 0.712 and ε_{Nd} = -22.2. These isotopic ratios place this rock suite within the “lower data array” of Wright and Wooden (1991), interpreted by them as recording interaction with ancient (Archean) crust depleted in U and Rb.

Geochronology: The age of the hornblende-biotite quartz diorite is constrained by a TIMS-ID U-Pb zircon age on five zircon size fractions from the northern part of

the Humboldt Peak quadrangle (Wright and Snoke, 1993). Although highly discordant, these data define a highly linear array with a lower concordia intercept of 40 ± 3 Ma interpreted as the crystallization age and an upper intercept of 2.39 ± 0.04 Ga interpreted as the age of resorbed xenocrystic cores (Wright and Snoke, 1993). The similarity of the inherited age to the 2.45-Ga zircon age on the orthogneiss of Angel Lake is notable, especially since the quartz diorite is intruded structurally beneath the Winchell Lake fold-nappe and the Precambrian gneiss complex of Angel Lake. This suggests that ca. 2.4-Ga gneiss may also form the basement at depth beneath the northern EHR as argued by Wright and Snoke (1993). Premo et al. (2014) report a SHRIMP-RG U-Pb zircon age of 40.9 ± 0.9 Ma for the same body for quartz diorite from a sample locality in the southern Humboldt Peak quadrangle east of Humboldt Peak.

Biotite monzogranite orthogneiss (lower Oligocene to middle Eocene)

Field description and petrography: Biotite monzogranite orthogneiss forms tabular bodies concordant and discordant to foliation in the country rocks, commonly with dikes connecting concordant sheets. Locally the unit forms plug-like bodies up to 200-m thick from which multiple sills originate (see, for example, the rear cirque walls between Smith Lake and Greys Lake on the map). Most commonly these sheet-like intrusions are 1–10 m thick. In a number of localities, they are partly to wholly involved in the final phase of folding (figure 4). They are finer grained than most leucogranitic bodies, although the margins of these sheets are locally marked by 5–20 cm-thick layers of leucogranite. Generally, more concordant and/or more deformed bodies show higher color index (commonly >8 % biotite), whereas more discordant members of this

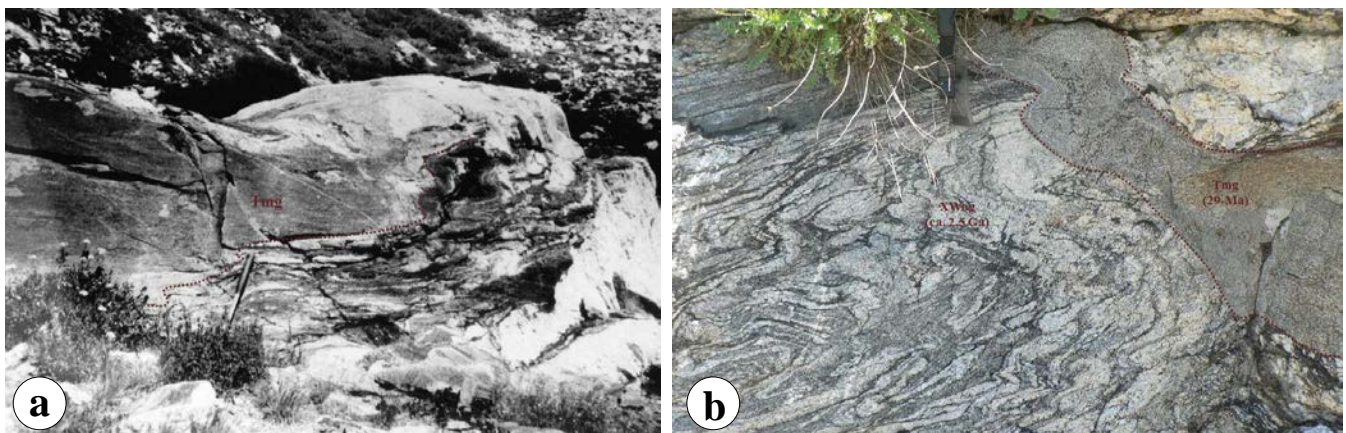


Figure 4. Field photographs illustrating relative age relationships between the biotite monzogranite (Tmg) and folding in country rock. (a) Monzogranitic sheet essentially fully involved in the final phase of folding ($F_{(n+1)}$). Light-toned, layered rocks are in the leucocratic border phase locally associated with the biotite monzogranite sheets. (b) Biotite monzogranitic dike cutting severely migmatized and intensely folded Paleoproterozoic to Neoproterozoic orthogneiss of Chimney Rock. Note that the biotite monzogranitic dike is itself partially involved in folding, probably reflecting intrusion into a vertical shortening field associated with late Oligocene extensional deformation.

suite show lower color index (<8 % biotite), suggesting a trend toward slightly more felsic composition through time. The biotite monzogranite commonly shows well-developed composite fabrics, especially at higher structural levels, with biotite concentrated along low-angle, normal-sense shear bands (interpreted as C'-planes) oriented at 20–30° to grain-shape foliations (figure 5). Such composite fabrics become less common at depth, where they commonly show a shear-sense to the ESE antithetic to the WNW-directed shear fabric characteristic of the unit in the overlying mylonitic zone.

The structurally early intrusive bodies exhibit compositions ranging from biotite tonalite through biotite granodiorite to the most characteristic biotite monzogranite composition (Batum, 2000). In addition to plagioclase, quartz, K-feldspar, and biotite the rock includes accessory apatite, zircon, allanite, monazite, and opaque oxides. Where the monzogranite intrudes into marble or calc-silicate host rock allanite is more abundant, and the accessory assemblage is expanded to include subhedral titanite and euhedral zoisite (Batum, 2000). Limited secondary alteration of biotite occurs

locally complete within ~1 cm thick bleach zones adjacent to late stage, northerly striking subvertical joints. Plagioclase ranges from unzoned to normally zoned from andesine cores to sodic oligoclase rims. Locally, it shows moderate sericitic alteration, especially along subgrain boundaries. In protomylonitic gneisses, asymmetrically disposed blebs of myrmekite are commonly observed in zones of expected localized stress concentration on opposite sides of small (3–5 mm) σ -type K-feldspar augen as described by Simpson and Wintsch (1989). Feldspar porphyroclasts are commonly microfractured, and the microfractures locally show small normal-sense offsets and “bookshelf-style” rotations. Feldspars commonly show signs of internal crystal-plastic strain ranging from undulose extinction to subgrain polygonization, with subgrains commonly showing serrate or cusped boundaries. In more intensely deformed rocks feldspars show incipient dynamic recrystallization, whereas quartz shows extensive subgrain polygonization, dynamic recrystallization, ribbon grains warping around feldspar augen, and locally well-defined S-C' fabrics, especially in more intensely

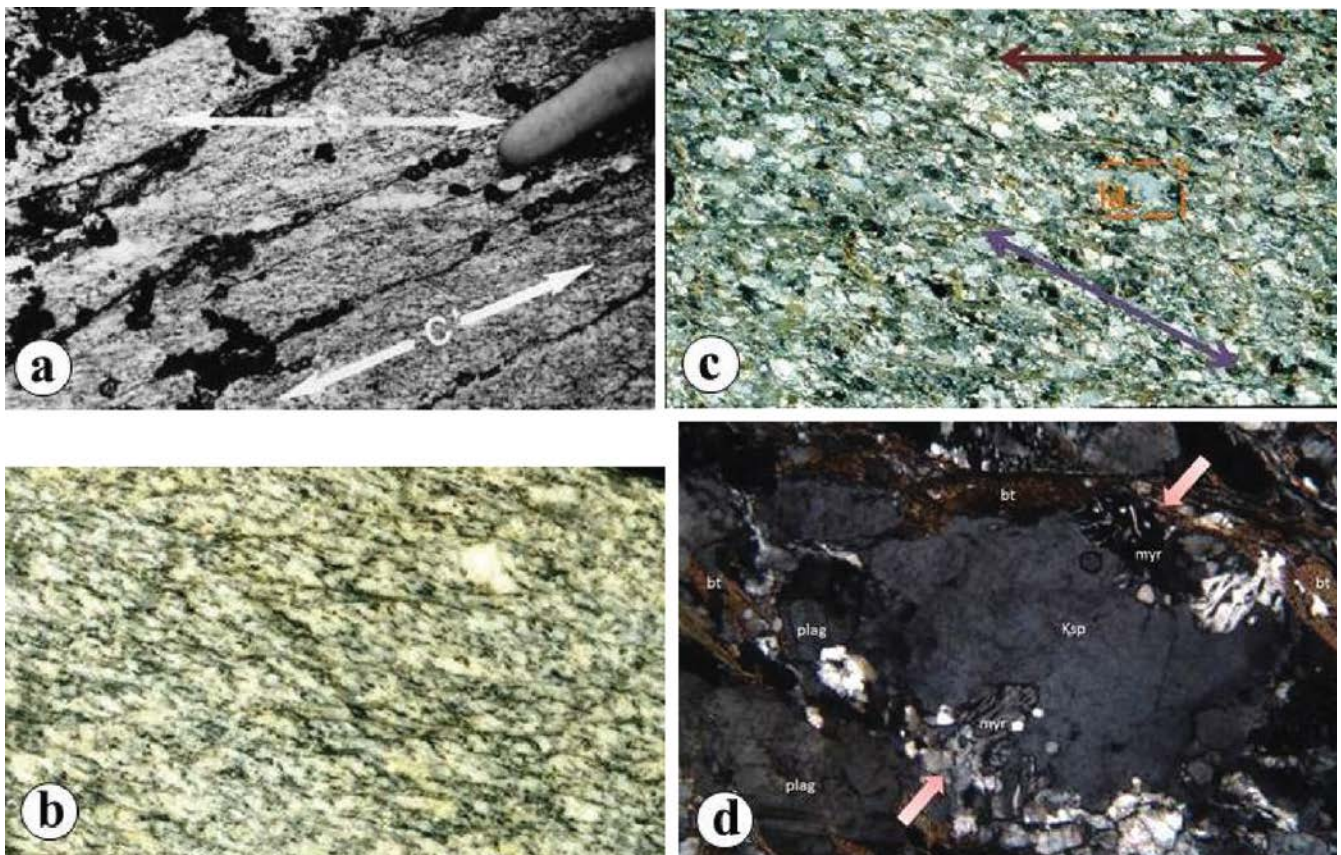


Figure 5. Photographs illustrating textural relationships in protomylonitic biotite monzogranite, indicating a post-29 Ma age for mylonitization. All photos are oriented with WNW to the left. (a) S–C' composite fabric relationships in outcrop, indicating top-to-WNW normal-sense shear. (b) S–C' composite fabric relationships in a scan of a polished slab of monzogranitic gneiss. Short dimension of slab is 27 mm. (c) Thin section scan of protomylonitic biotite monzogranitic orthogneiss illustrating S–C' relationships (crossed polars, vertical dimension 16 mm). The shear-band fabric (C'-planes) are oriented parallel to the red double arrow. The trace of grain-shape foliation (S-planes) parallels the violet double arrow. Box outlined by orange dashed line indicates area of photomicrograph (d). (d) Photomicrograph of K-feldspar porphyroclast in sample 870621-5 (crossed polars; vertical dimension of photograph approximately 2 mm). Pale red arrows indicate shortening direction. Note that the K-feldspar porphyroclast is being replaced by a myrmekite of qz+pl on the two sides facing the shortening direction, a relationship previously described from amphibolite-facies mylonitic orthogneisses (Simpson and Wintsch, 1989).

deformed shear bands. Biotite commonly forms offset fish-like grains and is dynamically recrystallized together with quartz in shear bands. In less deformed gneisses, biotite is aligned in grain-shape foliation.

Geochemistry: The geochemistry of the Oligocene monzogranitic intrusive suite has been investigated in detail by Batum (2000), who subdivided the suite into an earlier component and a structurally later, more leucocratic component based on cross-cutting relationships in the field. When pooled together the two components partly overlap, though the earlier component shows a range in weight percent SiO₂ from ~66.9–72.7% whereas the later, more leucocratic component ranges from ~72.9–75.9% SiO₂. In addition, the earlier component is slightly richer in MgO + Fe₂O₃, ranging from 0.5–1.5% in contrast with < 0.5 weight percent MgO + Fe₂O₃ for the more leucocratic phase. Taking CaO as the differentiation index, the suite as a whole shows a positive correlation between increasing CaO and increasing TiO₂, Al₂O₃, Fe₂O₃ and MgO and an inverse correlation between CaO and K₂O, whereas Na₂O and MnO show wide scatter, with increasing MnO and Na₂O in the first stage in contrast with decreasing MnO and Na₂O with increasing CaO in the second stage.

With regard to the large ion lithophile (LIL) trace elements, the first stage monzogranites show increasing Ba and Rb and decreasing Sr with increasing SiO₂ whereas in the second stage only Rb shows positive covariance with SiO₂ content (Batum, 2000). Among the high field strength (HFS) elements, Zr, Hf and Th decrease with increasing SiO₂ whereas U increases. Rare-earth element patterns from the monzogranitic suite show moderate to steep slopes in the light REE, a well-defined negative europium anomaly, and relatively flat heavy rare-earth elements spectra (Batum, 2000; McGrew, unpublished data).

Geochronology: Biotite monzogranite bodies are widespread in the RM-EHR metamorphic core complex and have mostly yielded middle Oligocene ages of ~29 Ma (Wright and Snoke, 1993). In the Welcome quadrangle, sample RM-5 (U-Pb Locality B on map) has been dated by ID-TIMS U-Pb zircon and monazite, yielding a well-defined discordia with a lower intercept age of 29 ± 0.5 Ma interpreted as the crystallization age of the sample and an upper intercept age of 2.43 ± 0.03 Ga, interpreted as the age of a xenocrystic zircon population. This upper intercept age is identical within error to the best-determined age of the orthogneiss of Chimney Rock (see above) and to the upper intercept inherited age of the hornblende-biotite quartz diorite unit. Given that this sample originated from the lower limb of the WLN beneath the orthogneiss of Chimney Rock, the presence of early Paleoproterozoic xenocrystic

zircon suggests that this rock may also be present in the underlying basement.

Basalt dikes (middle Miocene)

A suite of steeply dipping basaltic dikes (**Tb**) form a volumetrically minor but structurally significant phase because they represent the only entirely post-kinematic intrusive lithology exposed in the high-grade metamorphic core of the range. Rarely exceeding 2 m in thickness, they strike northwest to north-south and are nearly vertical. Calcite-filled amygdules, sharp contacts, and well-developed chilled margins all indicate that the metamorphic core had been exhumed to relatively shallow crustal levels by the time of their intrusion. Although undated in the EHR, Snoke (1980) reports a whole rock K-Ar age of ~17 Ma on a similar basaltic dike from the southwestern EHR, and Hudec (1990) reports two ⁴⁰Ar/³⁹Ar whole-rock plateau ages of ~15.5 ± 0.05 Ma from a basalt dike in the central Ruby Mountains. These basaltic dikes are probably related to a major swarm of northerly striking basalt dikes associated with the Northern Nevada Rift (Zoback and Thompson, 1978).

Rhyolite dikes (middle Miocene)

Scattered rhyolite dikes (**Trd**) intrude the sedimentary sequence of Clover Creek, Unit 2 of the Humboldt Formation, and metamorphic rocks exposed on Clover Hill. These rhyolites are quartz and feldsparphyric, characterized by relatively small phenocrysts of quartz (1–2 mm). Therefore, they are texturally distinct from rhyolite dikes of the quartz porphyry (**Tr₂**), which are characterized by conspicuously large phenocrysts of quartz (commonly 3–4 mm in diameter or even larger). Although these dikes are undated, they probably are roughly coeval with the basaltic dikes and therefore indicate late bimodal magmatism.

Quaternary Deposits

Introduction

Quaternary deposits in the Welcome quadrangle consist primarily of glacial, colluvial, or talus deposits at higher elevations (above ~7000 ft, 2150 m), whereas at lower elevations alluvial deposits predominate in the southeastern and northern parts of the quadrangle.

Youngest Alluvium (Qy – upper Holocene)

Alluvium and active channel deposits consist of unconsolidated silt, sand, gravel, and boulders mostly along modern stream courses and adjacent flood plains draining across alluvial fans.

Table 2. Thermobarometric results from the Welcome quadrangle summarized from McGrew et al. (2000) (localities 1–7) and Hodges et al. (1992). Map locations in parentheses, following sample numbers, refer to sample locations labeled with circled numbers.

Sample (Location)	Latitude	Longitude	Elevation	Assemblage	P (kb)	T (°C)
MP.AL196 (1)	41° 01' 52"	115° 05' 20"	2780 m (9120 ft)	amph+cpx+pl+[gt]+ q+ttn+ru	9.3 ± 1.1	752 ± 138
AJM.AL1 (2)	41° 01' 25"	115° 05' 13"	2633 m (8640 ft)	bt+sill+gt+qz+Ksp+ pl+mu	5.2 ± 1.4	630 ± 105
AJM.AL2 (3)	41° 01' 37"	115° 06' 14"	3146 m (10320 ft)	bt+sill+gt+qz+[ru]+ ilm+(chl)	8.3 ± 1.2	700 ± 125
MP.AL311 (4)	41° 01' 21"	115° 06' 13"	3194 m (10480 ft)	bt+sill+gt+qz+pl+ [ru]+ilm	7.4 ± 1.2	670 ± 100
MPAL312 (5)	41° 01' 20"	115° 06' 13"	3197 m (10490 ft)	bt+mu+sill+gt+pl+ qz+ilm+[ru]+[st]	7.4 ± 1.1	630 ± 90
AJM.AL3 (6)	41° 01' 18"	115° 06' 14"	3194 m (10480 ft)	bt+sill+gt+qz+pl+ mu+[ru]+(chl)	7.4 ± 1.2	710 ± 115
AJM.SC2 (7)	41° 00' 17"	115° 05' 57"	3078 m (10100 ft)	bt+sill+[ky]+qz+ pl+[ru]+ilm	6.7 ± 1.0	638 ± 47
1-15-17 (8)	41° 02' 53"	115° 00' 29"	2255 m (7400 ft)	bt+mu+ky+sill+gt+ qz+pl+ru+il	5.0 ± 0.6	622 ± 06
1-22-27 (9)	41° 02' 40"	115° 00' 28"	2205 m (7240 ft)	bt+mu+ky+sill+gt+ qz+pl+ru+il	5.7 ± 0.7	584 ± 40
554-34 (10)	41° 02' 29"	115° 00' 29"	2220 m (7280 ft)	bt+mu+ky+sill+gt+ qz+pl+ru+il	5.8 ± 0.9	623 ± 49

Landslide deposit (Q1s – Holocene)

A landslide deposit straddles the southern boundary of the Welcome quadrangle at 115° 5' W. It is marked by hummocky topography developed on a terrain of coarse, remobilized debris consisting of local bedrock and remobilized glacial deposits. It appears to overlap the range front fault system and plausibly could have been seismically triggered.

Colluvium (Qc – Holocene)

Colluvial deposits mantle and hide the underlying bedrock along many of the steep, densely vegetated slopes on both flanks of the crest of the EHR. These slopes are commonly underlain by thin soils intermixed with gravel and/or relatively fine talus.

Talus deposit (Qt – Holocene)

The steepest slopes near the crest of the EHR are commonly mantled by steep fields of coarse (10 cm to 2 m or more) angular blocks with little fine material between them to support vegetation. Such talus fields are particularly common where the crest of the range is upheld by quartzite.

Younger Alluvium (Qya – Holocene)

Unconsolidated silt, sand, and gravel of fluvial origin older than the active stream channels and adjacent flood plains. This unit exists as alluvial fans developed on the northern flank of the EHR and eastern flank of Clover Hill. Clasts include a wide sampling of rock types recognizable from the adjacent mountains.

Older Alluvium (Qoa – Pleistocene)

The alluvial fans mantling the east flank of the EHR are commonly visibly dissected by modern stream courses. The fan surfaces above these stream courses have been mapped as older alluvium and consist of unconsolidated or poorly consolidated alluvial and debris flow deposits of silt, sand, gravel, and boulders. The clasts include various rock types derived from the metamorphic and igneous source rock exposed in the higher parts of the range. The thickness of these deposits is unknown.

Glacial Deposits (Qg – Pleistocene)

The earliest descriptions of the glaciation of the Ruby Mountains and EHR were published by Blackwelder (1931) and subsequently mapped in detail by Sharp (1938), who divided them into two substages, the Lamoille substage and younger Angel Lake substage. Wayne (1984) subsequently differentiated the Lamoille and Angel Lake substages based on their contrasting weathering characteristics, and argued that only the Angel Lake substage correlates with the Wisconsin glaciation. Glacial deposits have not been subdivided on the geologic map, but include till, morainal deposits, and locally some glaciolacustrine sediment in the cirque lakes. Steep moraines occur at the mouth of each major cirque and commonly consist of ridges of coarse, angular boulders forming hummocky topography.

CONDITIONS OF METAMORPHISM

Metapelitic rocks on the upper limb of the WLN preserve pre-peak metamorphic kyanite (always mantled by sillimanite), rutile inclusions in garnet and rare relict staurolite inclusions in garnet. In contrast, on the lower limb of the WLN the older, kyanite-bearing assemblages appear to be completely obliterated by peak metamorphic $bt + sill + gt \pm Ksp$ assemblages, with abundant leucogranitic rock inferred to have been generated and injected synchronously with peak metamorphism (McGrew et al., 2000). In the Welcome quadrangle, the downward increase in leucogranite percentage is most clearly observed in the distinctive inferred Mississippian–Devonian rusty-weathering graphite-bearing schist unit (inferred Pilot Shale), which shows dramatically increasing visually estimated leucogranite percentages as it is traced into the nose of the WLN over the same interval that kyanite is replaced by sillimanite. On the lower limb of the WLN, this same unit commonly exists only as thin, discontinuous layers and selvages of biotite + graphite melanosome interlayered with leucogranitic sheets and boudins. Given that leucogranite from this same unit was folded around the nose of the fold-nappe and yielded a Late Cretaceous ID-TIMS U-Pb zircon age of 84.8 ± 2.8 Ma, McGrew et al. (2000) concluded that sillimanite-zone, upper amphibolite facies metamorphism must have accompanied both fold-nappe emplacement and leucogranite crystallization. Re-dating the same sample by SHRIMP-RG U-Pb zircon methods yields a revised age of 83.5 ± 1.5 Ma, similar to metamorphic zircons and zircon rims from numerous lithologies in the northern EHR (Premo et al., 2014). Clover Hill is inferred to correlate with the upper limb of the WLN, but the migmatitic overprint is less severe there and the older kyanite-bearing assemblage is much better preserved than in the EHR.

Quantitative thermobarometric results for the Welcome quadrangle are summarized in table 2 and synthesized with results from the entire EHR in figure 6. Mineral rim thermobarometry from the northern EHR yields a linear trend from 800°C , 9.0 kb to 630°C , 5 kb (McGrew et al., 2000) bracketed between ~ 85 Ma as described above and ~ 63 Ma, based on the oldest $^{40}\text{Ar}/^{39}\text{Ar}$ hornblende cooling age from high structural level (figure 6) (sample 870803-1 from McGrew and Snee, 1994). Applying contemporary quantitative thermobarometric methods integrated with SHRIMP-RG U-Pb monazite and zircon geochronology, Hallett (2012) and Hallett and Spear (2011) delineate a similar P – T – t path for the upper limb of the WLN, characterized by compressional metamorphism to $\sim 700^\circ\text{C}$, 10 kb bracketed between ~ 84 Ma and 78 Ma, followed by decompression and melting during continued heating to

740°C , 7 kb by ~ 70 Ma and then cooling with continued decompression to $\sim 650^\circ\text{C}$, 5 kb by ~ 60 Ma. Though no high resolution, quantitative geochronology exists for Clover Hill, Gibbs method modeling of mineral zoning similarly indicates an early phase of metamorphism at conditions of $\sim 500^\circ\text{C}$, 10 kb followed by peak metamorphism at lower pressure conditions, 550 – 600°C , 5.5–6.0 kb (figure 6) (Hodges et al., 1992). Before ~ 75 Ma, the WLN shows a distinctive metamorphic history from the underlying Lizzies Basin block, but after ~ 75 Ma both blocks converge on a similar decompressional P – T – t path suggesting that emplacement of the WLN over the Lizzies Basin block occurred during this time window (Hallett, 2012; Hallett and Spear, 2014). The final phase of the metamorphism is clocked by growth of monazite between 40 Ma and 30 Ma at temperatures of 550 – 600°C during decompression from 5 kb to 3 kb (Hallett, 2012; Hallett and Spear, 2014). The final phase of monazite growth overlaps with late Paleogene magmatism and with the youngest $^{40}\text{Ar}/^{39}\text{Ar}$ hornblende cooling ages of ~ 30 – 38 Ma observed at deeper structural levels in the EHR (McGrew and Snee, 1994).

Other diagnostic metamorphic rock types in the Welcome quadrangle include widespread calcareous and calc-silicate lithologies and metabasite assemblages represented by amphibolite and garnet amphibolite bodies scattered throughout the Angel Lake gneiss complex. Characteristic assemblages in the metabasites include: $amph + pl \pm bt \pm gt \pm qz \pm cpx \pm ilm \pm ttn \pm mt \pm ru \pm ap \pm chl \pm cc \pm white\ mica$ (McGrew et al., 2000). Where present, garnet commonly forms embayed relict porphyroblasts partly replaced to wholly pseudomorphosed by symplectic intergrowths of $pl + hb \pm bt$. Titanite is also commonly replaced by $ilm \pm pl$. Both textures record steeply decompressional P – T – t paths (McGrew et al., 2000). Just one garnet amphibolite sample has yet been quantitatively investigated, yielding a P – T estimate of $\sim 750^\circ\text{C}$, 9.3 kb that likely represents the conditions of Late Cretaceous peak metamorphism based on comparison with the metapelitic results outlined above (McGrew et al., 2000). Marble and calc-silicate typically occur with two distinct subassemblages. An early, diopside- and carbonate-rich assemblage probably equilibrated under relatively CO_2 -rich conditions at 550 – 750°C , ≥ 6 kbar whereas a secondary subassemblage consisting of amphibole + epidote + garnet records equilibration H_2O -rich fluid at temperatures that cooled from $>600^\circ\text{C}$ to $<525^\circ\text{C}$ as metamorphism progressed (Peters and Wickham, 1994). The secondary assemblage formed during extension as evidenced by the observation that actinolitic amphibole locally grew in extensional microstructures such as asymmetric microboudin necks, normal-sense shear bands and veins oriented perpendicular to mylonitic stretching lineation.

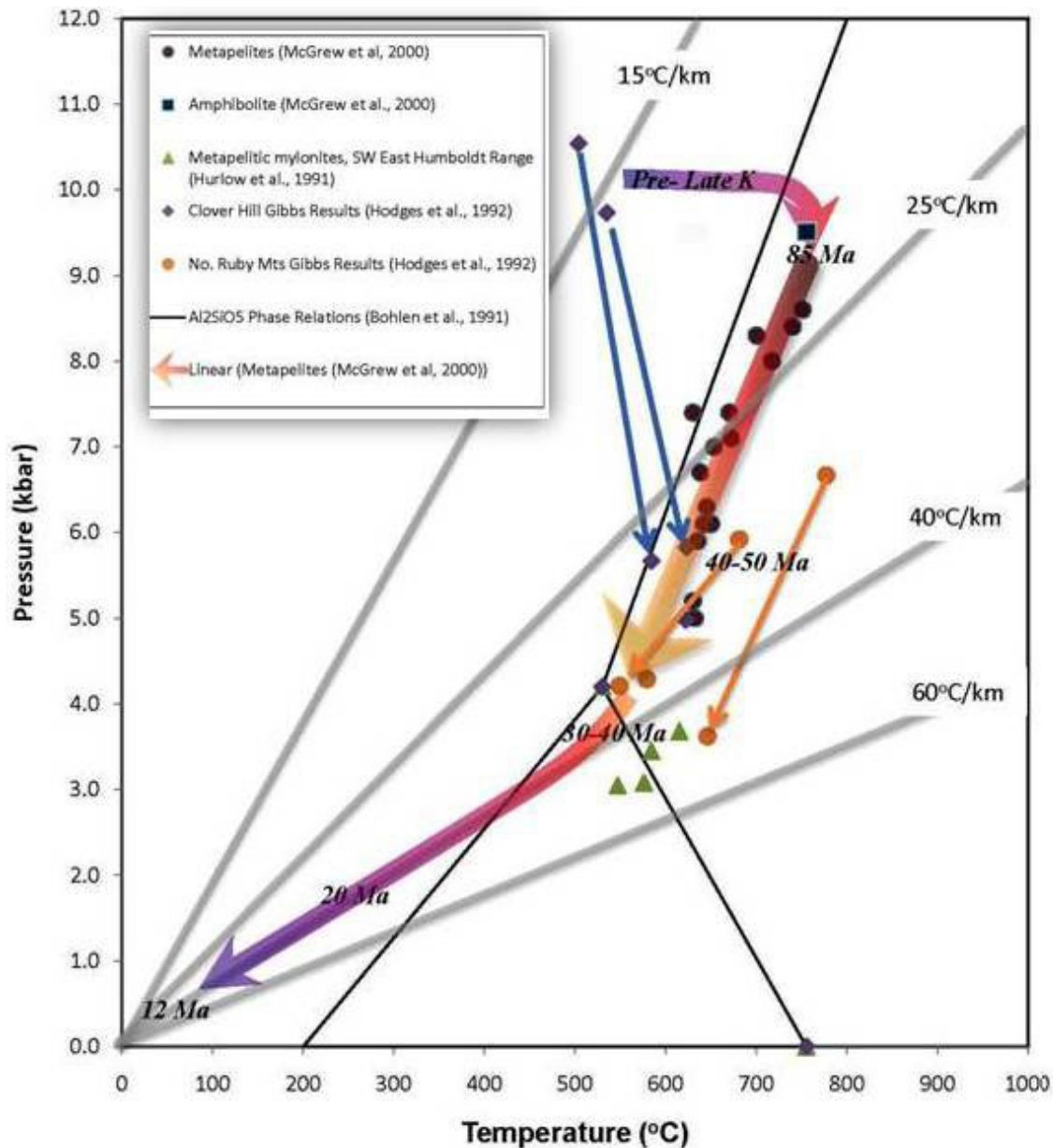


Figure 6. Interpretative diagram summarizing P-T results from rocks in the northern part of the Ruby-East Humboldt metamorphic core complex (Hurlow et al., 1991; Hodges et al., 1992; McGrew et al., 2000). Error ellipses left off to simplify viewing. The heavy-colored arrow shows the general clockwise P-T-t path inferred for the northern RM-EHR from Late Cretaceous to ~20 Ma based on integrating P-T results with thermochronological constraints (Dallmeyer et al., 1986; Dokka et al., 1986; McGrew and Snee, 1994). Shaded lines represent reference geotherms of 15°, 25°, 40°, and 60° C/km. The modern geothermal gradient in the Basin and Range Province is ~25° C/km, whereas geothermal gradients in the Battle Mountain heat-flow high range up to 40–75° C/km. Boundaries between stability fields of the Al₂SiO₅ polymorphs are included for reference (Bohlen et al., 1991).

THERMOCHRONOLOGY AND TIMING OF UNROOFING

In addition to the quantitative thermobarometry described above, the timing and progression of exhumation of the EHR is constrained by ⁴⁰Ar/³⁹Ar and fission-track thermochronology (Dallmeyer et al., 1986; Dokka et al., 1986; McGrew and Snee, 1994). ⁴⁰Ar/³⁹Ar geochronological results from the Welcome and adjacent part of the Wells quadrangle are summarized in table 3.

McGrew and Snee (1994) documented that structural levels above ca. 9350 ft (2850 m) preserve ⁴⁰Ar/³⁹Ar hornblende cooling ages ≥ 49 Ma, whereas deeper structural levels yield ⁴⁰Ar/³⁹Ar hornblende cooling ages of 30–38 Ma. Consequently, McGrew et al. (2000) concluded that the upper part of their P-T path from ca. 800 °C, 9 kb to ca. 630 °C, 5 kb must have predated 50 Ma, an interpretation further bolstered by the intrusion of the 40-Ma hornblende-biotite quartz diorite sill at pressures of 4.5–5.5 kb based on Al-in-hornblende barometry (McGrew and Snee, 1994). As noted above,

Table 3. $^{40}\text{Ar}/^{39}\text{Ar}$ Results from Welcome quadrangle. The map locations labeled in bold face correspond with the points in square text boxes on the map.

Map Location (Sample #)	Rock Type	Longitude Latitude	Elevation	Mineral	Integrated Age (Ma)	Plateau Age (Ma)	Isochron Age (Ma)	$^{40}\text{Ar}/^{39}\text{Ar}_i$	Citation
1	Willow Crk qtz porphyry rhyolite	115° 01' 13.3" 41° 04' 26.0"	2085 m (6840 ft)	san	-	15.25 ± 0.04	-	-	Brueseke & Hames, personal comm.
2	tuffaceous sandstone, Lower Humboldt Fm	115° 04' 53" 41° 05' 16"	2141 m (7020 ft)	Anorth- oclase	-	15.52 ± 0.12	-	-	Howard, Colgan & Henry, pers. comm.
3 (90B31B)	Tvs ash flow tuff	115° 04' 16.2" 41° 02' 52.7"	2225 m (7300 ft)	bt	-	38.0 ± 0.5	-	-	Brooks et al. (1995a, b)
4 (H10-79)	tuff of Campbell Creek	115° 04' 01.4" 41° 02' 37"	2195 m (7200 ft)	san	-	28.93 ± 0.07	-	-	Henry et al. (2012)
5 (NEV13-80)	mylonitic qtz dioritic orthogneiss	114° 59' 55" 41° 03' 21"	2012 m (6600 ft)	hb bt	117 ± 3	- 25.0 ± 0.8	-	-	Dallmeyer et al (1986)
6 (1-15-42)	mylonitic qtz dioritic orthogneiss	115° 00' 33" 41° 02' 42"	2268 m (7440 ft)	hb bt	72.8 ± 3.4 -	- 27.7 ± 0.8	-	-	Dallmeyer et al (1986)
7 (870623-2)	mu-bt-gt schist	115° 06' 15" 41° 02' 35.6"	2914 m (9560 ft)	mu	22.2 ± 0.3	22.1 ± 0.2	22.9 ± 0.1	253 ± 3	McGrew and Snee (1994)
8 (870614-3)	muscovite schist	115° 05' 49.5" 41° 02' 03.3"	2914 m (9560 ft)	mu	22.1 ± 0.2	22.0 ± 0.3	22.0 ± 0.1	299 ± 3	McGrew and Snee (1994)
9 (870625-1)	amphibolite	115° 05' 25.3" 41° 01' 50.5"	2877 m (9440 ft)	hb	65.5 ± 0.4	n.a.	51.0 ± 2	420 ± 90	McGrew and Snee (1994)
10 (860819-8)	Archean orthogneiss of Chimney Rock	115° 05' 33" 41° 01' 50"	2902 m (9520 ft)	Ksp	49.0 ± 0.2	-	-	-	McGrew and Snee (1994)
11 (AS-1-79)	amphibolite	115° 05' 52" 41° 01' 22"	2926 m (9600 ft)	hb bt	154 ± 6	- 25.3 ± 0.6	-	-	Dallmeyer et al. (1986)
12 (870719-2B)	biotite monzogranitic orthogneiss	115° 05' 26.25" 41° 00' 49"	2804 m (9200 ft)	bt	21.5 ± 0.2	21.4 ± 0.2	21.4 ± 0.1	298 ± 4	McGrew and Snee (1994)
13 (870803-1)	amphibolite	115° 06' 04.4" 41° 00' 35.6"	2999 m (9840 ft)	hb	80.6 ± 0.2	-	63.0 ± 2	310 ± 30	McGrew and Snee (1994)
14 (870718-1)	hb bt qtz dioritic orthogneiss	115° 05' 11.5" 41° 00' 32.7"	2579 m (8460 ft)	bt hb	20.89 ± 0.10 40.5 ± 0.3	- -	21.3 ± 0.1 30.3 ± 0.6	314 ± 2 629 ± 40	McGrew and Snee (1994)
15 (880706-2A)	amphibolite	115° 05' 46" 41° 00' 00"	3042 m (9980 ft)	bt hb	21.9 ± 0.2 44.6 ± 0.2	22.1 ± 0.2 -	22.53 ± 0.06 38.0 ± 0.5	267 ± 2 207 ± 10	McGrew and Snee (1994)

Hallett (2012) further refined the early stages of the exhumation history through SHRIMP-RG U-Pb monazite and zircon geochronology between 78 Ma and 60 Ma. Thus, a significant fraction of the decompressional history must have predated late Paleogene to Neogene extension and may either reflect a poorly understood older extensional episode or large-scale mass redistribution in the deeper crust by diapirism or deep-crustal flow.

The history of middle to late Cenozoic extensional exhumation appears to begin with the northern EHR and Clover Hill at pressures of approximately 5 kb, corresponding to paleodepths of ~18 km and temperatures in the range 450°–550°C because $^{40}\text{Ar}/^{39}\text{Ar}$ hornblende ages at deeper structural levels were reset whereas those at shallower structural levels did not close until approximately 30 Ma (McGrew and Snee, 1994). The final phase of monazite crystallization also occurred in the 30–40 Ma time range (Hallett, 2012), as did the final phase of growth of metamorphic rims on zircon at Angel Lake (Metcalf and Drew, 2011; Drew, 2013). Meanwhile, cooling through $^{40}\text{Ar}/^{39}\text{Ar}$ biotite closure temperatures occurred diachronously from ESE to WNW beginning at >30 Ma in the southeast to ~20 Ma in the northwestern part of the core complex (Kistler et al., 1981; Dallmeyer et al., 1986; McGrew and Snee, 1994). Thus, the southern part of the EHR was already cooling through $^{40}\text{Ar}/^{39}\text{Ar}$ biotite closure temperatures while rocks at deep structural levels in the central EHR were still above $^{40}\text{Ar}/^{39}\text{Ar}$ hornblende closure temperatures (approximately 200°C hotter). In the Welcome quadrangle, Dallmeyer et al. (1986) reported $^{40}\text{Ar}/^{39}\text{Ar}$ biotite cooling ages of 27.7 ± 0.8 Ma and 25.0 ± 0.8 Ma from Clover Hill and 25.3 ± 0.6 Ma at Angel Lake, whereas McGrew and Snee (1994) reported two $^{40}\text{Ar}/^{39}\text{Ar}$ muscovite cooling ages that statistically overlap at 22.0 Ma and three $^{40}\text{Ar}/^{39}\text{Ar}$ biotite cooling ages from the northern EHR that vary from 21.3 to 22.1 Ma. The WNW-directed cooling age progression is consistent with WNW-directed extensional shear sense indicators in the mylonitic zone and the overprinting of mylonitic fabrics on 29 Ma monzogranitic orthogneiss as discussed in the structural analysis section below. Little work has yet been done on lower closure temperature systems, but Dokka et al. (1986) reported a fission track titanite cooling age of 24.6 ± 2.3 Ma from Clover Hill. These authors also report a fission track apatite cooling age from Clover Hill of 26.5 ± 6.3 Ma, but the large error range and the fact that it predates nearby titanite and $^{40}\text{Ar}/^{39}\text{Ar}$ biotite cooling ages suggests that this is not a geologically meaningful result.

Despite the above cooling history, we note that a variety of evidence indicates that final exhumation of the EHR and Clover Hill did not occur until middle Miocene time. First, as shown in the *Structural Analysis* section below, strong rotation of the Miocene Humboldt Formation in Clover Valley implies that the detachment system was still active well into Miocene time. In fact,

farther south in Secret Pass, Haines and van der Pluijm (2010) report fault gouge ages of 13–11 Ma along the detachment system. In the Welcome quadrangle, clasts of lower-plate rock types derived from the EHR or Clover Hill do not appear in the stratigraphic section until deposition of Quaternary older alluvium, indicating that the metamorphic core of the EHR probably was not physically exposed at the surface until after the activation of the modern range-front fault system on the east side of the range.

STRUCTURAL ANALYSIS

As noted in the section on structural architecture above, the large-scale structure of the Welcome quadrangle is controlled by the following major features:

- a. The range-bounding normal fault systems on both sides of the EHR, and along the east side of Clover Hill (all inferred to have been active during Pleistocene to Holocene time).
- b. Clover Valley basin between Clover Hill on the east and the EHR on the west, consisting of late Paleozoic, Eocene to Oligocene, and Miocene sedimentary and volcanic rocks, all cut by brittle normal faults.
- c. A series of low-angle brittle normal faults (detachments) dropping the sedimentary and volcanic rocks of (b) down against the high-grade metamorphic core of Clover Hill.
- d. A thick zone of WNW-directed protomylonitic to mylonitic rocks several hundred meters thick increasingly well developed at higher structural levels in both the northern EHR and Clover Hill.
- e. A metamorphic core of upper amphibolite-facies migmatitic gneiss with locally developed protomylonitic zones showing a shear-sense antithetic to that of the overlying mylonitic zone.
- f. Within the metamorphic core, a multi-kilometer scale, southward-closing recumbent isoclinal fold (the WLN), cored by the Precambrian gneiss complex of Angel Lake.
- g. At least one major premetamorphic, pre-WLN thrust fault separating the gneiss complex of Angel Lake from the inferred Neoproterozoic to Paleozoic miogeoclinal sequence folded around it.

The detailed structural relationships within and between these features are more fully developed below.

Fold Relationships

The deformational history in the core of the EHR can be subdivided into at least three major fold phases, with the second fold phase being synkinematic with emplacement of the WLN and the third being synkinematic with the Cenozoic mylonitic shear zone. All three fold phases are essentially coaxial with each

other and with grain-shape lineation in the late Paleogene mylonitic shear zone, and thus identifying which of the fold phases is represented in a given outcrop is commonly problematic. We note the possibility that the older fold phases may not originally have formed coaxially but may have been rotated into coaxiality with the overprinting mylonitic stretching lineation. Accordingly, below we adopt a nomenclature with the WLN-related fold phase denoted as F_n , the younger folds as $F_{(n+1)}$ and the older folds as $F_{(n-1)}$. Despite these complexities, there are rare locations where all three fold phases can be observed in overprinting relationships, as illustrated in figure 7. This figure also serves to illustrate the style of fold transposition that commonly results in interdigitization of adjacent rock types near unit contacts. Note that figure 7 also demonstrates that the oldest generation of leucosome is folded by $F_{(n-1)}$ folds.

Foliation throughout the core of the EHR and Clover Hill is predominantly shallowly dipping (with a mean of 257° , 15° in the EHR and 206° , 8° on Clover Hill) and subparallel to small-scale fold axial surfaces with an average orientation of 264° , 14° (figure 8a, b and c). A best-fit great circle on poles to foliation defines a cylindrical fold axis oriented 300° , 11° in the EHR (figure 8a) and 279° , 8° in Clover Hill (figure 8b). These values statistically overlap the mean of small-scale fold hinge lines in the EHR, oriented 291° , 11° (figure 8c) and the mean lineation orientations in both the EHR (285° , 7°) (figure 8a) and Clover Hill (286° , 1°) (figure 8b). In addition, map-scale relationships tightly constrain the hinge line and the axial surface of the Greys Peak fold, a large second-order fold parasitic to the WLN exposed in the cirque wall west of Angel Lake (hinge line 290° , 14°).

Although the bulk of folding is probably related to the WLN, numerous folds also affect mylonitic foliation. In addition, at many localities Oligocene biotite monzogranitic sheets are also at least partially involved

in folding (figure 4). Moreover, mylonitic lineations developed in the Oligocene biotite monzogranitic rocks oriented approximately 285° , 8° are also oriented subparallel to small-scale fold hinge lines oriented on average 300° , 11° (compare figures 8c and 8d). Consequently, it is likely that the older folds were partly or wholly transposed by large magnitude extensional strain during late Paleogene deformation. Thus the original orientation of the WLN and associated folds is unknown.

Extensional Mylonitization

Overprinting the Mesozoic deformational history described above is a history of Cenozoic extension that ultimately resulted in the unroofing and exposure of the high-grade metamorphic core. The dominant feature of this history is the RM-EHR mylonitic shear zone and the overlying detachment fault. The kinematics of deformation during Cenozoic extensional unroofing are constrained by a variety of shear-sense indicators, including S-C-C' relationships, asymmetric mica fish, crystallographic preferred orientations in quartzites, extensional crenulation cleavage in pelitic schist, and shear band fabrics in quartzofeldspathic gneiss. Several lines of evidence suggest that a large fraction of the extensional strain occurred under amphibolite-facies conditions, including the following: widespread evidence of crystal-plasticity in feldspars, recrystallization of biotite along shear planes, and high-temperature quartz crystallographic preferred orientations (e.g., McGrew and Casey, 1998; McGrew and Rahl, 2014). However, locally chlorite occurs along shear planes or in the necks of asymmetrically boudinaged biotite or hornblende indicating that extensional deformation continued to lower greenschist-facies conditions, especially at higher structural levels in the mylonitic zone.

Figures 5 and 8d illustrate composite fabric



Figure 7. Field photograph illustrating interdigitization and fold transposition of the orthogneiss of Chimney Rock and the paragneiss of Greys Peak near the hinge zone of the Winchell Lake fold-nappe in central Angel Lake cirque. Three superimposed fold generations can be distinguished here. The hinge traces of each are labeled. The smaller $F_{(n+1)}$ generation folds are interpreted to be related to Cenozoic mylonitic shearing as they have the wrong sense of asymmetry to be parasitic to the larger F_n generation fold, which is isoclinally re-folds the older $F_{(n-1)}$ generation fold to form a Ramsey Type 3 interference pattern.

relationships defined by shear bands spaced at <5 mm with an average orientation of 227.5°, 22° transecting grain-shape orientation with a mean orientation of 271°, 6°. Grain-shape lineations exhibit a mean orientation of 8°, 285°, whereas “hot” slickenlines (inferred to represent the mean slip vector) plunge 24°, 275°, yielding a mean motion plane oriented 103°, 81°. With increasing structural depth there is a reversal in bulk shear-sense; >85% of shear indicators at high structural levels are WNW-directed whereas ~70% of shear-sense indicators at deeper structural levels indicate ESE-directed normal-sense shear. This suggests the existence of a large-scale, antithetic flow regime at deeper structural levels during extensional tectonism.

Upper Crustal Extensional History

The down-dropped Clover Hill fault block on the east side of the EHR affords an opportunity to appraise the relationship between upper levels of the metamorphic core complex as exposed in Clover Hill and the overlying brittlely extended cover sequence preserved in Clover Valley. The west flank of Clover Hill exposes a series of progressively younger and lower-grade to unmetamorphosed normal-fault slices listed from top to bottom as follows: 1) Cenozoic sedimentary and volcanic rocks faulted down against (2) unmetamorphosed Upper Devonian Guilmette Formation which is in turn faulted down against (3) Devonian and Silurian dolostone which is in turn faulted down against (4) a moderately metamorphosed extensional allochthon of Ordovician to Cambrian marble of Verdi Peak, which itself is faulted down against (5) the still higher grade quartzite, schist, gneiss and marble of the metamorphic core. The fact that the metamorphic core includes partly correlative but much higher grade Devonian to Cambrian marble and associated quartzite and schist implies that this extensional plexus must have overprinted a pre-existing contractile nappe stack in which lower parts were metamorphosed and upper parts were not.

Sedimentary strata in the hanging wall of the detachment fault on the west side of Clover Hill are strongly rotated to the east. Cenozoic strata define two dip domains, with the northern domain rotated to NE dips averaging 322°, 44° whereas strata in the southern domain are rotated to more SE dips averaging 034°, 33° (figure 8e). The Paleozoic strata flanking the northeastern EHR show more widely dispersed orientations no doubt partly reflecting pre-Cenozoic dips. However, they too show broadly easterly dips with a mean orientation of 342°, 32° (figure 8f). Together, these data suggest down-to-the-east rotations broadly compatible with the inferred slip direction on the underlying detachment.

Quaternary Normal Faulting

The final and demonstrably ongoing phase in the deformational history of the Welcome quadrangle is represented by the range-bounding faults. Arcing east-northeast to northeastward across the northern part of the Welcome quadrangle, the best-developed late Pleistocene to Holocene fault scarps are those of the Marys River fault system. As noted previously, this fault system extends southward along the west flank of the EHR, and the most recent rupture was likely mid-Holocene in age with an estimated recurrence interval bracketed between 5000 and 40,000 years (Wesnousky and Willoughby, 2003). We infer that the fault bounding the east side of the EHR cuts an Angel Lake-stage moraine along the north fork of Angel Creek in the eastern fore-range thus documenting it as a late Pleistocene fault system.

Farther east, the age of the Clover Hill fault is poorly constrained due to its weak geomorphic expression and the lack of well-dated Quaternary deposits on the east side of Clover Hill. However, Dohrenwend et al. (1991) infer that it cuts undivided Quaternary alluvium based on reconnaissance photogeologic mapping, and Henry and Colgan (2011) argue that the 2008 Wells Earthquake fault beneath Town Creek Flat basin represents a northward continuation of the Clover Hill fault system. Additionally, patches of boulder conglomerate exposed on the northwestern flank of Clover Hill include basalt clasts that we suggest could be sourced farther south from a small volcanic feature known as The Mound located in southern Clover Valley just north of Pleistocene Lake Clover. If correct, this hypothesis would imply a paleocourse for the Humboldt River or one of its tributaries flowing northward along the axis of Clover Valley over what is now Clover Hill, thus implying a late Pliocene to early Pleistocene age of initiation for the Clover Valley normal fault and the uplift of Clover Hill.

As the surface of the range-front fault system is not physically exposed no slickensides were observed to constrain the normal vs. strike-slip components of slip. However, the normal-sense dip separation on the range-bounding fault system on the east side of the EHR can be estimated at approximately 10,000–13,000 ft. (3000–4000 m) based on relationships in cross sections B–B' and C–C'. In addition, we note that the orthogneiss of Chimney Rock is exposed in the nose of a southward-closing map-scale fold on the east flank of Clover Hill and shows a similar occurrence in the core of the Greys Peak fold near 41° 2' 30" N on the east flank of the EHR. If these fold hinge lines are correlated, then they define a piercing point offset by the range-front fault system. A fault reconstruction can be completed based on this inferred piercing point assuming a fault orientation of 330°, 45° and a fold hinge line orientation of 290°, 10° based on map-scale fold relationships. This

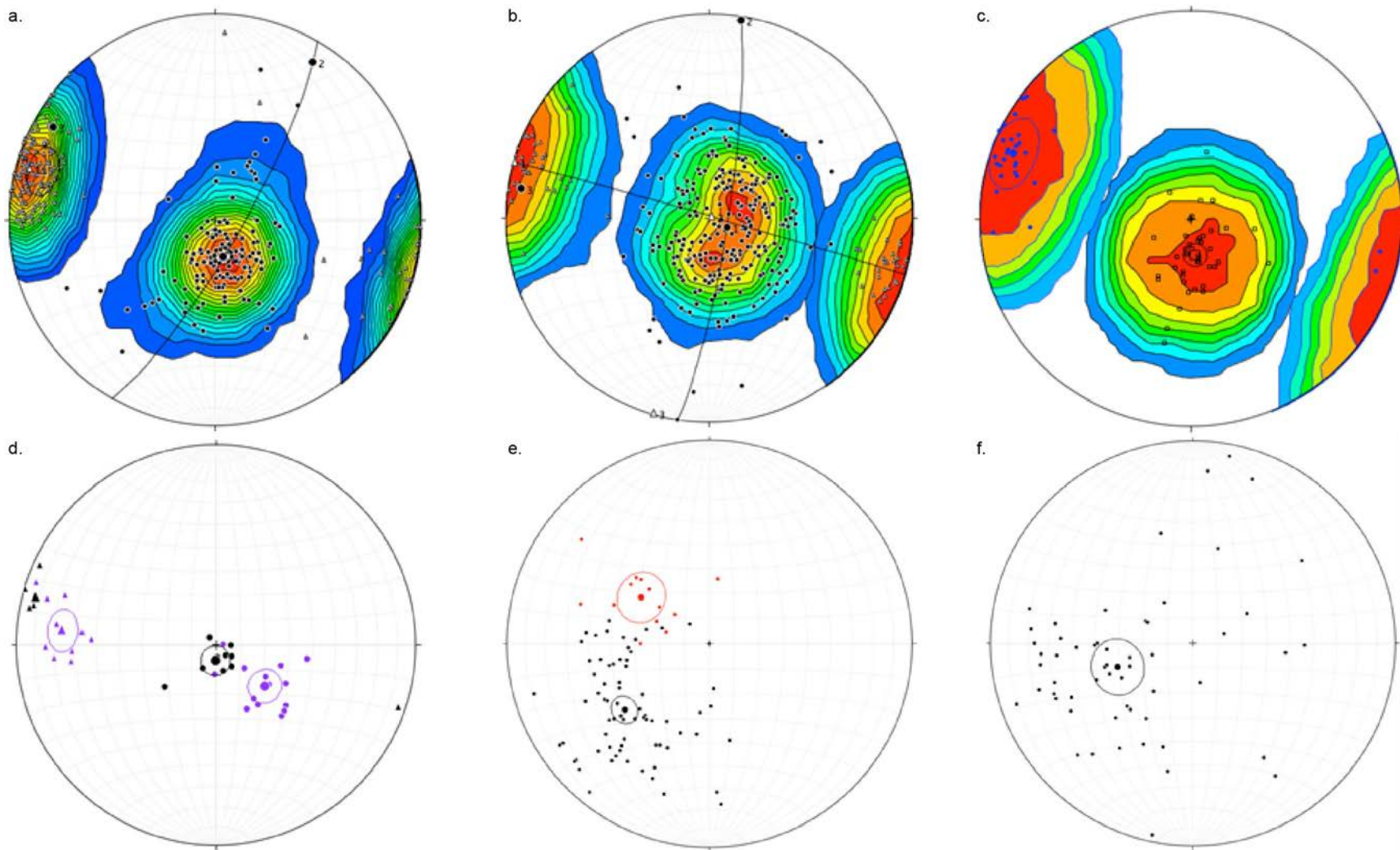


Figure 8. Equal-area, lower-hemisphere projections of structural data for the Welcome–Wells quadrangles. Kamb contours are at intervals of 2σ for all plots. (a) Foliations (filled black circles; $N = 135$) and lineations (open triangles; $N = 149$) from the EHR, with the Fisher mean foliation oriented 257° , 15° and the pole to the best-fit great circle indicating an average fold hinge line of 300° , 11° , subparallel to mean grain shape lineation oriented 285° , 7° . (b) Foliations (black filled circles; $N = 247$) and lineations (hollow black triangles; $N = 59$) from Clover Hill, with the mean foliation oriented 206° , 8° and the pole to the best-fit great circle indicating an average fold hinge line oriented 279° , 8° , subparallel to the Fisher mean grain shape lineation oriented 286° , 1° . (c) Small-scale fold data, EHR, recording a Fisher mean of small-scale fold hinge lines (blue filled circles; $N = 30$) oriented 291° , 11° and a Fisher mean of small-scale fold axial surfaces (black open squares; $N = 43$) oriented 83° , 14° . (d) S–C' relationships in protomylonitic quartzofeldspathic gneiss from the EHR (mostly 29 Ma biotite monzogranitic gneiss) recording Fisher mean of S planes (black filled circles, $N = 10$) of 271° , 6° as contrasted with the Fisher mean of C' planes (extensional shear bands) (purple filled circles; $N = 16$) oriented 227.5° , 22° . The mean of the “hot” slickenlines measured on the C' planes (purple filled triangles; $N = 12$) is oriented approximately 275° , 23° as compared with the mean of grain shape lineations (black filled triangles; $N = 6$) oriented approximately 285° , 8° . The best-fit motion plane for the deformation is oriented approximately 103° , 81° and the acute angle between the poles to C' and S-planes in this motion plane is approximately 18° , with a sense of asymmetry indicating WNW-directed extensional shear. Note: Much less widespread antithetically oriented (i.e., ESE-directed) shear-band fabrics observed mostly at deeper structural levels were omitted from this analysis. (e) Poles to bedding orientations for Tertiary strata in Clover Valley subdivided into two domains, south and north of the Angel Creek Campground road, respectively. The northern domain exhibits a mean pole orientation of 232° , 46° ($N = 74$); the southern domain shows a mean pole oriented at 304° , 56.6° ($N = 13$). (f) Poles to bedding orientations from Paleozoic units on the northeastern flank of the East Humboldt Range with the mean pole to bedding oriented at approximately 252.4° , 58° ($N = 57$). All stereonet analyses were performed using the program Stereonet 8.0 made available by R.W. Allmendinger of Cornell University (Allmendinger et al., 2012).

reconstruction yields a composite left-lateral, normal-sense displacement vector estimated at 4535 m and oriented 31°, 010°, with a rake of 48° NW, a dip-slip component of 3370 m and a strike-slip component of 3035 m. Because the fold hinge lines affect the same horizon even if they are not strictly correlative, we infer that the dip-slip component is more robustly determined than the strike-slip component. We also note the similarity of the dip-slip component to the dip separation determined above based on relationships in cross section C–C'.

Slip on the range-front fault system must have begun after 8 Ma based on cross-cutting relationships with the youngest strata rotated by the RM-EHR detachment fault (Mueller, 1992; Mueller and Snoke, 1993a, 1993b), and before 2.5 Ma based on the first appearance of lower plate clasts in Quaternary older alluvium. Consequently, the time-averaged slip rate can be bracketed between 0.5 and 1.8 mm/yr. If the fault system is assumed instead to be pure dip-slip, then the range of possible slip rates reduces to 0.37–1.35 mm/yr, but this still greatly exceeds the low slip rates (<0.2 mm/yr) inferred by Dohrenwend et al. (1991). This suggests either that the seismic risk on the east flank of the range has previously been underestimated or that the rate of slip on the eastern range-bounding fault system has greatly decelerated in the late Quaternary. This interpretation lends credence to the inference that the February 21, 2008 Wells earthquake fault correlates with the Clover Valley fault (Henry and Colgan, 2011), and raises concern for an enhanced level of seismic risk on the Clover Valley fault system despite the weak geomorphic expression of this fault.

SUMMARY AND CONCLUSIONS

In a remarkably small area, the Welcome quadrangle exposes a noteworthy array of critical relationships for understanding the geologic history of Nevada and the interior of the southwestern U.S. Cordillera. Nevada's oldest rocks (the gneiss complex of Angel Lake), and indeed its only exposures of Archean rock, form the core of a multi-kilometer scale, southward-closing recumbent fold-nappe (the Winchell Lake nappe). This fold-nappe transported what may be Nevada's most deeply exhumed rocks, with peak pressures ranging up to 10 kb and peak temperatures exceeding 750°C accompanied by widespread partial melting and *lit-par-lit* migmatization (McGrew et al., 2000; Hallett, 2012, Hallett and Spear, 2014). In addition, the Welcome quadrangle exposes an essentially complete—although intensely metamorphosed, profoundly attenuated, and tectonically shuffled—sequence of Paleoproterozoic to Mississippian metasedimentary rocks in the footwall of the RM-EHR detachment fault. Overprinting these rocks and immediately underlying the detachment fault is a WNW-directed kilometer-scale shear zone that accommodated

tens of kilometers of extensional displacement in mid- to late Cenozoic time, exhuming the terrain from mid-crustal depths. These high-grade rocks are extensively intruded by one of Nevada's most diverse suites of magmatic rocks, ranging in age from Archean to Miocene and in composition from mafic to felsic. Overlying the metamorphic complex, the detachment fault system forms a brittlely deformed plexus of partly correlative but lower grade to non-metamorphosed Paleozoic rocks. Structurally above the fault-bounded slices of Paleozoic rocks is a sequence of volcanic and sedimentary rocks, in part syntectonic that range in age from Eocene to Miocene and include a regionally rare exposure of Oligocene volcanic rock, the tuff of Campbell Creek (Henry et al., 2012). Finally, bounding the range today on both east and west are large, normal-fault systems that were demonstrably active in Quaternary time, and in the case of the Clover Hill fault, may represent a southerly extension of the blind fault that caused the 2008 M_w 6.0 Wells earthquake (Henry and Colgan, 2011).

DESCRIPTION OF MAP UNITS

Qy – Youngest alluvium (upper Holocene) – Unconsolidated silt, sand, and gravel of fluvial origin filling active stream channels and adjacent flood plains, mostly inset into coalesced alluvial fans on the northern flank of the East Humboldt Range. Clasts include a wide variety of rock types recognizable from the mountains to the south. At most about 5 m thick.

Qls – Landslide deposit (Holocene) – Coarse, unconsolidated debris consisting of local bedrock and remobilized glacial deposits; forms hummocky topography.

Qt – Talus deposit (Holocene) – Coarse (10 cm to >3 m), angular rock debris with little fine matrix and sparse vegetation, mostly occupying steep slopes beneath cliffs or moderate slopes in alpine environments subject to strong frost action.

Qc – Colluvium (Holocene) – Soil consisting of poorly sorted silt, sand, gravel, and locally some talus mantling steep slopes with enough fine matrix to support grassy or brushy vegetation.

Qya – Younger alluvium (Holocene) – Unconsolidated silt, sand, and gravel of fluvial origin older than the active stream channels and adjacent flood plains. This unit exists as alluvial fans developed on the northern flank of the East Humboldt Range and eastern flank of Clover Hill. Clasts include a wide sampling of rock types recognizable from the adjacent mountains. At most about 8 m thick.

Qoa – Older alluvium (Pleistocene) – Weakly consolidated or unconsolidated silt, sand, and gravel mantling alluvial fan surfaces away from or above active stream channels. This unit veneers terraces underlain by bedrock on the eastern flank of the northern East Humboldt Range. Clasts include a wide sampling of rock types recognizable from the adjacent mountains.

Qg – Glacial deposits (Pleistocene) – Chiefly includes morainal deposits, Lamoille and Angel Lake stages (Sharp, 1938; Wayne, 1984) undivided.

QTj – Jasperoid breccia (Quaternary to Tertiary, age uncertain) – Massive siliceous breccia, commonly re-cemented by quartz, associated with normal-sense fault zones (either high- or low-angle), commonly black to dark or medium gray on a fresh surface; a rusty red patina is characteristic of some outcrops. This unit also includes cream-colored to white siliceous breccia and vuggy siliceous veins. All these siliceous rock types are interpreted as the result of hydrothermal replacement of an original host rock. Some small bodies of jasperoid breccia are unmapped.

Tbc – Boulder conglomerate (upper Miocene or Pliocene?) – Flat-lying boulder conglomerate including boulders and cobbles of the Willow Lake rhyolite suite, metamorphosed Eureka Quartzite (equigranular to mylonitic texture), gray calcite marble with muscovite or siliceous layers, amygdaloidal pyroxene basalt, Paleozoic limestone ± chert, Mississippian Diamond Peak Formation, and Tertiary lacustrine limestone. The matrix is poorly sorted and consists of angular clasts (some reach up ~2 cm in diameter), grit, sand, and silt in a calcareous cement. 7 to 15 m thick.

Tls – Landslide deposit (upper Miocene) – Brecciated and silicified quartz porphyry rhyolite (**Tr₂**)

Th₂ – Humboldt Formation, Unit 2 (middle to upper Miocene) – Conglomerate, sandstone, siltstone, lacustrine limestone, and vitric ash. Rhyolite dikes (part of Willow Creek rhyolite suite) intrude the lower part of this unit. However, Mueller (1992) reports a fission-track zircon age of 8.3 ± 0.9 Ma on vitric ash from the upper exposed part of this unit (his sample WE-1). Clasts in conglomerate and sandstone beds are chiefly derived from the Mississippian Diamond Peak Formation, reworked Tertiary sedimentary and volcanic rocks, and metamorphosed white to light gray (graphite-bearing) Eureka Quartzite with an equigranular texture. At least 2000 m thick.

Tvb – Vesicular basalt (middle Miocene) – Lava flow with scattered phenocrysts of plagioclase.

Willow Creek rhyolite suite (middle Miocene)

Tr₃ – Maroon rhyolite with small phenocrysts of quartz and feldspar (1–2 mm).

Trvb – Volcaniclastic breccia – Silicified volcaniclastic breccia. Clasts are chiefly quartz and feldspar-phyric rhyolite but also include angular clasts to rounded cobbles of white metaquartzite (**Oe**). Possible talus deposit accumulated along the flank of an emergent rhyolite dome.

Tr₂ – Quartz porphyry rhyolite – Intrusive to extrusive phase (rhyolite dome). Brown to red-brown to deep red on weathered surfaces, pearly gray to red-brown on the fresh break. Conspicuously porphyritic (quartz and feldspar-phyric), locally vitrophyric. Massive with slabby cleavage locally developed. Commonly the small intrusive masses and dike-like bodies are autobrecciated. Sanidine from a sample of quartz and feldspar-phyric rhyolite porphyry, collected at Locality 1, yielded an $^{40}\text{Ar}/^{39}\text{Ar}$ age of 15.25 ± 0.04 Ma (M.E. Brueseke and W. Hames, unpublished data, personal comm., 2013). At most 500 m thick.

Tr₁ – Rhyolite – Commonly weathers brownish red to brick red to orange red. Small phenocrysts of feldspar and quartz (1–2 mm). Scarce black vitrophyre at the base of some flows (vitrophyre commonly contains green clinopyroxene). Locally vesicular, vesicles typically are filled with quartz and/or calcite. Jasper is common. Locally spectacular flow features including deformed vesicles, flow layering, flow breccia, and flowage folds. Some intercalated sedimentary rocks, chiefly yellow to orange-red siliceous siltstone. At most 500 m thick.

Tsu – Tertiary sedimentary rocks, undivided (lower to middle Miocene) – This unit is a composite of the sedimentary sequence of Clover Creek and Humboldt Formation, Unit 1.

Th₁ – Humboldt Formation, Unit 1 (middle Miocene) – Volcaniclastic pebble conglomerate and coarse sandstone, tuffaceous and siliceous siltstone, and lacustrine silty limestone (fossiliferous). Eleven anorthoclase grains from a tuffaceous sandstone collected by K.A. Howard and J.P. Colgan from locality 2 were dated at the New Mexico Geochronology Research Laboratory by C.D. Henry and yielded an $^{40}\text{Ar}/^{39}\text{Ar}$ age of 15.52 ± 0.12 Ma. Approximately 500 m thick.

Tcc – Sedimentary sequence of Clover Creek (lower Miocene?) – Thick-bedded, poorly sorted conglomerate

and sedimentary breccia, coarse sandstone, calcareous sandstone, lacustrine limestone (locally fossiliferous), and megabreccia (**Tmb**). The megabreccia deposits in the sedimentary sequence of Clover Creek are chiefly composed of brecciated, unmetamorphosed Upper Devonian Guilmette Limestone; however, several megabreccia bodies consist of brecciated Middle Devonian metadolomite and metasandstone. Approximately 900 m thick.

Tvs – Volcaniclastic conglomerate and sandstone, andesitic flows and flow breccia, dacitic to rhyolitic tuff, and rhyolite lavas (lower Oligocene to middle Eocene) – Brooks et al. (1995b) reported an $^{40}\text{Ar}/^{39}\text{Ar}$ biotite date of 38.0 ± 0.5 Ma (their sample 90B31B) from an ash-flow tuff collected from this unit (Locality 3). These authors considered this date as a minimum age. Henry et al. (2012) reported the presence of the early Oligocene tuff of Campbell Creek as an upper member in the **Tvs** unit. This correlation is based on an $^{40}\text{Ar}/^{39}\text{Ar}$ age of $28.93 \pm .07$ Ma and whole-rock geochemical data (their sample H10-79, Locality 4). Henry et al. (2012) interpret the tuff of Campbell Creek to be preserved in a paleovalley. Structural thickness at least 250 m.

Unmetamorphosed Sedimentary Rocks

Pm – Murdock Mountain Formation (Permian) – Light-gray dolomite with nodular chert, gray limestone, bedded chert, siltstone, fine- to coarse-grained sandstone, and chert-clast conglomerate. The Murdock Mountain is part of the Park City Group in eastern Nevada (Wardlaw and Collinson [1978] and Wardlaw et al., [1979]). Structural thickness at least 325 m.

Pp – Pequop Formation of Steele (1960) (Lower Permian) – Purplish-gray, platy (slope-forming) silty limestone and massive to thick-bedded, medium- to dark-gray, fine-grained limestone; locally fusulinid-rich coquina; yellow-weathering, calcareous fine-grained sandstone. Structural thickness at least 200 m.

Pe – Ely Limestone (Pennsylvanian) – Light- to medium-gray resistant thick-bedded limestone with gray to black nodular or lenticular chert; locally includes bioclastic limestone with brachiopod fauna, crinoid columnals, and other fossil fragments. Structural thickness at least 80 m.

Mdp – Diamond Peak Formation (Mississippian) – Dark yellow to red-weathering, subangular to subrounded chert/quartzite-clast conglomerate and grit, tan-weathering sandstone, black shale, and locally massive medium gray micritic limestone with sparse irregular chert nodules. Structural thickness at most 325 m.

Dg – Guilmette Formation (Upper Devonian) – Massive bedded, dark gray to black limestone that is highly veined by calcite. Commonly fossiliferous containing stromatoporoids, bryozoa, corals, crinoid debris, gastropods, and brachiopods (Snelson, 1957; Lush, 1982). This unit occurs as a fault-bounded slice on the southwestern flank of Clover Hill.

DSd – Dolostone (Devonian to Silurian, undivided) – Laminated black, fine- to medium-grained dolostone, thick-bedded medium- to dark-gray dolostone, and quartz sandstone (Lush, 1982). The unit is commonly brecciated and cemented by either a carbonate and/or siliceous matrix between the fragments. The lithologic character of this undivided dolostone unit suggests that it may include some elements of the Silurian Laketown Dolomite but mostly consists of Lower Devonian Sevy Dolomite and Middle Devonian Simonson Dolostone. This unit occurs as a fault-bounded slice between structurally higher, unmetamorphosed Upper Devonian Guilmette Formation and structurally lower Ordovician to Cambrian marble of Verdi Peak on the south end of Clover Hill. The same unit underlies most of Signal Hill, located immediately to the south, in the Humboldt Peak quadrangle (McGrew, in review).

Metamorphosed Sedimentary and Igneous Rocks

MCmu – Calcite and dolomite marble with calc-schist, calc-silicate paragneiss, and white metaquartzite (Mississippian to Cambrian, undivided) – In most areas this unit probably consists chiefly of Ordovician to Cambrian marble and associated calc-silicate schist, paragneiss, and quartzite. However, in places this unit cannot be reliably separated from overlying dolomitic and calcitic marble units, and so is left undivided. Common rock types include: coarse-grained white marble, medium- to coarse-grained gray marble (locally micaceous), dolomitic marble, coarse-grained cream- to yellow-weathering marble with large blades of tremolite, diopside-bearing white quartzite (probably Kanosh Formation), and thin layers of calcareous paragneiss or calc-schist. Overall, this unit is inferred to correlate with the carbonate-dominated part of the Cordilleran miogeoclinal sequence. This is commonly intruded by muscovite \pm biotite pegmatitic leucogranite and leucogranitic orthogneiss.

MDgs – Graphitic schist and calcareous paragneiss (Mississippian to Upper Devonian?) – Graphite-bearing micaceous feldspathic quartzite and quartzofeldspathic schist (commonly calcareous), pelitic schist, and local calc-silicate paragneiss, all rich in opaque minerals and hence weathering to a rusty red-brown. Characteristic metamorphic mineral assemblages in pelitic schist include biotite, sillimanite, kyanite

(thickly mantled or completely pseudomorphosed by sillimanite), garnet, plagioclase, and quartz with accessory rutile, ilmenite, and titanite. Inferred to correlate with the Pilot Shale.

Dgm – Metamorphosed Guilmette Formation (Upper Devonian) – Color-banded calcite ± dolomite marble, commonly graphitic. Equivalent to the “marble of Snell Creek” of Howard (1971, 2000).

DOdm – Dolomitic marble (Devonian to Ordovician, undivided) – White to dark gray, medium- to coarse-grained typically massive dolomitic marble with subordinate meta-sandstone and calc-silicate rock. Locally includes calcite marble (possibly correlating with Upper Devonian Guilmette Formation). Correlated with the Middle Devonian Simonson Dolomite, Lower Devonian Sevy Dolomite, Silurian Laketown Dolomite, and Upper Ordovician Fish Haven Dolomite. On the southwest flank of Clover Hill a fault-bounded slice of greenschist-facies metadolomite and metasandstone occurs above mylonitic marble of Verdi Peak (O€m) and below unmetamorphosed Guilmette Formation (Dg). Devonian Sevy Dolomite, Silurian Laketown Dolomite, and Upper Ordovician Fish Haven Dolomite. On the southwest flank of Clover Hill a fault-bounded slice of greenschist-facies metadolomite and metasandstone occurs above mylonitic marble of Verdi Peak (O€m) and below unmetamorphosed Guilmette Formation (Dg).

Oe – Metamorphosed Eureka Quartzite (Ordovician) – Coarse-grained, white metaquartzite, commonly with white diopside, forms thin, discontinuous layer (commonly 1–3 m thick) marking the contact between the marble of Verdi Peak (O€m) and dolomitic marble (DOdm). Locally pinches out due to tectonic attenuation.

O€m – Marble of Verdi Peak (Ordovician to Cambrian, undivided) – Pale gray, graphitic, muscovite-bearing calcite ± dolomite marble; calc-silicate marble; yellow-brown-weathering metadolomite. On Clover Hill, this unit is mylonitic and locally includes lenses of muscovite ± biotite leucogranite and leucogranitic orthogneiss.

€Zpm – Metamorphosed Prospect Mountain Quartzite (Cambrian to Neoproterozoic protolith age) and McCoy Creek Group (Neoproterozoic protolith age), undivided – Micaceous feldspathic quartzite with subordinate pelitic schist, and locally with calc-silicate gneiss and rare para-amphibolite. Commonly migmatitic, with pelitic rocks hosting a higher percentage of leucosome than quartzitic rocks. Leucosome occurs in centimeter-scale to meter-scale concordant pods, sheets, and lenses commonly bordered by mica and sillimanite-rich melanosome. Characteristic metamorphic mineral assemblages in pelitic schist

include biotite, sillimanite, kyanite (commonly thickly mantled or completely pseudomorphosed by sillimanite), garnet, plagioclase, and quartz with accessory rutile, ilmenite, and titanite. On Clover Hill the pelitic schist in this unit locally contains abundant kyanite porphyroblasts and only minor fibrolite sillimanite (Snoke, 1992).

Zc – Metaconglomerate and metaquartzite (Neoproterozoic?) – Mylonitic and strongly folded, quartz-pebble metaconglomerate and metaquartzite. This rock type occurs as a tectonic inclusion surrounded by the M€mu unit on the east face of Clover Hill. Inferred to correlate with Units G or F of the McCoy Creek Group of Misch and Hazzard (1962) and Miller (1983, 1984).

Gneiss Complex of Angel Lake

ZWal – Gneiss complex of Angel Lake, undivided (Neoproterozoic to Neoproterozoic) – This unit is a composite of the paragneiss of Greys Peak and orthogneiss of Chimney Rock.

ZXpg – Paragneiss of Greys Peak (Neoproterozoic to Paleoproterozoic) – Impure micaceous and/or feldspathic metaquartzite and metapsammitic paragneiss, biotite-sillimanite schist (locally with garnet), and rare white metaquartzite or pale to apple green fuchsitic metaquartzite. Also hosts widespread meter-scale layers and boudins of melanocratic amphibolite and garnet amphibolite interpreted as metamorphosed small mafic intrusions. Migmatization is widespread with more pelitic components commonly hosting large volumes of leucosome, especially at deeper structural levels on the lower limb of the Winchell Lake fold. Detrital zircon geochronology of most samples defines a strong minimum provenance of Grenville age (800–1250 Ma) supporting correlation with the McCoy Creek Group, but a sample of fuchsitic quartzite shows a much older minimum age provenance of ~2400 Ma suggesting that the unit may locally include Paleoproterozoic rocks (Premo et al., 2014).

XWpg – Paragneiss of Angel Lake (Paleoproterozoic to Neoproterozoic?) – Micaceous quartzofeldspathic paragneiss, rare metaquartzite, severely migmatized biotite and biotite-sillimanite schist (rarely with garnet) that commonly contains at least 50% leucogranitic rock. Also present are meter-scale sheets and boudins of melanocratic amphibolite and garnet amphibolite. Detrital zircon geochronology defines two provenance age groups: One group shows a near-singular provenance

age of ~2550 Ma and thus could be as old as Neoproterozoic, whereas the other group has a minimum provenance age of ~2450 Ma (Premo et al., 2014). Metamorphic zircon overgrowths at ~1770 Ma require that original deposition occurred no later than Paleoproterozoic (Premo et al., 2014).

XWog – Orthogneiss of Chimney Rock (Paleoproterozoic to Neoproterozoic) – Coarse-grained, light gray biotite quartzofeldspathic gneiss, locally with alkali feldspar augen up to 1 cm in diameter. Migmatization is nearly ubiquitous, with biotite selvages between stromatic leucosomes imparting a strong “striped” appearance. Meter-scale sheets and boudins of melanocratic amphibolite and garnet amphibolite are widespread but volumetrically minor. A minimally migmatized sample yielded a SHRIMP U-Pb zircon age of 2449 ± 3 Ma (Premo et al., 2014).

Intrusive Rocks

Trd – Rhyolite dikes (middle Miocene) – Dark pink-weathering quartz + feldspar-phyric dikes with small phenocrysts. These dikes are inferred to be petrogenetically and temporally associated with the Willow Creek rhyolite suite.

Tb – Basaltic dikes (middle Miocene) – Black, locally amygdaloidal, commonly with chilled margins and locally with diabasic cores. Dashed where approximately located.

Tmg – Biotite monzogranite orthogneiss (lower Oligocene to middle Eocene) – Weakly to moderately foliated medium grained, equigranular biotite monzogranite and subordinate tonalite and granodiorite, locally with small feldspar phenocrysts. At higher structural levels protomylonitic fabrics are well developed and indicate west- to northwest-directed shear. Contains approximately 10% biotite and subequal proportions of oligoclase, alkali feldspar and quartz. Accessory phases include apatite, zircon, monazite, allanite, and opaque phases. Typically forms meter-scale concordant to slightly discordant sheets, but locally forms laccolithic intrusive centers with dimensions on the order of tens of meters. Dated at 29 ± 0.5 Ma by U-Th-Pb zircon and monazite methods (Wright and Snoke, 1993, their sample RM-5, Locality B).

Tqd – Hornblende-biotite quartz diorite orthogneiss (middle Eocene) – Well-foliated (locally with well-developed, west- to northwest-directed-protomylonitic fabric at high structural levels), mostly equigranular-quartz-dioritic orthogneiss consisting of >60% andesine, 15–30% hornblende plus biotite, 10–20% quartz, and sparse to absent alkali feldspar. Titanite is the most

abundant accessory mineral, locally forming distinctive coarse amber-colored grains. Other accessories include: apatite, zircon, allanite, epidote, xenotime, scarce garnet, and relatively sparse opaque oxide phases. This intrusive body forms a thick sill centered on Lizzies Basin where it exceeds 500 m in thickness, tapering both northward and southward to thicknesses between 60 m and 200 m. Dated at 40 ± 3 Ma with U-Pb (zircon) techniques (Wright and Snoke, 1993).

TKlg – Leucogranite and leucogranitic orthogneiss (Paleogene to Cretaceous) – Predominantly moderately to strongly foliated granitic pegmatite, but also including trondhjemitic pegmatite, muscovite-rich two-mica leucogranite, and weakly foliated, late-stage garnet aplite dikes. Foliated leucogranites mostly form small concordant sheets, pods or lenses, commonly bounded by biotite-sillimanite melanosomes. In contrast, weakly foliated leucogranitic bodies commonly form dikes cutting gneissic foliation. A folded leucogranitic sheet in the hinge zone of the Winchell Lake fold-nappe yields a $^{207}\text{Pb}^*/^{206}\text{Pb}^*$ zircon date of 85 ± 3 Ma, resembling leucogranite ages from the southern East Humboldt Range and Ruby Mountains (Snoke et al., 1990; McGrew et al., 2000). Although much of the leucogranite is probably Late Cretaceous, a relatively small proportion of leucogranitic rocks are observed cutting or intermingled with the 40 Ma quartz diorite and 29 Ma biotite monzogranitic sheets and therefore must be mid-Tertiary in age.

ACKNOWLEDGMENTS

The geologic mapping of A.J. McGrew in the main range of the EHR could not have been completed without invaluable assistance from numerous undergraduate field assistants, including: Christopher Jayne and Brian Kirchner (both of Earlham College), and James P. Hogan, Andrew Folfas, Jared Stoffel, Anthony Asher, Brian Joyce, Timothy Cornett, and Will Vanderslice (all from the University of Dayton). In addition, this mapping project has profited greatly from discussions and collaborations with Melissa Batum, Calvin Barnes, Phyllis Camilleri, Callum Hetherington, Keith Howard, Michael Hudec, Hugh Hurlow, Karl Mueller, Mark Peters, Karri Sicard, Lawrence Snee, Charles Thorman, Steve Wickham, and numerous other colleagues who have visited the area on field trips. Ben Hallett generously shared access to his seminal results and ideas as his work in the area progressed. Wayne Premo, Christopher Henry, and Matthew Brueseke generously shared unpublished geochronological data. We thank Richard Allmendinger for making the Stereonet 8.0 software package freely available to us and the entire academic geological community. Finally, we thank Phyllis A. Ranz for her expert help on the cartography of

the geologic map as well as preparation of figures accompanying this report; and Rachel Wearne with the Nevada Bureau of Mines and Geology for her cartographic updates to the geologic map.

Funding for this project has derived from several sources over the years: multiple NSF Research Grants awarded to A.W. Snoke (University of South Carolina and University of Wyoming), University of Wyoming teaching and research fellowships, NSF Post-doctoral Research Fellowship EAR 92-08855 awarded to Allen J. McGrew, a Geological Society of Nevada quadrangle Mapping grant, a grant of financial assistance from Dale Kraemer, and University of Dayton Grants in Aid of Research.

Christopher Henry of the Nevada Bureau of Mines and Geology arranged much-appreciated office and field reviews of our geologic mapping as well as offering a broad array of insightful advice. Keith Howard and Joe Colgan provided detailed, informative, and helpful review comments that greatly improved the geologic map and accompanying pamphlet.

REFERENCES

- Allmendinger, R.W., Cardozo, N.C., and Fisher, D., 2012, structural geology algorithms—vectors & tensors: Cambridge, England, Cambridge University Press, 289 p.
- Armstrong, R.L., 1968, Mantled gneiss domes in the Albion Mountains, southern Idaho: Geological Society of America Bulletin, v. 79, p. 1295–1314.
- Armstrong, R.L., 1972, Low-angle (denudation) faults, hinterland of the Sevier Orogenic Belt, eastern Nevada and western Utah: Geological Society of America Bulletin, v. 83, p. 1729–1754.
- Batum, M.A., 2000, Petrology of Late Cretaceous and Cenozoic granitic rocks, East Humboldt Range, northeastern Nevada [M.S. thesis]: Lubbock, Texas Tech University, 167 p.
- Blackwelder, E., 1931, Pleistocene glaciation in the Sierra Nevada and basin ranges: Geological Society of America Bulletin, v. 42, p. 865–922.
- Bohlen, S.R., Montana, A., and Kerrick, D.M., 1991, Precise determination of the equilibria kyanite \leftrightarrow sillimanite and kyanite \leftrightarrow andalusite and a revised triple point for Al_2SiO_5 polymorphs: American Mineralogist, v. 76, p. 677–680.
- Brooks, W.E., Thorman, C.H., and Snee, L.W., 1995a, The $^{40}\text{Ar}/^{39}\text{Ar}$ ages and tectonic setting of the middle Eocene northeast Nevada volcanic field: Journal of Geophysical Research, v. 100, p. 10,403–10,416.
- Brooks, W.E., Thorman, C.H., Snee, L.W., Nutt, C.J., Potter, C.J., and Dubiel, R.F., 1995b, Summary of chemical analyses and $^{40}\text{Ar}/^{39}\text{Ar}$ age-spectra data for Eocene volcanic rocks from the central part of the Northeast Nevada Volcanic Field: U.S. Geological Survey Bulletin 1988-K, K1–K33.
- Brueseke, M., Calliccoat, J.S., Hames, W., and Larson, P.B., 2014, Mid-Miocene rhyolite volcanism in northeastern Nevada—the Jarbidge Rhyolite and its relationship to the Cenozoic evolution of the northern Great Basin (USA): Geological Society of America Bulletin, v. 126, p. 1047–1067.
- Bryant, B., 1988, Geology of the Farmington Canyon complex, Wasatch Mountains, Utah: U.S. Geological Survey Professional Paper 1476, 54 p.
- Camilleri, P.A., 2010, Geologic map of the Wood Hills, Elko County, Nevada: Nevada Bureau of Mines and Geology Map 172, 1 sheet, scale 1:24,000, 16 p.
- Coats, R.R., 1964, Geology of the Jarbidge quadrangle, Nevada–Idaho: U.S. Geological Survey 1141–M, M1–M24.
- Coats, R.R., 1987, Geology of Elko County, Nevada: Reno, Nevada Bureau of Mines and Geology Bulletin 101, 112 p.
- Colgan, J.P., Howard, K.A., Fleck, R.J., and Wooden, J.L., 2010, Rapid middle Miocene extension and unroofing of the southern Ruby Mountains, Nevada: Tectonics, v. 29, TC6022, doi:10.1029/2009TC002655.

- Compton, R.R., 1972, Geologic map of the Yost quadrangle, Box Elder County, Utah, and Cassia County, Idaho: U.S. Geological Survey Miscellaneous Geological Investigation Series Map I-672, scale 1:31,680, 7 p.
- Compton, R.R., 1975, Geologic map of Park Valley quadrangle, Box Elder County, Utah, and Cassia County, Idaho: U.S. Geological Survey Miscellaneous Geological Investigation Series Map I-873, scale 1:31,680, 6 p.
- Compton, R.R., Todd, V.R., Zartman, R.E., and Naeser, C.W., 1977, Oligocene and Miocene metamorphism, folding, and low-angle faulting in northwestern Utah: Geological Society of America Bulletin, v. 88, p. 1237–1250.
- Crittenden, M.D., Jr. and Sorenson, M.L., 1980, The Facer Formation, a new Early Proterozoic unit in northern Utah: U.S. Geological Survey Bulletin 1482-F, F1–F28.
- Dahl, P., Hamilton, M., Wooden, J., Foland, K., Frei, R., MacCombs, J., and Holm, D., 2006, 2480 Ma mafic magmatism in the northern Black Hills, South Dakota—a new link connecting the Wyoming and Superior cratons: Canadian Journal of Earth Sciences, v. 43, p. 1579–1600.
- Dallmeyer, R.D., Snoke, A.W., McKee, E.H., 1986, The Mesozoic–Cenozoic tectonothermal evolution of the Ruby Mountains, East Humboldt Range, Nevada—a Cordilleran metamorphic core complex: Tectonics, v. 5, p. 931–954.
- Dokka, R.K., Mahaffie, M.J., and Snoke, A.W., 1986, Thermochronologic evidence of major tectonic denudation associated with detachment faulting, northern Ruby Mountains–East Humboldt Range, Nevada: Tectonics, v. 5, p. 995–1006.
- Dohrenwend, J.C., McKittrick, M.A., and Moring, B.C., 1991, Reconnaissance photogeologic map of young faults in the Wells 1° by 2° quadrangle, Nevada, Utah, and Idaho: U.S. Geological Survey Miscellaneous Field Studies Map MF-2184, 1 sheet, scale 1:250,000.
- Drew, J., 2013, Cretaceous and Eocene U-Pb zircon migmatite ages from the East Humboldt Range metamorphic core complex, Nevada: University of Nevada, Las Vegas, M.S. thesis, 65 p.
- Eardley, A.J., and Hatch, R.A., 1940, Precambrian crystalline rocks of north-central Utah: Journal of Geology, v. 48, p. 58–72.
- Ehman, K.D., and Clark, T.M., 1990, Upper Proterozoic–Middle Cambrian miogeoclinal stratigraphy of the Bull Run Mountains, northern Nevada—implications for the early evolution of the Cordilleran rifted margin: Nevada Bureau of Mines and Geology, Open-file Report 90-5, 52 p.
- Frerichs, W.E., and Pekarek, A.H., 1994, Lower Miocene petroleum potential of northeast Elko County, Nevada, in Schalla, R.A., and Johnson, E.H., editors, Oil fields of the Great Basin: Reno, Nevada Petroleum Society, p. 151–158.
- Gans, P.B., and Miller, E.L., 1983, Style of mid-Tertiary extension in east-central Nevada, in Nash, W.P., and Gurgel, K.D., editors, Geological excursions in the overthrust belt and metamorphic complexes of the intermontane region: Utah Geological and Mineral Survey Special Study 59, p. 107–160.
- Good, S.C., Nester, P.L., and Snoke, A.W., 1995, Lacustrine mollusks from the Lower Humboldt Formation, northeastern Nevada, and possible late Eocene to Oligocene age: Geological Society of America Abstracts with Programs, v. 27, no. 1, p. 49.
- Hague, A., 1883, Report on the geology of the Eureka district, Nevada: U.S. Geological Survey, 3rd Annual Report, v. 37, p. 237–272.
- Hallett, B.W., 2012, Metamorphic history and timescales of cooling and exhumation of partially melted rocks—studies in the North American Cordillera: Troy, N.Y., Rensselaer Polytechnic Institute, Ph.D. Thesis, 213 p.
- Hallett, B.W., and Spear, F.S., 2011, Linking metamorphic monazite growth to the P–T path using major and trace element zoning in garnet and monazite from migmatitic pelites of the East Humboldt Range, Nevada: Geological Society of America Abstracts with Programs, v. 43, no. 5, p. 330.
- Hallett, B.W., and Spear, F.S., 2014, The P–T history of anatectic pelites of the northern East Humboldt Range, Nevada—evidence for tectonic loading, decompression, and anatexis: Journal of Petrology, v. 55, p. 3–36.
- Heaman, L., 1997, Global mafic magmatism at 2.45 Ga—remnants of an ancient large igneous province: Geology, v. 25, p. 299–302.
- Henry, C.D., and Colgan, J.P., 2011, The regional structural setting of the 2008 Wells earthquake and Town Creek Flat basin—implications for the Wells earthquake fault and adjacent structures, in dePolo, C.M. and LaPointe, D.D., 2011, The 21 February 2008 Mw 6.0 Wells, Nevada Earthquake—a compendium of earthquake-related investigations prepared by the University of Nevada, Reno, Nevada Bureau of Mines and Geology Special Publication 36, p. 53–64.
- Henry, C.D., McGrew, A.J., Colgan, J.P., Snoke, A.W., and Brueseke, M.E., 2011, Timing, distribution, amount, and style of Cenozoic extension in the northern Great Basin, in Lee, J., and Evans, J.P., editors, Geologic field trips to the Basin and Range, Rocky Mountains, Snake River Plain, and Terranes of the U.S. Cordillera: Geological Society of America Field Trip Guide 21, p. 27–66.
- Henry, C.D., Hinz, N.H., Faulds, J.E., Colgan, J.P., John, D.A., Brooks, E.R., Cassel, E.J., Garside, L.J., Davis, D.A., and Castor, S.B., 2012, Eocene–Early

- Miocene paleotopography of the Sierra Nevada–Great Basin–Nevadaplano based on widespread ash-flow tuffs and paleovalleys: *Geosphere*, v. 8, no. 1, p. 1–27, doi:10.1130/GES00727.1.
- Hope, R., 1972, Geologic map of the Spruce Mountain quadrangle, Elko County, Nevada: U.S. Geological Survey GQ-942, 1 sheet, scale 1:62,500, 3 p.
- Hintze, L.F., 1951, Lower Ordovician detailed stratigraphic section for western Utah: *Utah Geology and Mineral Survey Bulletin*, v. 39, 99 p.
- Hodges, K.V., Snoke, A.W., and Hurlow, H.A., 1992, Thermal evolution of a portion of the Sevier hinterland—the northern Ruby Mountains–East Humboldt Range and Wood Hills, northern Nevada: *Tectonics*, v. 11, p. 154–164.
- Howard, K.A., 1971, Paleozoic metasediments in the northern Ruby Mountains, Nevada: *Geological Society of America Bulletin*, v. 82, p. 259–264.
- Howard, K.A., 1980, Metamorphic infrastructure in the northern Ruby Mountains, Nevada, *in* Crittenden, M.D., Jr., Coney, P.J., and Davis, G.H., editors, *Cordilleran Metamorphic Core Complexes*, Geological Society of America Memoir 153, p. 335–347.
- Howard, K.A., 2000, Geologic map of the Lamoille quadrangle, Elko County, Nevada: Nevada Bureau of Mines and Geology Map 125, 1 sheet, scale 1:24,000, 4 p.
- Howard, K.A., and MacCready, T., 2004, Geologic map of the Verdi Peak quadrangle, Elko County, Nevada: Nevada Bureau of Mines and Geology Map 147, 1 sheet, scale 1:24,000, 4 p.
- Hudec, M.R., 1990, The structural and thermal evolution of the central Ruby Mountains, Elko County, Nevada: University of Wyoming, Laramie, Ph.D. dissertation, 272 p.
- Hurlow, H.A., 1987, Structural geometry, fabric, and chronology of a Tertiary extensional shear zone-detachment system, southwestern East Humboldt Range, Elko County, Nevada: University of Wyoming, Laramie, M.S. thesis, 141 p.
- Hurlow, H.A., Snoke, A.W., and Hodges, K.V., 1991, Temperature and pressure of mylonitization in a Tertiary extensional shear zone, Ruby Mountains–East Humboldt Range, Nevada—tectonic implications: *Geology*, v. 19, p. 82–86.
- Kellogg, K., Snee, L., and Unruh, D., 2003, The Mesoproterozoic Beaverhead impact structure and its tectonic setting, Montana and Idaho $^{40}\text{Ar}/^{39}\text{Ar}$ and U-Pb constraints: *Journal of Geology*, v. 111, p. 639–652.
- King, C., 1878, Systematic geology—geological exploration of the Fortieth Parallel, v. 1: Washington, D.C., U.S. Government Printing Office, 803 p.
- Kirk, E., 1933, The Eureka Quartzite of the Great Basin region: *American Journal of Science*, 5th series, v. 26, p. 27–44.
- Kistler, R.W., Ghent, E.D., and O'Neil, J.R., 1981, Petrogenesis of garnet two-mica granites in the Ruby Mountains, Nevada: *Journal of Geophysical Research*, v. 86, p. 10,591–10,606.
- Lawson, A.C., 1906, The copper deposits of the Robinson mining district, Nevada: University of California Department of Geology Bulletin, v. 4, p. 287–357.
- Link, P.K., and Johnston, S., 2008, Proterozoic paleogeography and stratigraphy of the Snake Range, eastern Nevada and Albion-Grouse Creek Ranges, southern Idaho; detrital zircon constraints and stratigraphic surprises: *Geological Society of America, Abstracts with Programs*, v. 40, no. 6, p. 145–146.
- Link, P.K., Dehler, C.M., Yonkee, A., 2011, Systematic regional patterns in detrital zircon populations from Cryogenian, Ediacaran and Cambrian sandstones, Brigham Group and Tintic Quartzite, northern Utah thrust belt: *Geological Society of America Abstracts with Programs*, v. 43, no. 4, p. 56.
- Long, S.P., 2012, Magnitudes and spatial patterns of erosional exhumation in the Sevier hinterland, eastern Nevada and western Utah, USA; insights from a Paleogene paleogeologic map: *Geosphere*, v. 8, p. 881–901, doi: 10.1130/GES00783.1.
- Lush, A.P., 1982, Geology of part of the northern East Humboldt Range, Elko County, Nevada: University of South Carolina, Columbia, M.S. thesis, 138 p.
- Lush, A.P., McGrew, A.J., Snoke, A.W., and Wright, J.E., 1988, Allochthonous Archean basement in the north East Humboldt Range, Nevada: *Geology*, v. 16, p. 349–353.
- Marcantel, J., 1975, Late Pennsylvanian and Early Permian sedimentation in northeast Nevada: *American Association of Petroleum Geologists Bulletin*, v. 59, p. 2079–2098.
- McGrew, A.J., 1992, Tectonic evolution of the northern East Humboldt Range, Elko County, Nevada: University of Wyoming, Laramie, Ph.D. dissertation, 191 p.
- McGrew, A.J., in review, Geologic map of the Humboldt Peak quadrangle, Elko County, Nevada: Nevada Bureau of Mines and Geology Map, 1 sheet, scale 1:24,000.
- McGrew, A.J., and Casey, M., 1998, Quartzite fabric transition in a Cordilleran metamorphic core complex, *in* Snoke, A.W., et al., editors, *Fault-related rocks—a photographic atlas*: Princeton, N.J., Princeton University Press, p. 484–489.
- McGrew, A.J., and Premo, W.R., 2011, The Angel Lake gneiss complex of northeastern Nevada and the southwestern limits of Archean to Paleoproterozoic basement in North America: *Geological Society of America Abstracts with Programs*, v. 43, no. 5, p. 435.
- McGrew, A.J., and Rahl, J.M., 2014, Pure and simple—SEM-EBSD analysis of quartzite CPOs

- from the Ruby-East Humboldt extensional shear zone, Elko County, Nevada: *Geological Society of America Abstracts with Programs*, v. 46, no. 5, p. 6.
- McGrew, A.J., and Snee, L.W., 1994, $^{40}\text{Ar}/^{39}\text{Ar}$ thermochronologic constraints on the tectonothermal evolution of the northern East Humboldt Range metamorphic core complex, Nevada: *Tectonophysics*, v. 238, p. 425–450.
- McGrew, A.J., and Snoke, A.W., 2010, SHRIMP-RG U-Pb isotopic systematics of zircon from the Angel Lake orthogneiss, East Humboldt Range, Nevada—is this really Archean crust?: *COMMENT: Geosphere*, v. 6, no. 6, p. 962–965, doi: 10.1130/GES00526.1.
- McGrew, A.J., Peters, M.T., and Wright, J.E., 2000, Thermobarometric constraints on the tectonothermal evolution of the East Humboldt Range metamorphic core complex, Nevada: *Geological Society of America Bulletin*, v. 112, p. 45–60.
- Merriam, C.W., 1940, Devonian stratigraphy and paleontology of the Roberts Mountains region, Nevada: *Geological Society of America Special Paper* 25, 114 p.
- Merriam, C.W., 1963, Paleozoic rocks of Antelope Valley, Eureka and Nye counties, Nevada: U.S. Geological Survey Professional Paper 423, 67 p.
- Metcalf, R.V., and Drew, J., 2011, Cretaceous and Eocene–Oligocene U-Pb zircon migmatite ages from the East Humboldt Range metamorphic core complex, Nevada: *Geological Society of America Abstracts with Programs*, v. 43, no. 5, p. 275.
- Miller, D.M., 1983, Allochthonous quartzite sequence in the Albion Mountains, Idaho, and proposed Proterozoic Z and Cambrian correlatives in the Pilot Range, Utah and Nevada, *in* Miller, D.M., Todd, V. R., and Howard, K.A., editors, *Tectonics and stratigraphic studies in the eastern Great Basin: Geological Society of America Memoir* 157, p. 191–213.
- Miller, D.M., 1984, Sedimentary and igneous rocks of the Pilot Range and vicinity, Utah and Nevada, *in* Kerns, G.J., and Kerns, R.L., Jr., editors, *Geology of northwest Utah, southern Idaho and northeast Nevada: Salt Lake City: Utah Geological Association Publication* 13, p. 45–63.
- Misch, P., and Hazzard, J.C., 1962, Stratigraphy and metamorphism of late Precambrian rocks in central northeastern Nevada and adjacent Utah: *American Association of Petroleum Geologists Bulletin*, v. 46, p. 289–343.
- Mueller, K.J., 1992, Tertiary basin development and exhumation of the northern East Humboldt Range–Wood Hills metamorphic complex, Elko County, Nevada: University of Wyoming, Laramie, Ph.D. dissertation, 205 p.
- Mueller, K.J., and Snoke, A.W., 1993a, Cenozoic basin development and normal fault systems associated with the exhumation of metamorphic complexes in northeast Nevada, *in* Lahren, M.M., Trexler, J.H., Jr., and Spinoso, C., editors, *Crustal evolution of the Great Basin and Sierra Nevada: Cordilleran/Rocky Mountain Section, Geological Society of America Guidebook*, Department of Geological Sciences, University of Nevada, Reno, p. 1–34.
- Mueller, K.J., and Snoke, A.W., 1993b, Progressive overprinting of normal fault systems and their role in Tertiary exhumation of the East Humboldt Range–Wood Hills metamorphic complex, northeast Nevada: *Tectonics*, v. 12, p. 361–371.
- Mueller, P.A., Wooden, J.L., Mogk, D.W., and Foster, D.A., 2011, Paleoproterozoic evolution of the Farmington zone—implications for terrane accretion in southwestern Laurentia: *Lithosphere*, v. 3, p. 401–408.
- Munroe, J.S., and Laabs, B.J.C., 2011, New investigations of Pleistocene glacial and pluvial records in northeastern Nevada, *in* Lee, J., and Evans, J.P., editors, *Geologic field trips to the Basin and Range, Rocky Mountains, Snake River Plain, and terranes of the U.S. Cordillera: Geological Society of America Field Guide* 21, p. 1–25.
- Munroe, J.S., and Laabs, B.J.C., 2013, Temporal correspondence between pluvial lake highstands in the southwestern US and Heinrich Event 1: *Journal of Quaternary Science*, v. 28, p. 49–58.
- Nolan, T.B., 1935, The Gold Hill mining district, Utah: U.S. Geological Survey Professional Paper 177, 172 p.
- Nolan, T.B., Merriam, C.W., and Williams, J.S., 1956, The stratigraphic section in the vicinity of Eureka, Nevada: U.S. Geological Survey Professional Paper 276, 77 p.
- Oversby, B.S., 1973, New Mississippian formation in northeastern Nevada and its possible significance: *American Association of Petroleum Geologists*, v. 57, p. 1779–1783.
- Peters, M.T., and Wickham, S.M., 1994, Petrology of upper amphibolite facies marbles from the East Humboldt Range, Nevada, USA—evidence for high-temperature, retrograde, hydrous volatile fluxes at mid-crustal levels: *Journal of Petrology*, v. 35, p. 205–238.
- Premo, W.R., Castiñeiras, P., and Wooden, J.L., 2008, SHRIMP-RG U-Pb isotopic systematics of zircon from the Angel Lake orthogneiss, East Humboldt Range, Nevada—is this really Archean crust?: *Geosphere*, v. 4, no. 6, p. 963–975.
- Premo, W.R., Castiñeiras, P., and Wooden, J.L., 2010, SHRIMP-RG U-Pb isotopic systematics of zircon from the Angel Lake orthogneiss, East Humboldt Range, Nevada—is this really Archean crust?: *REPLY: Geosphere*, v. 6, no. 6, p. 966–972, doi: 10.1130/GES00592.1.
- Premo, W.R., Moscati, R.J., McGrew, A.J., and Snoke, A.W., 2014, New U-Pb geochronology of Precambrian paragneisses and late Phanerozoic

- orthogneisses of the Angel Lake–Lizzies Basin region of the East Humboldt Range, northeastern Nevada—a comparison with the thermal chronology at Lamoille Canyon in the adjacent Ruby Mountains: *Geological Society of America Abstracts with Programs*, v. 46, no. 5, p. 33.
- Premo, W.R., and Van Schmus, W.R., 1989, Zircon geochronology of Precambrian rocks in southeastern Wyoming and northern Colorado, *in* Grambling, J.A., and Tewksbury, B.J., editors, *Proterozoic geology of the southern Rocky Mountains*: Boulder, Colorado, Geological Society of America Special Paper 235, p. 13–32.
- Ramelli, A.R., and dePolo, C.M., 2011, Quaternary faults in the 2008 Wells earthquake area: Nevada Bureau of Mines and Geology Special Publication 36, p. 79–88.
- Reheis, M.C., Sarna-Wojcicki, A.M., Reynolds, R.L., Repenning, C.A., and Mifflin, M.D., 2002, Pliocene to middle Pleistocene lakes in the western Great Basin—ages and connections, *in* Hershler, R., Madsen, D.B., and Currey, D.R., editors, *Great Basin aquatic systems history*: Washington, D.C., Smithsonian Institution Press, *Smithsonian Contributions to the Earth Sciences*, no. 33, p. 53–108.
- Richardson, G.B., 1913, The Paleozoic section in northern Utah: *American Journal of Science*, v. 36, p. 406–413.
- Rodgers, D.W., 1984, Stratigraphy, correlation, and depositional environments of upper Proterozoic and Lower Cambrian rocks of the southern Deep Creek Range, Utah: *Utah Geological Association Publication*, v. 13, p. 79–91.
- Schneck, W.M., 1986, Lithostratigraphy of the McCoy Creek Group and Prospect Mountain Quartzite (upper Proterozoic and Lower Cambrian), Egan and Cherry Creek ranges, White Pine County, Nevada: Eastern Washington University, Cheney, M.S. thesis, 120 p.
- Sharp, R.P., 1938, Pleistocene glaciation in the Ruby–East Humboldt Range, northeastern Nevada: *Journal of Geomorphology*, v. 1, no. 4, p. 296–323.
- Sharp, R.P., 1939a, Basin-Range structure of the Ruby–East Humboldt Range, northeastern Nevada: *Geological Society of America Bulletin*, v. 50, p. 881–920.
- Sharp, R.P., 1939b, The Miocene Humboldt Formation in northeastern Nevada: *Journal of Geology*, v. 47, p. 133–160.
- Sharp, R.P., 1940, Geomorphology of the Ruby–East Humboldt Range, Nevada: *Geological Society of America Bulletin*, v. 51, p. 337–372.
- Sharp, R.P., 1942, Stratigraphy and structure of the southern Ruby Mountains, Nevada: *Geological Society of America Bulletin*, v. 53, p. 647–690.
- Sicard, K.R., 2012, The relationship between Cretaceous and Tertiary magmatism and structural development in the southeastern East Humboldt Range, part of the Ruby–East Humboldt core complex, northeast Nevada: University of Wyoming, Laramie, M.S. thesis, 138 p.
- Simpson, C., and Wintsch, R.P., 1989, Evidence for deformation-induced K-feldspar replacement by myrmekite: *Journal of Metamorphic Geology*, v. 7, p. 261–275.
- Smith, J.F., Jr., and Ketner, K.B., 1976, Stratigraphy of post-Paleozoic rocks and summary of resources in the Carlin–Piñon Range area, Nevada: U.S. Geological Survey Professional Paper 867-B, B1–B48.
- Snelson, S., 1957, The geology of the northern Ruby Mountains and the East Humboldt Range, Elko County, Nevada: University of Washington, Seattle, Ph.D. dissertation, 214 p.
- Snoke, A.W., 1980, Transition from infrastructure to suprastructure in the northern Ruby Mountains, Nevada, *in* Crittenden, M.D., Jr., Coney, P.J., and Davis, G.H., editors, *Cordilleran metamorphic core complexes*: Boulder, Colorado, Geological Society of America Memoir 153, p. 287–333.
- Snoke, A.W., 1992, Clover Hill, Nevada: structural link between the Wood Hills and East Humboldt Range, *in* Wilson, J.R., editor, *Field guide to geologic excursions in Utah and adjacent areas of Nevada, Idaho, and Wyoming*: Miscellaneous Publication 92-3, Utah Geological Survey, p. 107–122.
- Snoke, A.W., and Miller, D.M., 1988, Metamorphic and tectonic history of the northeastern Great Basin, *in* Ernst, W.G., editor, *Rubey Volume VII, Metamorphism and crustal evolution of the western United States*: Prentice-Hall, p. 606–648.
- Snoke, A.W., McGrew, A.J., Valasek, P.A., and Smithson, S.B., 1990, A crustal cross section for a terrain of superimposed shortening and extension: Ruby Mountains–East Humboldt Range metamorphic core complex, Nevada, *in* Salisbury, M.H., and Fountain, D.M., editors, *Exposed cross sections of the continental crust*: Dordrecht, The Netherlands, Kluwer Academic Publishers, p. 103–135.
- Snoke, A.W., Howard, K.A., McGrew, A.J., Burton, B.R., Barnes, C.G., Peters, M.T., and Wright, J.E., 1997, The grand tour of the Ruby–East Humboldt metamorphic core complex, northeastern Nevada—part 1, Introduction & Road Log, *in* Link, P.K., and Kowallis, B.J., editors, *Proterozoic to Recent stratigraphy, tectonics, and volcanology, Utah, Nevada, southern Idaho and central Mexico*: Provo, Utah, Brigham Young University Geology Studies, v. 42, Part 1, p. 225–269.
- Spencer, A.C., 1917, The geology and ore deposits of Ely, Nevada: U.S. Geological Survey Professional Paper 96, 189 p.
- Steele, G., 1959, Basin and Range structure reflects Paleozoic tectonics and sedimentation: *American*

- Association of Petroleum Geologist Bulletin, v. 43, p. 1105.
- Steele, G., 1960, Pennsylvanian–Permian stratigraphy of the east-central Nevada and adjacent Utah, *in* Eleventh Annual Field Conference Guidebook: Intermountain Association of Petroleum Geologists, p. 91–113.
- Stevens, C.H., 1979, Lower Permian of the central Cordilleran miogeocline: Geological Society of America Bulletin, Part II, v. 90, p. 381–455.
- Strickland, A., Miller, E.L., Wooden, J.L., Kozdon, R., and Valley, J., 2011, Syn-extensional plutonism and peak metamorphism in the Albion-Raft River-Grouse Creek metamorphic core complex: American Journal of Science, v. 311, p. 261–314.
- Sullivan, W.A., and Snoke, A.W., 2007, Comparative anatomy of core-complex development in the northeastern Great Basin, U.S.A.: Rocky Mountain Geology, v. 42, p. 1–29.
- Taylor, G.K., 1984, Stratigraphy, metamorphism, and structure of the southeastern East Humboldt Range, Elko County, Nevada: University of South Carolina, Columbia, M.S. thesis, 148 p.
- Thorman, C.H., 1970, Metamorphosed and nonmetamorphosed Paleozoic rocks in the Wood Hills and Pequop Mountains, northeast Nevada: Geological Society of America Bulletin, v. 81, p. 2417–2448.
- Van Houten, F.B., 1956, Reconnaissance of Cenozoic sedimentary rocks of Nevada: Bulletin of the American Association of Petroleum Geologists, v. 40, p. 2801–2825.
- Voice, P., Kowalewski, M., and Eriksson, K., 2011, Quantifying the timing and rate of crustal evolution—global compilation of radiometrically dated detrital zircon grains: Journal of Geology, v. 119, p. 109–126.
- Walcott, C.D., 1908, Smithsonian Miscellaneous Collection: Washington, D.C., v. 53, no. 1812, 184 p.
- Wallace, A.R., Perkins, M.E., and Fleck, R.J., 2008, Late Cenozoic paleogeographic evolution of northeastern Nevada—evidence from the sedimentary basins: Geosphere, v. 4, no. 1, p. 36–74; doi: 10.1130/GES00114.1.
- Wardlaw, B.R., and Collinson, J.W., 1978, Stratigraphic relations of Park City Group (Permian) in eastern Nevada and western Utah: American Association of Petroleum Geologists Bulletin, v. 62, p. 1171–1184.
- Wardlaw, B.R., Collinson, J.W., and Maughan, E.K., 1979, The Murdock Mountain Formation—a new unit of the Permian Park City Group, *in* Wardlaw, B.R., editors, Studies of the Permian Phosphoria Formation and related rocks, Great Basin–Rocky Mountain region: U.S. Geological Survey Professional Paper 1163–B, p. 5–7.
- Wayne, W.J., 1984, Glacial chronology of the Ruby Mountains–East Humboldt Range, Nevada: Quaternary Research, v. 21, p. 286–303.
- Webb, G.W., 1956, Middle Ordovician detailed stratigraphic sections for western Utah and eastern Nevada: Salt Lake City, Utah Geological and Mineralogical Survey Bulletin, v. 57, 77 p.
- Wesnousky, S.G., and Willoughby, C.H., 2003, Neotectonic note—the Ruby–East Humboldt Range, northeastern Nevada: Bulletin of the Seismological Society of America, v. 93, no. 3, p. 1345–1354.
- Willden, R., and Kistler, R.W., 1979, Precambrian and Paleozoic stratigraphy in central Ruby Mountains Elko County Nevada, *in* Newman, G.W., and Goode, H.D., editors, Basin and Range Symposium and Great Basin field conference, RMAG-UGA, p. 221–243.
- Woodward, L.A., 1967, Stratigraphy and correlation of late Precambrian rocks of Pilot Range, Elko County, Nevada, and Box Elder County, Utah: American Association of Petroleum Geologists Bulletin, v. 51, p. 235–243.
- Woodward, L.A., 1965, Late Precambrian stratigraphy of northern Deep Creek Range, Utah: American Association of Petroleum Geologists Bulletin, v. 49, p. 310–316.
- Wright, J.E., and Snoke, A.W., 1993, Tertiary magmatism and mylonitization in the Ruby–East Humboldt metamorphic core complex, northeastern Nevada—U-Pb geochronology and Sr, Nd, Pb isotope geochemistry: Geological Society of America Bulletin, v. 105, p. 935–952.
- Wright, J.E., and Wooden, J.L., 1991, New Sr, Nd, and Pb isotopic data from plutons in the northern Great Basin—Implications for crustal structure and granite petrogenesis in the hinterland of the Sevier thrust belt: Geology, v. 19, p. 457–460.
- Yonkee, A., Willis, G.C., and Doelling, H.H., 2000, Petrology and geologic history of the Precambrian Farmington Canyon complex, Antelope Island, Utah, *in* King, J.K., and Willis, G.C., editors, The geology of Antelope Island, Davis County, Utah: Salt Lake City, Utah Geological Survey Miscellaneous Publication 00-1, p. 5–36.
- Zoback, M.L., and Thompson, G., 1978, Basin and Range rifting in northern Nevada—clues from a mid-Miocene rift and its subsequent offset: Geology, v. 6, p. 111–116.

Suggested Citation:

McGrew, A.J., Snoke, A.W., 2015, Geologic map of the Welcome quadrangle and an adjacent part of the Wells quadrangle, Elko County, Nevada: Nevada Bureau of Mines and Geology Map 184, scale 1:24,000, 40 p.